MULTIMODAL NEUROIMAGING IN DRUG NAÏVE GENETIC GENERALISED EPILEPSY PATIENTS

Perani, Suejen

Awarding institution:
King's College London

MULTIMODAL NEUROIMAGING IN DRUG NAÏVE GENETIC GENERALISED EPILEPSY PATIENTS

Suejen Perani, BSc, MSc

DEPARTMENT OF BASIC AND CLINICAL NEUROSCIENCE
INSTITUTE OF PSYCHIATRY, PSYCHOLOGY AND NEUROSCIENCE (IoPPN)
KING'S COLLEGE LONDON
UNITED KINGDOM

THESIS SUBMITTED TO KING'S COLLEGE LONDON
FOR THE DEGREE OF DOCTOR OF PHILOSOPHY, 2016

DECLARATION OF OWN WORK

I, Suejen Perani, confirm that the work presented here is my own. Where information has been derived from other sources, I confirm that this has been indicated in the thesis.

The scientific studies presented in this thesis reflect the contributions of a team of researchers including colleagues from the Developmental Imaging and Biophysics Section, UCL Institute of Child Health and the epilepsy group at King's College London. This thesis only presents studies where I conducted data collection, data analysis and interpretation of the results following discussions at supervision meetings. I have outlined my own individual contribution to each of the studies presented here and the contributions of my main co-workers and collaborators.

All the figures and illustrations are my own.

Information derived from other sources has been indicated and referenced in this thesis.

Signature

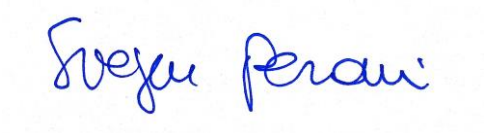

ABSTRACT

Neuroimaging has advanced the knowledge of genetic generalised epilepsy via the improvement of methods and technology. The current understanding is that patients with GGE are characterised by abnormalities in the cortical-thalamic network, functionally and also structurally; and in the default mode network, mainly functionally. However, most studies have been performed on treated patients often with poor seizure control. This leaves uncertainty regarding the status of the brain at the onset of the disease and mechanisms that lead to positive and negative treatment outcome. Also, the systematic measurements of epileptic activity during resting fMRI has left questions about the interaction between cognitive status and the brain networks that have been identified as associated with generalised spike waves (GSW).

In this thesis I focused on three rarely and/or uniquely explored issues in the field of neuroimaging in GGE to reach a more comprehensive understanding of GGE.

First, I undertook a study of brain structure and function free from any effects of anti-epileptic medication. In drug naïve patients, I measured grey matter volume and shape and fMRI BOLD changes related to GSW onset and prior to GSW. I showed that previous findings can be interpreted and confirmed without the potential influence of AEDs.

Secondly, I applied a prospective approach via longitudinally following patients from pre-treatment to post-treatment stages to explore treatment response and to identify markers of treatment outcome. I compared grey matter volume and shape between drug

naïve pre-treatment patients with good and bad outcomes. I identified a trend of decreased grey matter volume in patients with bad outcome suggesting the existence of differences at baseline between patients with different treatment response. I compared cerebral blood flow (CBF) longitudinally and found a trend of decreased CBF post-treatment. This suggests that BOLD changes post-treatment may be related to CBF differences.

Thirdly, I explored the relationship between brain networks associated with GSW and the brain state via measuring BOLD changes associated with GSW recorded during periods of rest and while watching a cartoon. Evidence of different BOLD maps during rest and cartoon is reported suggesting the need to consider initial brain state in defining the GSW related BOLD response.

Methodological constraints, clinical applications and future perspectives are discussed.

TABLE OF CONTENT

LIST OF TABLES

LIST OF FIGURES

LIST OF ACRONYMS

AE = Absence epilepsy

AED = Anti-epileptic medication

AM = Ante-meridiem

ASL = Arterial spin labelling

BCG = Ballistocardiographic

BD = Bis Die – two times a day

BOLD = Bold oxygen level dependent

CAE = Childhood absence epilepsy

CBF = Cerebral blood flow

Cl = Chlorine

CLB = Clobazam

CLZ = Clonazepam

CNS = Centre for neuroimaging sciences

DARTEL = Diffeomorphic Anatomical Registration Through Exponentiated Lie

DMN = Default mode network

DN = Drug naïve

DTI = Diffusion tensor imaging

ECG = Electrocardiogram

EEG = Electroencephalography

EEG-fMRI = Simultaneous electroencephalography and functional magnetic resonance imaging

EMA = Eye myoclonia with absences

EPI = Echo planar imaging

EPSP = Excitatory post synaptic potential

ETX = ethosuximide

F = Female

FC = Frontal cortex

FDR = False discovery rate

FIACH = Image artefact correction heuristic

FLAIR = Fluid-attenuated inversion recovery

fMRI = Functional magnetic resonance imaging

FOV = Field of view

FWE = Familywise error

FWHM = Full width at half maximum

GA = Gradient artefact

GABA = Gamma-aminobutyric acid

GAERS = Genetic absence epilepsy rats from Strasbourg

GGE = Genetic generalised epilepsy

GLM = General linear model

GM = Grey matter

GOSH = Great Ormond street hospital

GSW = Generalised spike wave

GTCS = Generalised tonic clonic seizure (seizure)

GTCSO = Generalised tonic clonic seizure only (syndrome)

HC = Healthy control

HRF = Haemodynamic response function

ICA = Independent component analysis

IED = Interictal epileptic discharge

IFG = Inferior frontal gyrus

IGE = Idiopathic generalised epilepsy

ILAE = International league against epilepsy

IPSP = Inhibitory post synaptic potential

JAE = Juvenile absence epilepsy

JME = Juvenile myoclonic epilepsy

K= Potassium

KCH = King's college hospital

L = Left

LCM = Lacosamide

LEV = Levetiracetam

LFP = Local field potential

LTG = Lamotrigine

M = Male

MEG = Magnetoencephalography

MFG = Middle frontal gyrus

MNI = Montreal neurological institute

MR = Magnetic resonance

MRI = Magnetic resonance imaging

MRS = Magnetic resonance spectroscopy

MTG = Middle temporal gyrus

MUA = Multi unit activity

Na = Calcium

NBV = Normalised brain volume

NHS = National Health Service

PA = Pulse artefact

PBT = Phenobarbital

PCC = Posterior cingulate cortex

PD = Proton density

PET = Positron emission tomography

PhMRI = Pharmacological magnetic resonance imaging

PM = Post-meridiem

PT = Post-treatment

R = Right

REC = Research ethic committee

RF = Radio frequency

ROI = Region of interest

SD = Standard deviation

SFG = Superior frontal gyrus

SMA = Supplementary motor area

SPECT = Single photon emission tomography

SPM = Statistical parametric mapping

SPM[F] = Statistical parametric mapping F-test contrast

SPM[T] = Statistical parametric mapping T-test contrast

SPSS = Statistical package for the social science

STG = Superior temporal gyrus

T = Tesla

TMS = Transcranial magnetic stimulation

TPM = Tissue probability map

VBM = Voxel base morphometry

VPA = Valproate acid

WAG/Rij = Wistar albino Glaxo from Rijswijk

WM = White matter

AKNOWLEDGEMENTS

This thesis would have not been created without all the patients and patients' families that kindly agreed to participate in the project.

I want to thank my supervisors: Prof. Richardson (Mark) and Dr Carmichael (David). The support I have been given has been essential and priceless. In addition to the amount of knowledge provided, I have also felt supported along the whole process, from the design of the project until the thesis writing. I think this has really made this thesis possible and the time of my PhD memorable. I want to thank Prof. Cross for her support as without her I would not be able to have such a great approval from so many paediatricians across London. Also, I want to thank her as she is an inspiration for me not only as a professional but especially as a woman. Having had three mentors of this kind is rare and I think this has positively shaped my professional character. Thank you.

This thesis would have not been possible without the support of the research teams from King's and UCL. Particularly, I want to thank Isabella, Toni and Amber. Isabella, thank you for the psychological support; Toni, thank you for chasing Mark and organising his time for me; Amber, you solved some of this R&D issues for me…you know how this was important! Also, I want to thank Maria, Tim, Elli, Sara and Merina. In addition to the help I received in data acquisition, Maria, you stood beside me since the beginning of this project and I really felt I had a very good friend next to me. Tim and Elli, thank you for the long talk and the support in data acquisition and data analysis. Tim, I will never forget your face when I drag you to the methods meeting at the FIL and you saw me standing up next to Prof. Friston. Sara, you just arrived in the team but you already

supported me with precious answers. Merina, you are a friend with work-related knowledge so thank you for sharing bad and good moments with me, you remember, this PhD started also with your help in reading my application!

I want to thank all the radiographers from Great Ormond Street hospital and King's College London. It would have been impossible to scan patients within one week if it wasn't for your effort too. Jess and Tina, I cannot thank you enough for lunch breaks you used for fitting my scanning.

Last but not least, my family and friends; you have been a rock through all the process. I want to particularly thank Filippo, my 8 years old nephew, who was brave enough to be scanned as a healthy control, and my sister, Gessica, to let me do this. I want to thank my mother Lena, I felt her support and love every day of this journey.

I want to thank Mazzone who helped me keep going by yelling at me: 'PERANI STUDIA!' and Enni, who called me every day to check on me and she kept me motivated. I think that without recreational breaks with you, I would have not be able to finish this thesis.

FUNDING SOURCES

During this PhD thesis, I was supported by a 3+1 studentship from the NIHR Maudsley Biomedical Research Centre (BRC), Institute of Psychiatry, Psychology and Neuroscience, King's College London. I am also thankful to Medical Research Council (MRC grant MR/K013998/1), the Maudsley/IoPPN BRC Neuroimaging Theme funding scheme and Epilepsy Research UK (grant PGE1402) which partly funded the scanning costs of the project. I am also thankful to the Action Medical Research (SP4646) for funding Dr Centeno and the scanning cost used for acquiring children healthy control data in addition to the Engineering and Physical Sciences Research Council grant (EP/M001393/1) for funding the MRI-compatible EEG equipment at ICH, UCL.

I am thankful to Guarantors of Brain and to the BRC, IoPPN for the travel grants awarded which allowed the presentation of part of the current research in international conferences.

PREFACE

This thesis presents the first body of research aimed to study the first sample of drug naïve patients diagnosed with genetic generalised epilepsy which was followed longitudinally from the diagnosis up to 6 months after the first drug intake. The motivations behind the acquisition of brain measures in such a challenging group of patients came from the continuous requirement by the neuroscience and clinical communities to understand generalised epilepsy further, via the acquisition of unbiased neuroimaging data. Indeed, current knowledge is mainly based on studies of patients taking treatment for a long time, mostly with a poor treatment outcome and, in the majority of the cases, the epileptic network was only investigated during rest.

We (Prof. Richardson, Dr Carmichael, Prof. Cross and I) took the challenge of acquiring neuroimaging data in a group of 31 drug naïve patients diagnosed with GGE and related follow-up. Here, I present different measures we used to explore treatment effect on grey matter structures and GSW related BOLD maps. I report that structural grey matter volume may contribute to understanding treatment outcome. I present results suggesting that BOLD maps post-treatment may be influenced by differences in the level of cerebral blood flow due to treatment. I describe how the interaction with brain state (for example at rest or during a task) may influence brain networks involved in GSW.

Bearing in mind the rarity of this sample, I believe that the results I report give novel insights to the current knowledge of GGE mechanisms.

OUTLINE AND STATEMENT OF PERSONAL CONTRIBUTION

This thesis is structured as follows:

SECTION 1: INTRODUCTION

Chapter 1 introduces the clinical aspects of genetic generalised epilepsy. I describe epilepsy classification, diagnosis, treatment and current understanding of underlying mechanisms.

Chapter 2 describes the use of neuroimaging in genetic generalised epilepsy, including current knowledge and related flaws.

SECTION 2: GENERAL METHODS

Chapter 3 summaries the general methods used to acquire and analyse the sample investigate in the experimental studies. It describes recruitment strategies, MRI protocol and generalities of the sample. Here I would like to thank Prof. Helen J. Cross and Prof. Mark P. Richardson for providing clinicians' names and allow me to develop a strong network between myself and the clinical team. I would like to thank Dr. David W. Carmichael who helped me to set-up simultaneous EEG-fMRI at King's College London together with the help of Prof. Gareth Barker and Mr David Gasston.

SECTION 3: EXPERIMENTAL STUDIES

Chapter 4 – 7 describes experimental studies.

In Chapter 4 I present analysis on cortical and subcortical structural grey matter, demonstrating the existence of abnormalities at new onset of the disease in the absence of antiepileptic medication. Here, I would like to thank Dr. Jonathan O'Muircheartaigh and Dr. Simone Keller for their advice in data analysis.

In Chapter 5 I introduce the first EEG-fMRI study in which I explored GSW BOLD changes in the biggest drug naïve population. I also explored BOLD changes prior to GSW to identify their temporal evolution.

In Chapter 6 I describe the second EEG-fMRI study in which I tested differences in BOLD changes related to GSW arising in different brain states. Here, I want to thank Tim Tierney for the support in the statistical modelling and Elli Shamshiri for providing cartoon network maps.

In Chapter 7 I compare the differences in cerebral blood flow between drug naïve and post-treatment patients. Here I want to thank Dr. Patrick Hale for providing me with the Matlab code for the 1.5T data and Dr. Fernando Zelaya for the support in data analysis for 3T data.

SECTION 4: DISCUSSION AND CONCLUSION

In Chapter 8 I summarise the main results reported in the experimental chapters and I also discuss how this new information improves the current status of knowledge in seizure generation, drug effects, treatment outcome and brain states in GGE. I introduce plans for future studies in structural and functional connectivity which will provide the

most comprehensive picture of the evolution of GGE and differences in treatment outcome in the first longitudinal sample.

In Chapter 9 I conclude summarising the main findings and providing a comprehensive picture of the relationship between these discoveries and the novelty they provide to understand GGE.

CONFERENCE, POSTERS AND TALKS RELATED TO THIS THESIS

Posters

- Tangwiriyasakul, C., Perani, S., Nurbaya Yaakub, S., Richardson M.P., (2016). Using a temporal decomposition technique to investigate dynamic changes in subnetworks derived from resting state fMRI during generalised spike-and-wave discharges: an EEG-fMRI pilot study: a pilot study. INFC, Poster.
- Tangwiriyasakul, C., Perani, S., Nurbaya Yaakub, S., Richardson M.P., (2016). Investigation of kuramoto's critical value during generalised spike-and-wave (GSW) discharge periods: a pilot study. Biodynamics, Poster.
- Perani, S., Centeno, M., Tierney, T., Shamshiri, E.A., Cross, H.J., Carmichael, D.W., Richardson, M.P., (2015). EEG-fMRI: generalised spike wave networks in newly diagnosed-drug naïve absence epilepsy children. BACI, Poster.
- Perani, S., Centeno, M., Tierney, T., Shamshiri, E.A., Cross, H.J., Carmichael, D.W., Richardson, M.P., (2015). EEG-fMRI: generalised spike wave networks in newly diagnosed-drug naïve absence epilepsy children. Human Brain Mapping, Poster and published abstract.
- Perani, S., Centeno, M., Tierney, T., Cross, H.J., Carmichael, D.W., Richardson M.P., (2014). Simultaneous EEG-fMRI: posterior slow-waves compared with occipital alpha in childhood absence epilepsy. European Congress Epilepsy, Poster.

- Perani, S., Centeno, M., Tierney, T., Cross, H.J., Carmichael, D.W., Richardson M.P., (2014). Simultaneous EEG-fMRI: posterior slow-waves compared with occipital alpha in childhood absence epilepsy. Human Brain Mapping, Poster and published abstract.

Invited talks

- Preliminary results of Drug Naïve patients: an MRI study in absence epilepsy and juvenile myoclonic epilepsy. Young Epilepsy Retreat, UCL, GOSH (2016).
- Effect of treatment on brain networks changes: an EEG-fMRI study in absence epilepsy and juvenile myoclonic epilepsy. Centre for Neuroimaging Science, King's College London (2015).
- Update on the effect of treatment on brain networks changes: an EEG-fMRI study in absence epilepsy and juvenile myoclonic epilepsy. Young Epilepsy Retreat, UCL, GOSH (2015).
- Update on the effect of treatment on brain networks changes: an EEG-fMRI study in absence epilepsy and juvenile myoclonic epilepsy. Young Epilepsy Retreat, UCL, GOSH (2014).
- Effect of treatment on brain networks changes: an EEG-fMRI study in absence epilepsy and juvenile myoclonic epilepsy. UKERN, Epilepsy Research Forum, Birmingham Medical institute (2013).
- Update on the effect of treatment on brain networks changes: an EEG-fMRI study in absence epilepsy and juvenile myoclonic epilepsy. Young Epilepsy Retreat, UCL, GOSH (2013).

SECTION 1: INTRODUCTION

Chapter 1 : Introduction to Genetic Generalised Epilepsy

Epilepsy is a common disease known from Mesopotamian civilisations that has been considered a medical condition since the late 19th century (Chaudhary et al., 2011). Since then, the knowledge of epilepsy has expanded thanks to the invention of anti-epileptic drugs, neuroimaging methods, and genetics (Magiorkinis et al., 2014). Nevertheless, neuroscience and medicine are working together to understand unknown elements such as the cause/origin of epilepsy, the unpredictability of seizures (Carney et al., 2011; Ramgopal et al., 2014) and the unknown predictors of treatment outcome (Perucca, 1997).

Clinical definition and classifications of epilepsies has been reached via the taxonomy that the ILAE (International League Against Epilepsy) has drafted (Berg et al., 2010; Fisher et al., 2014). Generalised and focal epilepsies are defined by seizures engaging bilateral distributed networks or circumscribed within one smaller region, respectively. This thesis will be exclusively concerned with what is defined as generalised seizures manifested in the presence of a diagnosis of genetic generalised epilepsy (GGE) syndromes such as childhood and juvenile absence epilepsies, juvenile myoclonic epilepsy and generalised tonic-clonic seizures only.

1.1 Genetic Generalised epilepsies - GGE

Genetic generalised epilepsy is the current term for what was called idiopathic generalised epilepsy (IGE) in the previous ILAE classification (Engel and International

League Against, 2001). The name has been changed under the assumption that the aetiology of the syndromes is a genetic defect directly contributing to the epilepsy, and that seizures are the core symptom of the disorder (Berg et al., 2010). Idiopathic was previously regarded as meaning "presumed genetic aetiology". GGEs are characterised by different ages of onset and seizure semiology. Given that this work is focusing on childhood absence epilepsy (CAE), juvenile absence epilepsy (JAE), juvenile myoclonic epilepsy (JME) and epilepsy with generalised tonic-clonic seizures only (GTCSO) (Caraballo and Dalla Bernardina, 2013), specification of each syndrome will be presented in the following paragraphs.

There are commonalties across these syndromes. For example, they are all characterised by electrophysiological changes recorded with electroencephalography (EEG) of a frequency of 3-5 Hz called Generalised Spike Wave (GSW) discharges which disrupt normal background activity (Smith, 2005). Photosensitivity is found in about 5% of patients diagnosed with GGEs and 75% of them have had the first photic induced seizure between the ages of 8 and 20 years old (Quirk et al., 1995).

1.1.1 Absence epilepsy

The first recording of GSW in absence epilepsy was performed by Gibbs and colleagues in 1935 (Gibbs et al., 1935).

Absence epilepsy is divided in two syndromes based on age: childhood absence epilepsy (CAE) and juvenile absence epilepsy (JAE).

1.1.1.1 CAE

Absence epilepsy is a common type of generalised epilepsy in childhood (about 7/100,000 children per year) (Chang and Lowenstein 2003). Typical CAE occurs in otherwise normal children during childhood (onset between age 4 and 10) and it has a strong genetic predisposition. Seizures are characterised by typical absences described as brief non-convulsive absence seizures (AE) which can be detected by electroencephalography (EEG) showing electrophysiological changes at 2.5–4 Hz generalised, bilaterally and synchronous GSW (Blumenfeld 2005). The interictal EEG is normal, or may show runs of occipital rhythmic delta (in 15–40% of cases) which might be a sign of good treatment outcome (Caraballo and Dalla Bernardina, 2013), persisting in some children after remission of absences. Seizures are frequent, varying from tens to hundreds per day and lasting from 4 to 20 seconds. Clinically, the most important feature of the absences is severe impairment of consciousness with unresponsiveness and interruption of the ongoing voluntary activity, which is restored immediately after the seizure finishes. Automatisms occur in two-thirds of the seizures, and are stereotyped. At the beginning of the absences, mild myoclonic movements of the eyes, eyebrows, and eyelids may be seen. Absences are often easily triggered by hyperventilation (Caraballo and Dalla Bernardina, 2013). As part of the GGEs, CAE has a strong genetic aetiology given recent evidence suggesting mutation in genes encoding GABA receptors or brain-expressed voltage-dependant calcium channels (Panayiotopoulos, 2010b). Diagnosis of epilepsy is effectively made via clinical history and routine EEG with hyperventilation and photic stimulation, but may require short ambulatory EEG recording. CAE is treated with monotherapy AED with valproate,

ethosuximide or lamotrigine. In refractory patients, polytherapy with valproate combined with ethosuximide or lamotrigine is the most common combination. Prognosis is good for CAE with usually a remission before age 12 and less than 10% develops GTCSs during adolescence or adulthood (Caraballo and Dalla Bernardina, 2013).

1.1.1.2 JAE

Juvenile absence epilepsy onset is around 9-13 years of age. JAE is characterised by typical absence seizures like CAE. Automatisms are also present and eye myoclonic movements are often seen. Patients with JAE present with GTCSs in 80% of cases and myoclonic jerks in 15-25%. Ictal EEG is similar to CAE, however, they are more likely to show polyspike discharges or a spike wave frequency above 3 Hz; runs of occipital rhythmic delta are not found (Smith, 2005). Additionally, focal abnormalities and spike/polyspike discharges are seen asymmetrically. Background EEG is otherwise normal. Ictal events are triggered by photosensitivity in 8% of patients (Panayiotopoulos, 2010b). As for CAE, there is a strong component of genetic aetiology in JAE. JAE is easily diagnosed with video-EEG. The only way to distinguish JAE from CAE is the age of onset and the presence of occasional myoclonus. Drug therapy is the same as for CAE. JAE has a worse prognosis than CAE and is typically a life-long disorder. However, 80% of patients are well controlled with AED if the treatment is initiated at the early stage of onset (Panayiotopoulos, 2010b).

1.1.2 JME

Juvenile myoclonic epilepsy was recognised as a distinct clinical syndrome in 1957 (Janz, 1957).

In juvenile myoclonic epilepsy, the interictal and ictal EEG characteristic is brief bursts of polyspike (sometimes single spike) and wave discharge at 3-6Hz. Variable asymmetry or lateralised emphasis of discharge is common, and focal abnormalities are described in up to 40% of cases during interictal period (Smith, 2005).

Juvenile myoclonic epilepsy accounts for 8-10% of patients with epilepsy. It is characterised by myoclonic jerks in the limbs particularly on awakening. Most of the patients also manifest with GTCS which may follow on from periods of continuous myoclonic jerks. One third of patients also have absences that are brief compared to those typically found in CAE and JAE. Seizures are triggered by sleep deprivation, fatigue, stress, emotion and alcohol intake. Personality, behavioural, cognitive, and psychological disturbance are often observed in JME (Koepp et al., 2014). A family history of epilepsy was found in about 40-50% of patients with JME showing a big genetic component in the aetiology. Treatment with valproate is the most effective for men but is teratogenic, hence lamotrigine or levetiracetam is often the best solution for women; a combination of lamotrigine with valproate or topiramate are alternatives. Benzodiazepines may be used during clusters of myoclonic jerks. As for JAE, seizures are probably suffered life-long but 90% of patients have seizures well controlled with AED (Caraballo and Dalla Bernardina, 2013).

1.1.3 GTCSO

Epilepsy with GTCS only is characterised by generalised tonic clonic seizures predominantly occurring 1 or 2 hours after awaking. However, undetected jerks or absence seizures may occur before the onset of GTCS. Age of onset varies from 6 to 47 years of age with a peak between 16 and 17 years. The prevalence of GTCSO is debated as some studies reported that these patients account for only 0.9% of all GGE (Panayiotopoulos, 2005), others for 13-15% (Roger, 1994). Seizures are triggered by sleep deprivation, fatigue and alcohol consumption. There is a strong genetic aetiology for GTCSO with high incidence of family history in patients. GTCSO is a life-long disease with an 83% relapse rate on withdrawal of treatment. (Panayiotopoulos, 2010b)

1.2 Diagnoses of GGE

As mentioned in the previous paragraphs, EEG is the best clinical tool to provide evidence for a diagnosis of epilepsy. In a clinical setting, it is used to determine seizure type and specific epilepsy syndrome along with the clinical history and to help identify possible precipitants to epileptic seizures. Clinical EEG is routinely recorded in outpatient clinics first in normal wakefulness before asking the patients informed consent to perform intermittent photic stimulation and hyperventilation. If the diagnosis is still unclear, sleep EEG can be advised. The EEG recording is abnormal in about 80-90% of patients in a population with untreated GGE, especially absence epilepsies with presence of photosensitivity (Panayiotopoulos, 2010c).

1.3 Treatment in GGE

Treatment of genetic generalised epilepsy consists of a daily long-term intake of antiepileptic drug (AED) regime. There is a long list of AED available in the market. However, we will only cover those used in GGE. Those are: clobazam (CLB), clonazepam (CLZ), ethosuximide (ETX), lacosamide (LCM), lamotrigine (LTG), levetiracetam (LEV), phenobarbital (PBT), topiramate (TPM) and valproate (VPA) (Panayiotopoulos, 2010a). These are, in reality, anti-seizure drugs as they stop the manifestation of seizures but do not cure epilepsy (French et al., 2004).

General guidelines suggest that for patients with GTCS of unknown cause (ie. not known whether due to GGE or focal epilepsy), valproate is effective. Valproate is the drug of choice for patients with GSW on the EEG in general and in particular for all the forms of GGE. Ethosuximide and lamotrigine (French et al., 2004) are also useful drugs for absence seizures. For patients who have both absence seizures, GTCS and/or myoclonic jerks, valproate is preferable (Brodie and Dichter, 1996).

Clobazam is licensed only as adjunctive therapy in epilepsy. Its efficacy is not the same as that of clonazepam. It may be more efficacious in focal than generalised epilepsies (Childhood, 1998; Montenegro et al., 2001). Clonazepam is licensed for any type of epileptic seizure, but it is mainly used as one of the most efficacious AEDs for myoclonic jerks. It may not suppress GTCS of juvenile myoclonic epilepsy and patients may be deprived of the warning jerks, which herald the onset of GTCS (Obeid and Panayiotopoulos, 1989). Ethosuximide may be effective in negative myoclonus (Oguni et al., 1998). Lamotrigine may aggravate myoclonic jerks in juvenile myoclonic epilepsy and some progressive myoclonic epilepsies (Guerrini et al., 1998b; Guerrini et al., 1999;

Gayatri and Livingston, 2006). The effect of levetiracetam on absences is not well documented, although clinical series have shown a significant beneficial effect in childhood and juvenile absence epilepsy (Di Bonaventura et al., 2005; Verrotti et al., 2008).

In case the first AED does not control seizures, polytherapy is advised. In the case of refractory epilepsy in patients with GTCS of unknown cause, the combination of the first drug with carbamazepine, valproate acid and/or phenytoin is advised. For patients with myoclonic seizures who do not have a response to valproate, clonazepam can be added, whereas patients with intractable typical or atypical absence seizures may have a response to valproate combined with ethosuximide (Brodie and Dichter, 1996).

The type of AED prescribed depends not only on the specific diagnosis but also on the specific medical situation of the patient. For example, women in their first trimester of pregnancy might have an increased risk of foetal malformation if under valproate monotherapy and/or polytherapy (Harden et al., 2009) and therefore a different drug might be preferable. For example, levetiracetam is advisable if myoclonic seizures are predominant; lamotrigine would be favoured if absence seizures are the main seizure type to control (Montouris, 2009). Another risk factor to account for is weight gain and loss. For those people already overweight, AED with weight gain as a side effect (valproate) may be avoided; vice versa, in people under weight, AED of which side effect is weight loss may be avoided (ethosuximide and topiramate) (Panayiotopoulos, 2010a).

1.3.1 Pharmacodynamics

Although the mechanisms of action of AED are not fully clarified, the main mechanisms of action known of the available AEDs are blockage of voltage-dependent ion channels (K+, Na+ and Ca2+ channels), increasing the activity of the inhibitory GABAergic system and decreasing the activity of the excitatory glutamatergic system.

Among those AEDs used in GGE, phenobarbitan, topiramate and valproate are found to use all mechanisms, clobazam and clonazapam function by increasing GABA inhibition, ethosuximide blocks Ca2+ channels and lamotrigine blocks voltage dependent Na+ channels (Panayiotopoulos, 2010a).

In clinical practice, knowledge about the mechanism of action is important, particularly in the treatment of seizure types with known pathophysiology; for example, primarily GABA-ergic AEDs such as clobazam are contraindicated in absence seizures that are facilitated by GABA activation. Furthermore, in polytherapy, combining AEDs with the same action is ill-advised because their combination is unlikely to have a better success and more likely to have additive side effects (Panayiotopoulos, 2010a).

1.4 Treatment outcome

It has been estimated that more than 30% of patients diagnosed with GGE have an inadequate control of seizures (Kwan and Brodie, 2000). In fact, monotherapy with an appropriately selected AED at an appropriate target dose achieves complete control of seizures in 50–70% of patients (Panayiotopoulos, 2010a).

Rational polytherapy is often needed for 30–50% of patients who are unsatisfactorily controlled with a single AED. Recent studies showed that the chance to become seizure

free declines by 50% every 1.5-2 AEDs that has proved ineffective in the past, leaving up to 16.6% of patients uncontrolled after failure of three previous AEDs (Kwan and Brodie, 2001; Schiller and Najjar, 2008). Polytherapy with more than three drugs is discouraged because adverse reactions become more prominent, with little, if any, seizure improvement (Panayiotopoulos, 2010a).

For those patients who are seizure free for more than 3–5 years, consideration of total withdrawal of AEDs is needed. However, particular attention is required for those who suffer from epileptic syndromes requiring long-term treatment such as JME. Discontinuation of AEDs should be extremely slow, in small doses and in long steps of weeks or months. The rate of relapse increases with a faster rate of AED discontinuation (Panayiotopoulos, 2010a).

The current state of knowledge is that treatment outcome cannot be predicted. This leaves clinicians and patients with the only option of trying an AED and adjusting treatment based on the patient-specific outcome. Some studies have tried to estimate treatment response based on number of seizures pre-treatment but this measure was found not be a key element to predict treatment outcome (Kwan and Brodie, 2000). However, given the reduced percentage of treatment response from first AED to polytherapy or change of first drug (< 14%) (Kwan and Brodie, 2000), it is important to identify predictors for unsuccessful treatment outcome.

1.5 Animal models of GGE

Understanding the mechanisms of GGE would help in understanding also mechanisms of treatment outcome. There are two well-established inbred rat strains with inherited

GSW, accompanied by absence seizure-like phenomena: Wistar Albino Glaxo from Rijswijk (WAG/Rij) (Coenen et al., 1992) and Genetic Absence Epilepsy Rats from Strasbourg (GAERS) (Danober et al., 1998). Given the similarities between the ictal EEG and behavioural manifestations of GAERS and WAG/Rij rats and those of typical absence (Crunelli and Leresche, 2002), rat models provide important insight regarding mechanisms of seizure generation in humans.

It has been possible to identify different theories of GSW generation from these models: the centrencephalic theory in which GSW have been described as originating from subcortical areas (Jasper HH, 1947; Buzsaki, 1991) and the cortical theories in which GSW has a focus in the cortex (Gloor, 1968; Niedermeyer, 1972; Luders et al., 1984). A compromise of the two is the cortico-reticular theory in which a functionally intact thalamo-cortical network is required for the generation of spike-wave discharges. This theory was generated by results in GAERS and WAG/Rij in which GSW were recorded at first in somatosensory cortex and 500ms after in the thalamus. The proposed mechanism describes that the first cycles of the seizure in the cortex drives the thalamus, while thereafter cortex and thalamus drive each other, thus amplifying and maintaining the rhythmic discharge (Meeren et al., 2002; Meeren et al., 2005).

More recent evidence supports the cortico-reticular theory. For example, intracerebral electrodes in several brain sites in GAERS showed that the neural driver of GSW was in somatosensory cortex (David et al., 2008). Preictal activity has been found in somatosensory cortex. In WAG/Rij rats, increased EEG power was seen prior to GSW in a range of brain areas, especially in somatosensory cortex (Luttjohann et al., 2013). Multisite local field potential recordings in GAERS showed that the onset of GSW was

preceded by abnormal 5-9Hz oscillations in a localised area of somatosensory cortex (Zheng et al., 2012). Additionally, strong functional connectivity between hemispheres was demonstrated in the interictal state, particularly involving somatosensory regions where seizures appear to arise (Mishra et al., 2013). Whole-brain network imaging in both strains has shown a very similar pattern to that seen during GSW in humans. Simultaneous EEG-fMRI in WAG/Rij and GAERS rats during GSW showed increased BOLD in bilateral sensorimotor cortex and thalamus, as well as decreased BOLD in striatum (David et al., 2008; Mishra et al., 2013).

Neuroimaging results in humans are discussed in the following Chapter.

1.6 Conclusion

In this chapter the clinical picture of GGEs was presented. Clinical practice and classification of syndromes are well established allowing researchers to easily and unequivocally target patients with a consistent electro-clinical features and a well-defined syndrome. However, there is lack of knowledge of the mechanisms behind variability in treatment outcome which has prevented the improvement of good treatment outcome rate, patient management and health services costs. Given that treatment outcome may be linked with the underlying mechanisms of GGEs itself, in the following chapter I will cover the broad range of knowledge that neuroscience has reached in understanding GGE using neuroimaging in humans.

Chapter 2 : Introduction to Neuroimaging in Genetic Generalised Epilepsy

The importance of neuroimaging to study genetic generalised epilepsy has been fully recognised (Anderson and Hamandi, 2011; Richardson, 2012) given the progress made over the last 20 years in the imaging of the brain in epilepsy. Different techniques, as for example T1-weighted, magnetic resonance spectroscopy (MRS), single photon emission tomography (SPECT), positron emission tomography (PET) and functional magnetic resonance imaging (fMRI) have contributed to enrich with information the current status of knowledge of the disease (Duncan, 2005) underlying how the relationship of structure with function is essential in the understanding of disease aetiology, progression and outcome. In the clinical domain, the Neuroimaging Commission of the International League Against Epilepsy has developed guidelines for the implementation of MRI protocol in epilepsy. The rationale for imaging the brains of patients with epilepsy is first to identify underlying pathologies; and second to assist the formulation of syndrome and etiological diagnoses (Duncan, 2000). However, there are still numerous unknown mechanisms behind epilepsies, particularly GGE. Yet, with the advanced in MR methods and technology, some advanced in knowledge have been achieved. For example, it was long established that brains of patients with GGE do not show radiological abnormalities, but abnormalities in grey matter volume reduction have been identified with more advanced measures (Duncan, 2005). Therefore, further use of

neuroimaging techniques will provide additional information regarding underpinning mechanisms in GGE.

In the following chapter, I will focus on MRI techniques that have contributed to improve current knowledge in GGE, particularly emphasising those applied in this thesis. Those methods are T1-weighted imaging, simultaneous video-EEG-fMRI and arterial spin labelling. Although DTI was acquired in our MRI protocol (Chapter 3, Paragraph3.4), I will not cover the contribution of this MRI technique as no analysis of DTI data is presented in this thesis (Chapter 8, Paragraph 8.4).

2.1 T1 weighted imaging

A T1-weighted image is a standard MRI technique in which differences in the T1 relaxation times of the tissues are used to create the contrast. The computer-based analysis of grey matter from T1-weighted MRI scans can provide estimates of local brain volume, shape and cortical thickness that are indicative of underlying patho-physiological processes (Ashburner et al., 2003). For example, this technique is applied to reveal grey matter malformation and, or, lesions in focal epilepsy (Urbach, 2012). In GGE, although visual inspection of routine MRI in patients appears normal, neuropathological autopsy studies have provided evidence of grey and white matter microdysgenesis (Meencke and Janz, 1984). Therefore, quantitative analysis of structural MRI like T1-weighted image can elucidate subtle changes in the ratio of cortical and subcortical tissues, providing a means of detecting structural changes not normally visible using high-resolution MRI (Sisodiya et al., 1995).

2.1.1 Quantitative measures

Quantitative measures of high-resolution T1-weighted MRI of the human brain provide a powerful tool for characterizing individual differences and abnormalities in brain anatomy. Several methods have been developed to quantify and systematically compare morphological differences in grey matter brain structures.

One of the method most commonly used is voxel-based morphometry (VBM) (Ashburner and Friston, 2000). Typically, VBM involves segmentation of anatomical MRI images into tissue types such as grey matter, white matter and cerebrospinal fluid. Images from each participant are then spatially warped into a common stereotactic space and the gross morphological differences across participants are removed. These pre-processing procedures ensure that the original regional grey matter volume is maintained (Ashburner, 2007). Processed images represent regional grey/white matter volumes or density of each participant and are used for statistical analysis. In most VBM studies the quantity assessed is the local grey matter volume at individual locations (voxels) in the brain (Raz et al., 2005).

Another quantitative method involves the use of an anatomical segmentation procedure for grey matter and statistically measure volumes of specific areas of interest. This method creates masks of the structures that can be additionally used to measure the shape of the selected grey matter structures by providing a local and direct measure of geometric changes (Patenaude et al., 2011).

However, as grey matter volume is a product of thickness and surface area, differences in local grey matter volume can also arise from differences in cortical thickness and variation in surface area due to the folding pattern (Bernhardt et al., 2009). Cortical

thickness and surface area can be independently estimated at each point on the cortical surface using fully automated procedures (Fischl and Dale, 2000; MacDonald et al., 2000; Hutton et al., 2008).

2.1.2 Grey matter changes in GGE

T1-weighted imaging has been used to demonstrate subtle but widespread cerebral structural changes in patients with GGE (Woermann et al., 1998). In fact, studies in humans have shown compelling evidence for thalamic dysfunction and structural abnormality in GGE (Bernasconi et al., 2003; Chan et al., 2006; Pardoe et al., 2008) in which a reduction of the grey matter volume in thalamus, putamen, caudate and globus pallidus was found (Seeck et al., 2005; Bernhardt et al., 2009; Du et al., 2011; Keller et al., 2011; Kim et al., 2013; Saini et al., 2013). VBM studies on cortical grey matter, however, provided conflicting results. While some reported increased grey matter in frontal areas (Woermann et al., 1999; Kim et al., 2007), others found decreased volumes in frontal, parietal, and temporal cortices (Ciumas and Savic, 2006; Tae et al., 2006; Tae et al., 2008; Bernhardt et al., 2009; O'Muircheartaigh et al., 2011a).

Although current genetic evidence supporting that the same inherited factor may give rise to different GGE syndromes in different individuals (Kjeldsen et al., 2003; Dibbens et al., 2009; Helbig et al., 2009; de Kovel et al., 2010), most of the studies looked at heterogeneous GGE syndromes (Savic et al., 2004), therefore it is possible to speculate that inconsistencies in the cortical grey matter structures may underlie differences among syndromes. However, other factors can explain such differences. For example, there is evidence supporting correlations between the status of grey matter and disease durations (Bernhardt et al., 2009; Kim et al., 2013; Saini et al., 2013). Variability in this

parameter may lead to inconsistent results. Moreover, the effects of antiepileptic drug effects on brain atrophy are unclear. Some studies have indicated that antiepileptic drugs can influence nerve morphology, causing changes such as pseudoatrophy of the brain (Papazian et al., 1995; Guerrini et al., 1998a) or neurogenesis (Hao et al., 2004). Therefore, given that in the majority of cases, patients had taken multiple antiepileptic drugs for several years before participating in these studies, medication effects need to be considered in the interpretation of the results together with disease duration.

To date, the effects of disease duration and AEDs on structural changes in the brain have been explored in just two studies. Pulsipher et al. (2001) measured prospective changes in the grey matter volumes in a group of CAE, JAE and JME (together and separated) longitudinally from maximum to 12 months after the diagnoses and to 24 months after the diagnoses for the follow-up. Therefore, for the first time, the experimental design was built to look at prospective rather than retrospective changes in grey matter volumes, and different and homogenous syndromes were considered. However, the effect of AED was not fully controlled as patients were already taking AEDs. Their contribution is still valuable as they found no differences between syndromes in grey matter volumes, but rather consistent changes compared to controls, suggesting commonalities across syndromes. Also, they reported a smaller thalamic volume at follow-up but not at baseline and no differences in the frontal lobe volumes suggesting that effects of disease durations were most prominent in subcortical areas (Pulsipher et al., 2011). Only recently, one study examined grey matter volume in a group of drug naïve CAE finding differences in bilateral thalami before starting treatment (Wang et al., 2016) providing evidence that these structures may show abnormalities independently of

AED. However, this study does not provide proof of prospective changes to AED intake.

The next step is to build a study using the prospective approach as Pulsipher et al. (2011) possibly enlarging the group to other GGE syndromes but using drug naïve patients as in Wang et al. (2016). This will be useful to verify previous results and achieve the gold standard for longitudinal comparisons. Indeed, this was one drive for the foundation of the studies I present in the following thesis.

Overall, to date, the findings all suggests abnormalities in cortico-thalamic structures underlying GGE.

2.2 Simultaneous video EEG-fMRI

Simultaneous video EEG-fMRI is a neuroimaging technique that combines the recording of electroencephalography with functional MRI.

Since its invention (Ogawa and Lee, 1990; Ogawa et al., 1990b; Ogawa et al., 1990a; Kwong, 2012), fMRI has been used to map physiological and pathological BOLD networks during task-based experiments (Cabeza and Nyberg, 2000; Richardson et al., 2006; Price, 2010; Bonelli et al., 2011) and in the resting state (Biswal et al., 1995; Fox and Raichle, 2007).

Functional MRI has a good spatial resolution (millimetres) but low temporal resolution (seconds); particularly when compared to the timescale of epileptic activity which is typically occurring in the range of milliseconds. On the other hand, EEG has good temporal resolution (milliseconds) but low spatial resolution (centimetres). Therefore, the combination of the two techniques has allowed the acquisition of data that has high

spatial-temporal resolution. This technique has been used, and was initially developed to map haemodynamic changes related to epileptic event (Ives et al., 1993; Lemieux et al., 2001). Indeed, the application of EEG-fMRI to study both focal and generalised epilepsies is well established (Rosenkranz and Lemieux, 2010; Gotman and Pittau, 2011; Centeno and Carmichael, 2014). In focal epilepsy EEG-fMRI is typically used to map the irritative zone which is often similar to the seizure onset zone and so can improve the localisation of epilepsy foci (Salek-Haddadi et al., 2006; van Houdt et al., 2013; Centeno et al., 2016). In generalised epilepsy EEG-fMRI has been used to identify the brain networks that are related to GSW in humans (Gotman et al., 2005; Hamandi et al., 2006; Kay and Szaflarski, 2014).

In the following paragraphs I will separately describe both EEG and fMRI techniques before moving on to examine the potential gain in information when the simultaneous combination of the techniques is used to perform what is termed EEG-fMRI. I will then explain how the two signals can be related to each other with a focus on epilepsy.

2.2.1 Electroencephalography recording

Neurons are excitable cells with characteristic intrinsic electrical properties, and their activity produces electrical and magnetic fields. The EEG signals consist of the summed electrical activities of populations of neurons. These fields are recorded by means of electrodes at a long distance from the source (usually at the scalp) using EEG (Speckmann, 2005).

We have two types of neuronal activation. The first is the fast depolarisation and repolarisation of neuronal membranes, known as an action potential which is mediated

by the sodium and potassium voltage-dependent channels. The action potential in a neuron is propagated along axons and dendrites, with no propagation to the extra-cellular space. The second kind of neuronal current is a post-synaptic potential (PSP) and it is related to slow changes (from 15 to more than 200 ms) in membrane potential due to synaptic activity. PSPs may be excitatory (EPSP) or inhibitory (IPSP) potentials. At the level of synapses, in the case of ESPS, the transmembrane current is carried by positive sodium (Na+) ions inwards. In the occurrence of IPSP, negative ions such as chlorine (Cl^-) are carried inwards and positive ions as potassium (K+) outwards. Thus, the positive electric current is directed to the extracellular medium in the case of an EPSP and is directed from the inside of the neuron to the extracellular medium in the case of IPSP (Lopes da Silva, 2010). The two mechanisms are connected as action potentials occur when the neuronal membrane is depolarised beyond a critical level and by depolarising and inducing the same sequence of events in neighbouring membrane, the action potential travels from the axon to the dendrite terminal where the depolarisation releases neurotransmitter from the cell causing the EPSP or IPSP in other neurons (Lopes da Silva, 2005; Speckmann, 2005).

The electrical signals recorded by scalp EEG are the weighted sum of EPSP and IPSP predominantly from the vertically oriented pyramidal cells in the cortex (Lopes da Silva, 2005; Olejniczak, 2006). Indeed, a PSP can sum into an effective current source due to the particular geometry and organisation of cortical pyramidal cells which are arranged parallel to each other, with apical dendrites on one side and soma on the other making these neurons able to receive similar input and response to it with potential changes that produce electrical currents. Due to the head tissue conductor properties, this current

source can be large enough to be remotely recorded by scalp EEG (Niedermeyer, 2005; Speckmann, 2005). For example, IEDs recorded on the human scalp using EEG represent synchronised cortical activity from 6-10 cm2 area of brain (Tao et al., 2005; Ray et al., 2007).

Different distributions of intracerebral sources can result in the same distribution of electrical potentials recorded by the scalp EEG. This is called the inverse problem and it has no unique solution (Lopes da Silva, 2005). Although, currently, there are methods that are attempting to solve the problem by making prior assumptions on the number, geometry, and/or location of the current sources (Lopes da Silva, 2005; Yao and Dewald, 2005), fundamental uncertainty on the origin of the measured signals is introduced (Yao and Dewald, 2005). This and the need of large cortical generators to allow the signal to be detected from the scalp are the main sources of the limited spatial resolution intrinsic to EEG.

2.2.2 fMRI and the BOLD response

During information processing, there is an increase of neuronal activity in parts of the brain allocated for a specific function. This increase in neuronal activity elicits an increase in oxygen and glucose consumption supplied by the vascular system, as a result, the ratio of diamagnetic oxy-haemoglobin to paramagnetic deoxy-haemoglobin changes. The MRI signal recorded in functional imaging measures changes in this microvasculature oxygenation level non-invasively over the entire brain. The relationship between venous oxygenation and the MR signal strength corresponds to

images called Blood Oxygenation Level Dependent (BOLD) images (Ogawa and Lee, 1990; Ogawa et al., 1990a).

The standard time course of the BOLD signal response to a stimulus has been well described and it defines the poor temporal resolution of fMRI. It has been reported that the BOLD signal starts with an initial dip (although this is not always found) and increases about 2s after the neural activity; it then reaches a plateau at about 5-6s post-stimulus. Once the neural activity stops, the signal returns to baseline by around 8s post-stimulus and a transient change referred to as the undershoot then occurs around 8-12s and resolves approximately 20-30s post stimulus (Logothetis et al., 1999). This time course shape has been called the canonical haemodynamic response function (HRF) (Glover, 1999) and can be thought of as the transfer function between neural input and fMRI signal changes.

Physiological correlates to the HRF have been shown. For example, the initial dip in the signal is attributed to the rapid increase in deoxy-haemoglobin (Malonek and Grinvald, 1996; Zhong et al., 1998), although there are controversial findings regarding this initial change (Hu and Yacoub, 2012). The increase in BOLD signal reflects increased blood flow overcompensation for the decreased oxygen due to the oversupply of oxygenated blood. The under shoot reflects changes in blood volume and the decrease in BOLD signal from peak maybe also be reflecting neuronal inhibition (Logothetis et al., 1999; Logothetis et al., 2001; Logothetis and Pfeuffer, 2004; Logothetis and Wandell, 2004).

However, variance of the BOLD response has been observed between subjects and across different brain regions (Aguirre et al., 1998; Buckner, 1998). This has led to revisiting the exclusive use of a standard and completely fixed HRF in fMRI models

where more flexible shapes of the BOLD response have been used instead (Dale and Buckner, 1997; Josephs et al., 1997; Friston et al., 1998; Bagshaw et al., 2004). This is the case of fMRI studies using pathological features where the effect of interest to be modelled is treated as if it was a 'stimulus', such as epileptic EEG features in epilepsy studies (Jacobs et al., 2008; Storti et al., 2013). This is particularly relevant for the analysis presented in the following chapters where we used a more flexible model of BOLD responses as introduced in Chapter 5, Paragraph 5.2.4. This is consistent with a reduced certainty regarding the nature of the responses to epileptic events.

2.2.3 BOLD effect and neuronal activity

Over the last decade, efforts have been made to understand the exact relationship between the haemodynamic changes recorded with fMRI and the neuronal activity recorded with EEG. It has been found that the BOLD signal reflects the firing of neural populations as a correlation exists between the BOLD amplitude and Multi Unit Activity (MUA)[1]; however the strongest correlate was the local field potential (LFP)[2] data in anesthetised (Logothetis et al., 2001) and awake (Goense and Logothetis, 2008) monkeys.

The contribution of LFP activity to the BOLD signal has also been supported by autoradiography studies of the energy consumption underlying neuronal signals (Jueptner and Weiller, 1995). As for example, measures of the energy budgets required

[1] MUA reflects the weighted sum of the output signal of a neuronal population within a radius of 50-350 microns (Legatt AD, Arezzo J, Vaughan HG (1980) Averaged Multiple Unit-Activity as an Estimate of Phasic Changes in Local Neuronal-Activity - Effects of Volume-Conducted Potentials. Journal of neuroscience methods 2:203-217.).

[2] "*The local field potential is the extracellular current flow that reflects […] the linearly summed postsynaptic potentials from local cell groups*" (Buzsaki G (2004) Large-scale recording of neuronal ensembles. Nat Neurosci 7:446-451.)

for different processes have shown that post-synaptic effects of glutamatergic neurons (glutamate recycling) accounts for 74% of the brain energy consumption (Attwell and Laughlin, 2001; Lennie, 2003).

The sustained BOLD increases (Logothetis and Wandell, 2004) and decreases (Shmuel et al., 2002) for a particular stimulus or task can be conceptualised to reflect a balance between local neuronal excitation and inhibition (Lauritzen, 2005). Although there are still uncertainty regarding the relationship between direct and indirect inhibitory activity and changes in metabolic energy consumption (Logothetis, 2008), there is evidence supporting that increases in synaptic inhibition is likely to reflect decreased BOLD response (Logothetis, 2008) and that negative BOLD response seems to reflect neural activity decreases (Shmuel et al., 2006; Devor et al., 2007).

Accordingly, data in humans suggest that in conditions where mainly inhibitory circuits are involved, inhibition and negative BOLD responses could be detected (Shmuel et al., 2002; Stefanovic et al., 2004; Pasley et al., 2007). Current understanding is thus that synaptic activity related to PSP leads to observe a positive BOLD response; but a decrease in the same neural activity leads to a negative BOLD response (Shmuel et al., 2002; Shmuel et al., 2006; Devor et al., 2007; Carmichael et al., 2008).

From current evidence, it is clear that there is a strong coupling between the haemodynamic changes and neuronal signals (Logothetis and Pfeuffer, 2004) during visual and or motor tasks (Shmuel et al., 2002; Stefanovic et al., 2004). In particular, the coupling was not seemingly altered during neurological activity such as epileptic activity (Stefanovic et al., 2005; Carmichael et al., 2008).

2.2.4 Recording EEG inside MRI scanner

Combining EEG and MRI together raises challenges for EEG data quality and patient safety. Following well-established set-up procedure of the EEG in the MR environment, both EEG quality and patients' safety can be ensured.

2.2.4.1 Safety and data quality considerations

Scalp EEG recording inside the scanner requires the electrodes and leads to be placed within the imaging field of view (FOV) which can result in possible interactions between the magnetic fields of the scanner and metal electrodes. The main sources of artefact on EEG recorded inside the scanner are the strong static magnetic field, switching magnetic fields gradient, electrical and magnetic components of radio frequency (RF) pulses, cardiac pulse-related and head and body movements within the static magnetic field. Any change in magnetic flux over time through a conducting medium (loop, surface, volume) can produce an induced current. This change in magnetic flux and the induced current can be caused by movement (i.e. change of position, orientation or shape) of the conducting medium in a magnetic field or due to a change in the magnetic field to which the conducting medium is exposed (i.e. MRI gradient switching and RF pulses). This can cause additional health hazards and EEG quality degradation in the form of EEG artefacts related to image acquisition (Lemieux et al., 1997; Goldman et al., 2000; Konings et al., 2000; Krakow et al., 2000a; Krakow et al., 2000b; Lemieux et al., 2001; Benar et al., 2003; Laufs et al., 2008).

An important safety consideration to reduce the risk of heating is to limit the RF power exposure. This can be done by only using low RF power MRI sequences when the EEG cap is used. To avoid RF antenna effects, the length of wires (exposed to the electrical

component of the field) has to be as short as possible and their path avoids regions of high electric RF field. (Lemieux et al., 1997; Goldman et al., 2000; Konings et al., 2000; Krakow et al., 2000a; Krakow et al., 2000b; Lemieux et al., 2001; Benar et al., 2003; Laufs et al., 2008).

Current commercially available MR-compatible EEG system, as used by most of the EEG-fMRI studies in epilepsy to date (i.e. http://www.brainproducts.com) (Hamandi et al., 2006; Laufs et al., 2006; Moeller et al., 2008a; Gotman and Pittau, 2011; Centeno et al., 2016), provides customised electrode caps. In this MR-compatible scalp EEG system, an extra 10 kΩ current-limiting resistor is used in each electrode lead and electrode leads are twisted in a bundle which has been designed to reduce the possibility of forming large loops between subject's head, electrode, electrode lead and EEG amplifier. This is aimed at preventing health hazards from induced currents in the loops causing heating of EEG components in contact with the subject.

Additional safety guidelines are provided, as for example, regarding EEG cap preparation. Indeed, it is recommended to have low impedance (≤10 kΩ) to guarantee good safety and artefact characteristics. The amount of conductive agent between electrodes and scalp should be minimised to avoid forming bridges between electrodes and the wires connecting the cap to the EEG recording system needs to be secured in place by sand bag to avoid vibration and or formation of loops (Lemieux et al., 1997; Laufs et al., 2008).

2.2.4.2 EEG-fMRI setup

The signal recorded by EEG electrodes is relayed to the EEG recording amplifier through wires. Currently, with the availability of MR-compatible equipment, the EEG

signals are amplified and digitised within the scanner room using MR-compatible amplifiers and passed to the recording equipment, outside of the electro-magnetically shielded room, through optical fibres. In the recording suite, the EEG clock is synchronised with the MRI clock to allow perfect simultaneous recording and to improve scanner artefact removal from EEG (Mandelkow et al., 2006; Laufs et al., 2008).

2.2.5 EEG-fMRI networks in GGE

The first study by Salek-Haddadi and colleagues (Salek-Haddadi et al., 2003) using simultaneous EEG-fMRI has described two patterns of BOLD changes during absence seizures in a single patient: BOLD increases bilaterally in thalamic nuclei, and widespread and symmetrical decreases in the cortex, maximum in the frontal lobes. Subsequently, group studies of GGE patients (Aghakhani et al., 2004; Gotman et al., 2005; Hamandi et al., 2006; Moeller et al., 2010a) also revealed common patterns of BOLD decrease in the frontal and parietal cortices, posterior cingulate and precuneus, and predominant BOLD increase in the thalamus and medial frontal region.

2.2.5.1 GSW-related brain networks significance

Areas involved in GSW related cortical BOLD decrease resemble the default mode network (DMN) which is found active in healthy control during rest (Raichle et al., 2001). It can be argued that the BOLD signal decreases in these areas, in relation to GSW, represents the physiologic suspension of conscious rest or an fMRI signature of the negative clinical phenomenology of absences during which cognitive processes may be impaired (Laufs et al., 2006). However, another valid argument refers to the idea that

DMN deactivation is an epiphenomenon related to the brain state during the recording rather than strictly related to GGE (Archer et al., 2003; Aghakhani et al., 2004; Gotman et al., 2005). Current evidence is lacking to determine which potential explanation is correct; Chapter 6 explores this issue further.

Further evidence regarding the direct involvement of the thalamic-cortical network in GGE comes from animal models (Danober et al., 1998) and studies in humans using other technique such as transcranial Doppler, H2(15)O PET (Prevett et al., 1995; Diehl et al., 1998) and invasive recordings (Avoli and Kostopoulos, 1982; Avoli et al., 2001).

To summarise, although there are still open questions regarding the direct role of DMN in GGE, it has been proven that the cortico-subcortical/striato-cortico-thalamic network is associated to GSW in patients with GGE.

2.2.5.2 GSW duration effect and BOLD signal

Although GSW have stereotypical features of 3Hz frequency discharges, their durations vary across events. Evidence showed that BOLD changes were in the same brain areas for shorter (< 3s) and longer (> 3s) bursts of GSW in 3/4 cases and one case did not reveal any BOLD changes for shorter discharges but diffuse response for long bursts (Aghakhani et al., 2004). On the contrary, it has been discussed that BOLD changes were of greater magnitude (Carney et al., 2010) and more frequent in the thalamus (Hamandi et al., 2006; Li et al., 2009) when GSW were of longer duration (suggesting the presence of seizures) and higher in number. This may be explained by a simple signal to noise ratio phenomena or may reflect the role of thalamus in maintaining the GSW (Avoli et al., 2001) for longer duration discharges which is reflected in stronger thalamus BOLD changes. A recent study reported a linear relationship between GSW

duration and BOLD response identifying that a larger amplitude BOLD response was associated with longer GSW. However, the same thalamic-cortical and DMN were found associated with short and long GSW across different GGE syndromes (Pugnaghi et al., 2014). Given that this relationship was found significant with GSW of a range duration of 0-5.2s and that the conventional and pragmatic definition of the interictal state required the presence of GSW < 3s (Goode et al., 1970), these results provide evidence for the involvement of the same brain networks during ictal and interictal states in GGE.

2.2.5.3 BOLD changes before GSW onset

Recent studies tried to evaluate the dynamics of GGE to understand if there is a signature prior to GSW events that might elucidate the mechanisms of seizures generation and transition between inter-ictal and ictal states (Petkov et al., 2014; Schmidt et al., 2014). Animal models of absence seizures reported BOLD changes prior to GSW onset showing changes in concentration of oxy/deoxy-haemoglobin (Roche-Labarbe et al., 2010). Invasive recordings in rats also identified that low frequency activity in the delta range was predictive of GSW onset. This activity was measured first in the cortex and next from the thalamus (van Luijtelaar et al., 2016).

GLM based data analysis of EEG-fMRI have also evaluated the presence of activity prior to the electrophysiological onset of GSW and earlier studies found that BOLD increases peaked earlier than BOLD decreases (Aghakhani et al., 2004; Moeller et al., 2008a; Bai et al., 2010). Different results have been presented by different studies in which both positive and negative responses were reported in the same brain areas. In fact, by modelling the HRF before the EEG onset of GSW in the GLM framework

(Moeller et al., 2008b) the temporal pattern of BOLD changes was different from a canonical response. By investigating the mean time course of GSW-related haemodynamic changes, it was shown that BOLD increased in the thalamus (Moeller et al., 2008b), parietal cortex and precuneus (Carney et al., 2010) before GSW onset. In contrast, the thalamus was mostly found activated at GSW onset only (Carney et al., 2010; Kay and Szaflarski, 2014) and the BOLD changes in various anatomical areas such as thalamus, cortex and caudate, were dynamic (evolving at different time points) throughout the duration of absence seizure rather than static (Moeller et al., 2010b). BOLD increases in frontal cortex preceding GSW onset and followed by BOLD decreases in the same areas lasting after GSW have also been reported (Bai et al., 2010). This is important because it suggests that BOLD responses to GSW are not canonical and that they may precede EEG changes which suggest there is a hemodynamic signature of the transition to the GSW before they occur electrographically. Further discussion on this issue is presented in Chapter 5.

The inconsistency of the temporal evolution of GSW related BOLD changes in GGE may result from variable modelling strategies applied (Moeller et al., 2008b; Bai et al., 2010), different types of epileptic discharges (polyspikes and waves and GSW) (Pillay et al., 2013), biological differences between adults (Benuzzi et al., 2012) and children (Moeller et al., 2008b), genetic and phenotypic heterogeneity of individuals (Bai et al., 2010; Carney et al., 2010), and of our main interest, treatment outcome (Szaflarski et al., 2010) and treatment intake (Szaflarski et al., 2013).

Although more studies need to be conducted to resolve the inconsistency across the results presented, evidence reporting focal BOLD increases in cortex prior to GSW

electrophysiological onset (Bai et al., 2010; Carney et al., 2010; Benuzzi et al., 2012) is consistent with the theory that seizures in GGE have a focal cortical initiation (Koepp, 2005; Meeren et al., 2005; Vaudano et al., 2009; Westmijse et al., 2009; van Luijtelaar et al., 2014) which would, if true, challenge the current approach to classification of epilepsy.

2.3 Arterial Spin Labelling for pharmacological studies

Arterial spin labelling (ASL) is a perfusion MRI sequence that uses radiofrequency pulses to magnetically label the water molecules in the subject's own arterial blood, usually at the base of the brain. The magnetically labelled blood water is then used as an endogenous tracer for the measurement of CBF, which has a half-life (determined by blood T1), on the order of 1s to 2s. The effects of ASL are measured by comparing images acquired with active or control labelling, and this signal difference is used to non-invasively quantify CBF (Buxton et al., 1998b; Buxton et al., 1998a).

In focal epilepsy, the use of ASL has been limited to identifying seizure onset zone (Pizzini et al., 2008; Storti et al., 2014), and in studying metabolic abnormalities related to interictal activity (Wolf et al., 2001; Lim et al., 2008; Pizzini et al., 2013).

In GGE, ASL was implemented in combination with simultaneous EEG-fMRI to examine the relationship between CBF and BOLD measurements in pathological condition. This is important for interpreting studies using fMRI given the interconnected relationship between neuronal activity and oxygenation, the basis of the BOLD signal (Ogawa et al., 1990b; Hoge et al., 1999; Stefanovic et al., 2005). A positive correlation between BOLD changes and CBF irrespective of the sign of BOLD change was

reported. Particularly, this association was found to be stronger during GSW than during background activity suggesting preserved (i.e. within normal limits) neurovascular coupling (Carmichael et al., 2008; Hamandi et al., 2008).

However, all these analyses were performed in patients under the influence of AEDs. Given the alteration in CBF after drug intake (Bartenstein et al., 1991; Gaillard et al., 1996; Spanaki et al., 1999; Joo et al., 2006), further analysis needs to disentangle the association between CBF alteration, BOLD response alteration and AED effects. Because of the lack of absolute quantification and poor reproducibility over time scales longer than hours or across scanning sessions, BOLD fMRI may not be suitable to track long-term drug effects on baseline brain function. An alternative and non-invasive method is therefore ASL which provides absolute quantification of cerebral blood flow both at rest and during task activation. ASL perfusion measurements have been shown to be highly reproducible over minutes and hours to days and weeks. These two characteristics make ASL an ideal tool in pharmaco-MRI for studying both intravenous and oral drug action as well as understanding drug effects on baseline brain function and brain activation. When ASL is combined with BOLD fMRI, drug-induced changes in cerebral metabolic rate of oxygen can also be inferred (Wang et al., 2011).

2.4 Anti-epileptic medication effect

All the studies presented in the previous paragraphs included patients who were already taking antiepileptic medication (monotherapy and/or polytherapy) for various lengths of time. Treatment outcome was mostly unknown or unreported.

There is no clear understanding of the effects that AEDs have on the measures of the brain we are acquiring with neuroimaging techniques. There is evidence supporting differences in BOLD signals in patients responding and not responding to VPA (Szaflarski et al., 2013) but the effects that VPA has on cortical excitability is still unclear (Reutens et al., 1993; Cantello et al., 2006). Further evidence has indicated that antiepileptic drugs can influence nerve morphology, causing changes such as pseudo-atrophy of the brain (Papazian et al., 1995) or neurogenesis (Hao et al., 2004). Alteration in CBF after drug intake has been reported (Bartenstein et al., 1991; Gaillard et al., 1996; Spanaki et al., 1999; Joo et al., 2006) supporting that an alteration of neuronal functioning related to AEDs might influence BOLD findings.

There are numerous studies recording cortical excitability with TMS in patients who were naïve to AEDs (Cantello et al., 2006; Badawy et al., 2007; Joo et al., 2008b; Badawy et al., 2009; Badawy et al., 2010). They reported that cortical excitability is reduced after the administration of AED (Joo et al., 2008b) only in patients responding to treatment but not in those who are not responding (Badawy et al., 2010) casting light on possible treatment outcome measures and measures which relate to AED exposure.

The field of neuroimaging lacks this information despite the importance of AED effects measure to understand the origin, the evolution and potential treatment outcome of the disease. To my knowledge, only two studies used EEG-fMRI to investigate GSW related BOLD response in drug naïve patients (Moeller et al., 2008a; Li et al., 2009), two studies recorded MEG data (Tenney et al., 2013; Miao et al., 2014), one study measured regional cerebral blood flow with SPECT (Joo et al., 2008a), one study looked

at white matter integrity (Yang et al., 2012) and one explored grey matter volume (Wang et al., 2016).

Although their results reported an involvement of thalamic-cortical areas (in agreement with the findings reported in treated patients), the number of studies and especially the number of patients reported in each study are too small to allow definitive conclusions. Moreover, no follow-up comparisons were made to relate findings to treatment outcome.

The work presented in the following chapters was conceived to address this need of providing measures from drug naïve patients in which there is no AED effects and prospective longitudinal outcome information.

2.5 Data quality

Combined multimodal measurement is generally prone to data quality degradation due to interactions between the recording instruments such as EEG and fMRI. Here, I discuss these issues in some detail.

2.5.1 EEG-fMRI specific artefacts

EEG recordings inside an MRI scanner are obscured by gradient artefact (GA) and pulse artefact (PA) or ballistocardiographic (BCG). The GA is produced by the rapidly changing magnetic field used for fMRI acquisition and is superimposed on the EEG signal making it uninterpretable (Allen et al., 2000). Current equipment with sufficient bandwidth, sampling rate (1-20 KHz) and dynamic range (~20 mV) can capture the artefact in detail, allowing its removal, and significantly improve the quality of EEG recorded inside the scanner (Laufs et al., 2008; Mulert, 2010).

Different methods are available for GA correction: frequency domain method (Hoffmann et al., 2000), average image artefact subtraction, average image artefact subtraction and adaptive noise cancellation (Allen et al., 2000) and principal component analysis (PCA) (Negishi et al., 2004; Niazy et al., 2005). To date the most commonly used method is average image artefact subtraction and adaptive noise cancellation (Allen et al., 2000), which is used both for online and off-line EEG artefact removal. This works on the basis of the principle that physiological signals and the GA are not correlated and the gap between acquired volumes and slices and the pattern of the GA remains stable. As a result, the GA is estimated and removed by averaging the EEG over a number of epochs corresponding to individual volume (Allen et al., 2000) or slice (Niazy 2005) repetitions.

BCG artefact results from the pulsatile movement of the head and scalp due to blood vessel expansion in relation to the cardiac cycle which results in induced voltages (artefacts) in the EEG recording circuit (Debener et al., 2008), head rotation originating from blood momentum transfer into axial body motion (Bonmassar et al., 2002), and Hall[3] voltages arising from the flow of conductive blood in the magnetic field (Yan et al., 2010). BCG artefact may make the identification of epileptic events difficult in some patients, especially for focal discharges. Here again methods based on the average artefact subtraction principle (Allen et al., 1998) are the most commonly applied technique for removing the BCG artefact. Other methods include applying adaptive

[3] When an electric current flows through a conductor in a magnetic field, the magnetic field exerts a transverse force on the moving charge carriers which tends to push them to one side of the conductor. A build-up of charge at the sides of the conductors will balance this magnetic influence, producing a measurable voltage between the two sides of the conductor. The presence of this measurable transverse voltage is called the Hall effect after E. H. Hall (Hall EH (1879) On a new action of the magnetic on electric currents. Am J Math 2:287-292.

filtering (Bonmassar et al., 2002), weighted average subtraction (Goldman et al., 2000), median filter template (Ellingson et al., 2004) or independent component analysis (ICA) (Srivastava et al., 2005). All these methods have been validated in a number of studies and provide adequate solutions although methods to improve the quality of EEG inside the scanner are under continuous development (LeVan et al., 2013; Maziero et al., 2016). Despite these improvements, it is a common view that a certain degree of loss of EEG data quality cannot be avoided (Debener et al., 2007; Debener and Herrmann, 2008; Debener et al., 2008).

2.5.2 Motion artefacts

The imaging sequence mostly used for simultaneous EEG-fMRI is gradient echo-planar imaging (EPI) which is prone to distortion and local signal dropout (Krakow et al., 2000b). Artefacts produced in the imaging data due to electromagnetic interference can be minimised by proper selection, design and placement of EEG recording equipment as introduced in Paragraph 2.2.4.

However, head motion is unavoidable, especially in paediatric population (i.e. drug naïve CAE), together with intrinsic pulse and respiration related motion artefacts. Methods to reduce and correct for this are needed. Currently, one practical way to diminish head motion is the usage of vacuum cushion that braces the head limiting motions.

The effect of motion on fMRI is tackled using available off-line motion correction methods. One of the most commonly used is implemented in the SPM framework and calculates rigid-body realignment of the image data and provides motion-related

nuisance regressors that are included as nuisance covariates in GLM analyses (Friston et al., 1996; Ashburner J, 2012a). From this method, other nuisance regressors have been implemented to improve motion and physiological artefact suppression. For example, a vector with values of volumes with gross movements that are discarded from the analysis (Lemieux et al., 2007; Power et al., 2012) and extra physiological noise regressors (Chaudhary et al., 2012a). However, these approaches required the inclusion of several numbers of regressors and while extra explanatory regressors can increase specificity, it should be noted that they can also dramatically reduce sensitivity by reducing the amount of degrees of freedom (Friston et al., 1999). Therefore, another method that creates a mask of the total displacement (motion fingerprint) at each voxel per subject and generates a synthetic time series individually for each subject was implemented (Wilke, 2012) to try to ameliorate the statistical power for single-subject and group analyses. However, these methods rely on the realignment for providing motion measurements which have been shown to be a poor representation of subject movement in some circumstances (Beall and Lowe, 2014).

In addition, in common across all these methods is the focus on global corrections which leads to the assumption that any motion/noise would affect the whole brain. Therefore, in the case of data scrubbing, this would mean for example the removal of 35%-39% of the total amount of volumes acquired when scanning a paediatric population (Power et al., 2012). Given that it has been proven that local changes in the data would not affect the entire volume (Tierney et al., 2016), a new method for noise correction that corrects local changes called FIACH will be applied in this thesis. It is a newly implemented prospective and automated motion and physiological-noise correction method designed

for paediatric population but applicable to adult populations. This method provides a local assessment and correction of non-physiological fMRI signal changes and a parsimonious model of noise (e.g. motion, cardiac and respiration changes) from the data. The advantages of this approach are the ability to correct local changes due to fast motion, discarding only the noisy data-point via the interpolation of the nearest noise-free corresponding data and a model of physiological noise and motion which does not dramatically alter the degrees of freedom. These have been proven to increase statistical power during movement in particular recovering changes in problematic areas for fMRI such as temporal poles and the hippocampus (Tierney et al., 2016).

Motion artefact affects structural imaging as well, provoking misclassification of tissues and preventing from correct segmentation of the structures. This leads to reduced volume or cortical thickness estimates and reduce reliability (Reuter et al., 2015). To date, the most common approach applied in the literature is the visual inspection of the MR images and consequent qualitative assessment of the image. If corrupted, then the data are removed from the analysis.

2.6 General consideration

It is evident, from previous paragraphs, that we have reached an advanced stage in using neuroimaging to study GGE. However, there are some gaps in our knowledge that need to be addressed to reach a more comprehensive understanding of GGE. In this thesis I will be focussing on three.

I am particularly interested in AED effects. By imaging the brain of newly diagnosed and AED free patients, previous findings can be interpreted without the potential

influence of AEDs and cement the current knowledge. Therefore, I will answer the question: do the neuroimaging results in drug naïve patients replicate those reported in patients on treatment?

I will explore treatment effects as follow:

- Measuring grey matter volume and shape in drug naïve patients (Chapter 4).
- Measuring BOLD changes related to GSW in drug naïve patients at GSW onset and pre-GSW. This will explore not only spatial EEG-fMRI models but it will add knowledge regarding temporal aspects of the signal changes to examine evidence for the focal onset theory and a pre-ictal state (Chapter 5).

Secondly, there is a missing prospective approach. Most of the treatment outcome and disease duration effect evidence is from retrospective data. By following patients longitudinally from pre-treatment to post-treatment we aim to answer questions related to treatment response and find markers of treatment outcome prior to treatment in the long-term.

I will apply a prospective/longitudinal approach as follow:

- Grey matter volume and shape will be compared between drug naïve pre-treatment and post-treatment and between drug naïve responding and not responding patients to identify baseline differences following treatment outcome (Chapter 4).
- Global CBF will be measured before treatment intake and after treatment intake to identify changes that may be linked with BOLD changes post-treatment (Chapter 7).

Thirdly, I am interested in disentangling the relationship between brain networks related with GSW and brain state given that most of the current studies performed EEG-fMRI during resting state. Therefore I will answer these questions: What is the relationship with GSW related brain network in a situation different from rest? And, what is the role of the DMN?

I will then explore the effect of brain state as follow:

- BOLD response of GSW recorded during period of rest and during a low demand task will be compared (Chapter 6).

2.7 Conclusion

The state of knowledge in GGE is advanced, however multimodal imaging needs to provide missing and complementary knowledge regarding treatment effects in GGE via the study of drug naïve patients. Longitudinal follow-up of these patients will contribute in exploring how baseline measures pre-treatment can disentangle possible treatment outcome measures. Functional brain states different from rest will also help in understanding roles of GSW related brain networks. In the following chapters I present work that I have performed to explore this. I will present results from the data I have obtained in drug naïve patients newly diagnosed with CAE, JAE, GTCSO and JME and their longitudinal follow-up using multimodal imaging.

SECTION 2: GENERAL METHODS

Chapter 3 : METHODS

In this chapter I describe the experimental methods commonly used for the empirical studies I will present in chapters 4, 5, 6 and 7.

The experimental methods were specifically designed to achieve the highest data quality taking into consideration a paediatric population.

3.1 Recruitment

The targeted population included 15 drug naïve AE patients, 15 drug naïve JME/GTCSO patients, 30 age matched controls, 5-10 refractory AE patients, 5-10 refractory JME/GTCSO patients.

Drug naïve patients' inclusion criteria: i) diagnosis of GGE made by an epilepsy specialist based on clinical decision following examination; ii) normal cognitive development from age 6 to allow MRI scan without sedation. Exclusion criteria: i) history of any neurological condition other than epilepsy; ii) history of brain active drug intake (i.e. drug or alcohol misuse and active brain prescribed medications).

Refractory patients' inclusion criteria: i) diagnosis of GGE made by an epilepsy specialist based on clinical decision following examination; ii) on treatment for at least 1 year and continuing to have seizures; iii) cognitive age from age 6 to allow MRI scan without sedation. Exclusion criteria: i) history of any neurological condition other than epilepsy; ii) presence of seizures occurrence as a consequence of drug/alcohol misuse and/or following not appropriate AED intake.

Healthy controls inclusion criteria: i) cognitive age from age 6 to allow MRI scan without sedation. Exclusion criteria: i) history of brain active drug intake (i.e.: drug or alcohol misuse, active brain prescribed medications); ii) medical history of any neurological/neurodevelopmental conditions; iii) family history of epilepsy in a first degree relatives.

All participants had minimum age of 5.9 years; no upper age limit was set. All participants were included if they did not present any contraindication of having MRI. Patients were identified by the treating clinicians in clinics across London (King's College Hospital NHS Foundation Trust, Great Ormond Street Hospital for Children NHS Foundation Trust, University College London Hospitals NHS Foundations Trust, Barnet and Chase Farm Hospitals NHS Trust, Lewisham and Greenwich NHS Trust, East Kent Hospital University NHS Foundation Trust, Maidstone and Tunbridge NHS Trust, Barts Health NHS Trust, Guy's and St Thomas' NHS Foundation Trust, Croydon Health Service NHS Trust, Royal Free Hampstead NHS Trust) and via screening neurophysiological reports at King's College Hospital and Evelina London Children Hospital.

In order to study patients while drug naïve, the timing of recruitment was crucial given that our intervention had to fit between the first declaration of the diagnosis to patients/families and the start of AED. Therefore, patients were approached in different ways based on advice from the clinical team. Going from the least common to the commonest strategy: i) the clinical team contacted us with names and contact details after having explained the project to the patient and obtained consent from him/her/family to be contacted by us; ii) patient was identified by us in the EEG

department. We then contacted the clinical team with names and project information and the clinical team discussed the project with the patient/family in clinic and obtained consent to be contacted by us. Following notification of the consent from the clinical team, we contacted the patient; iii) patient was identified by us in the EEG department. We then contacted the clinical team with names and we attended the clinic on the day of the appointment with the named patient to discuss the project directly with his/her/family.

An appointment within 5 working days from the day of the diagnosis was provided to all the drug naïve patients to avoid treatment delay.

Refractory patients were identified from clinic lists from King's College Hospital (KCH), Evelina London Children Hospital and Great Ormond Street Hospital (GOSH). As this sample did not need to be scanned urgently, their study visit was arranged at a convenient time.

Healthy controls from age 18 were identified using advertisement on King's College London Research Volunteer Recruitment Webpage. Healthy controls from age 6 to 18 were identified via advertisement on the Great Ormond Street Hospital webpage in collaboration with an ongoing project funded by Action Medical Research, led by Dr David Carmichael and Dr Maria Centeno.

The study took place in two centres: King's College Hospital and Great Ormond Street Hospital, London, UK. Individuals were allocated to be studied in one centre or the other on the basis of age and syndrome. Patients (drug naïve and refractory) with a diagnosis of AE and healthy controls from age 5.9 to about 14 were invited to GOSH for the study. Patients (drug naïve and refractory) with a diagnosis of JME/GTCSO and

healthy controls from about age 14 were invited to come to King's College Hospital. This allocation of subjects was based on child oriented facilities available at Great Ormond Street Hospital.

All subjects having legal age of 18 gave informed, written consent. One parent or the nominated legal carer gave informed and written consent on behalf of the participant below the age of 18. The study was approved by the Riverside Research Ethics Committee (REC approval number 12/LO/2006). The study from which we shared the healthy control children population was approved by the London-Surrey Border Research Ethics Committee.

3.2 Prospective longitudinal approach

We designed the experiment longitudinally to allow comparisons related to AED changes. Drug naïve patients were invited for the first visit before starting treatment and for a second visit after six months since the first drug intake. The same experimental protocol was applied for both visits. Six months' time for the repeated measure was decided accordingly as the minimum clinical time needed to judge treatment outcome. Throughout the manuscript, I will refer to drug naïve for scan time 1 and post-treatment for scan time 2.

Healthy control and refractory subjects were studied only once as the experimental design was built to compare pre and post-treatment with healthy control and refractory groups.

3.3 Subjects

We acquired data in 16 drug naïve patients diagnosed with AE and in 15 drug naïve patients diagnosed with JME/GTCSO (3 drug naïve of JME/GTCSO presented only GTCS at the drug naïve stage). For simplicity, this group will be referred as JME only through the thesis. The number of patients recruited was different in the AE group compared to the original target and to the JME group. This was due to the greater proportion of drug naïve patients diagnosed with AE in clinics. Most of the JME we encountered had a history of epilepsy in their past; therefore, they were not classified as drug naïve. 54.8% (17 patients) of all the drug naïve patients came back for the post-treatment scan. Among this group, 62.5% (10 patients) were diagnosed with AE and 46.6% (7 patients) diagnosed with JME. In regards to the patients who did not come for the follow-up, 64.2% (9 patients) decided not to start treatment, 7.1% (1 patient) got pregnant and decided to stop treatment, 21.4% (3 patients) are currently still waiting to start treatment due to clinical delay.

We acquired data in 9 refractory AE patients and in 9 refractory JME patients. We acquired a total of 42 healthy controls, 21 children below age 18 and 21 adults/adolescents from age 17. Demographics of the sample are listed in Table 3.1.

Table 3.1: Demographic characteristics of the sample.

GROUP	CODE	GENDER	AGE	AGE AT SEIZURE ONSET	AED
DRUG NAÏVE AE	#1	M	6.03	6	/
	#2	M	14.00	5	/
	#3	M	10.51	10	/
	#4	M	6.37	6	/
	#5	M	10.58	10	/
	#6	F	13.65	13	/
	#7	M	8.03	8	/
	#8	F	7.73	7	/
	#9	M	10.28	10	/
	#10	F	9.72	9	/
	#11	F	16.18	6	/
	#12	M	7.15	7	/
	#13	M	9.26	9	/
	#14	M	5.92	5	/
	#15	M	6.84	6	/
	#16	F	13.50	13	/
POST-TREATMENT AE	#3b	M	11.49	AS ABOVE	LMT 47.5 mg BD
	#5b	M	11.30		unknown
	#6b	F	14.21		ETX 250

					mg AM+500 mg PM
	#7b	M	8.54		VPA (dose unknown)
	#8b	F	8.25		VPA 300 mg BD
	#9b	M	10.77		VPA 500 mg AM+100 mg PM
	#11b	F	16.78		ETX (dose unknown)
	#13b	M	9.78		ETX 200 mg BD
	#14b	M	6.43		VPA (dose unknown)
	#15b	M	7.56		VPA 500 mg + LMT 10 mg BD
REFRACTORY AE	#17	M	8.60	4	VPA + ETX
	#18	F	12.33	~6	ETX 650 mg + TPM 50 mg BD
	#19	M	10.45	2.5	LMT 150 mg + LEV 750 mg BD
	#20	M	8.34	4	VPA + ETX (dose unknown)
	#21	F	13.12	4/5	VPA 700 mg BD
	#22	F	9.66	4.5	LMT 100 mg AM + 125 mg PM
	#23	F	9.93	6/7	LMT 25 mg BD
	#24	F	7.00	2	LMT 50 mg + VPA 300

					mg BD
	#25	M	10.98	2.5	ETX 700 mg + CBZ 7.5 mg BD
CONTROL CHILDREN	#26	M	14.08	N/A	N/A
	#27	F	9.72		
	#28	F	13.62		
	#29	F	15.59		
	#30	F	18.08		
	#31	M	8.34		
	#32	F	16.73		
	#33	F	8.32		
	#34	F	9.08		
	#35	M	6.61		
	#36	M	12.00		
	#37	F	12.14		
	#38	F	9.08		
	#39	M	10.32		
	#40	F	8.85		
	#41	M	14.20		
	#42	M	7.50		
	#43	F	7.23		
	#44	F	14.22		
	#45	F	12.67		

	#46	F	9.58		
DRUG NAÏVE JME	#47	M	21.71	21	/
	#48	M	16.75	16	/
	#49	F	16.58	16	/
	#50	F	13.64	13	/
	#51	F	20.11	20	/
	#52	M	35.98	16	/
	#53	F	15.38	15	/
	#54	F	17.69	17	/
	#55	F	26.04	26	/
	#56	M	14.44	14	/
	#57	F	25.94	25	/
	#58	F	31.23	31	/
	#59	F	16.46	16	/
	#60	M	20.86	20	/
	#61	F	19.18	19	/
POST-TREATMENT JME	#47b	M	22.95	AS ABOVE	VPA 600 mg BD
	#50b	F	14.14		LMT 100 mg BD
	#51b	F	20.78		LEV 250mg BD
	#52b	M	36.44		VPA 500 mg BD
	#54b	F	18.26		(treatment unknown)
	#56b	M	14.94		VPA 500 mg

	#57b	M	26.48		LMT 150 mg
REFRACTORY JME	#62	F	18.18	14	LEV, LMT (dose unknown)
	#63	F	22.18	18	LMT (dose unknown)
	#64	M	39.10	28	LEV 500 mg BD
	#65	M	40.06	8	VPA 1500 mg BD
	#66	M	21.39	7 (AE), 14 (GTCS)	VPA 1500 mg BD
	#67	M	20.69	16	VPA 1200 mg + LEV 1000 mg BD
	#68	F	22.33	Jerks since young age, 15 GTCS	LMT 1000 mg + LEV 1250 mg BD
	#69	F	30.86	7 AE, 15 GTCS	VPA 600 mg + LEV 1250 mg BD + parampanel 2 mg alternate PM only
	#70	M	40.84	15	VPA 500 mg BD
CONTROL ADOLESCENTS/ ADULTS	#71	F	23.89	N/A	N/A
	#72	F	20.28		
	#73	M	24.98		
	#74	F	25.64		
	#75	M	22.26		

	#76	M	23.00
	#77	F	25.14
	#78	F	23.34
	#79	F	22.85
	#80	F	20.47
	#81	M	21.09
	#82	M	21.28
	#83	F	28.71
	#84	F	27.00
	#85	M	24.00
	#86	M	34.77
	#87	M	26.00
	#88	F	17.10
	#89	M	29.00
	#90	M	24.00
	#91	F	24.00

LMT=Lamotrigine, ETX=Ethosuximide, TPM=Topiramade, VPA=Valproate, LEV=Levetiracetam, CBZ=Clobazam, BD=(bis die) – 2 times a day, PM=post meridiem, AM=ante meridiem, #...b=post-treatment.

Descriptive statistics of the sample are summarised in Table 3.2. There were no significant differences between the age of drug naïve AE patients and the age of AE refractory patients groups, U=63, p=0.61. No differences were also found between the age of drug naïve AE patients and children healthy control groups, U=120.5, p=0.145. No difference between the refractory AE group and the children healthy control group

was found, U=78.5, p=0.469. Drug naïve JME patients were found to be statistically significantly younger than adults/adolescents healthy control groups, U=85, p=0.019. No differences between the refractory JME group and the adults/adolescents healthy control group were found, U=86, p=0.722. Significant difference was found between the age of the drug naïve JME patients and the age of JME refractory patients, U=29, p=0.022. The effect of age will be accounted for as a covariate in the analysis performed where we have reasons to believe that the differences in age might impact the results.

Table 3.2 : Descriptive of the sample

GROUP	MEDIAN AGE	MEAN AGE	SD AGE	GENDER
DRUG NAÏVE AE	9.49	9.73	3.19	5F, 11M
POST-TREATMENT AE	10.28	10.51	3.15	3F, 7M
REFRACTORY AE	9.93	10.05	1.94	5F, 4M
CONTROL CHILDREN	10.32	11.33	3.31	14F, 7M
DRUG NAÏVE JME	19.18	20.80	6.44	10F, 5M
POST-TREATMENT JME	20.78	22.00	7.71	3F, 4M
REFRACTORY JME	28.40	28.40	9.35	4F, 5M
CONTROL ADULTS/ADOLESCENTS	23.00	24.22	3.7	11F, 10M

We classified the patients that completed the post-treatment scan as responding or not responding to the first AED. We considered 2 aspects for the classifications: i) family/personal report following clinical practice; ii) presence/absence of GSW in the EEG recording during the second visit. Details of classification are listed in Table 3.3. We collected families and personal reports up to April 2016; this period was more than

2 years from first diagnoses for some patients. We have 4 patients diagnosed with AE who are responding to treatment and the information from families and the EEG is concordant as we did not record any GSW. We classified them as responders. We have 1 patient who started presenting with seizures after the 6 moths of follow-up; we considered this subject as not responder as the seizures re-occured whilst under the first medication prescribed. We have two patients who did not present with any GSW during the EEG but the family reported seizures occurrence. We classified them as not-responders considering that we may not have sampled spontaneous GSW during the limited time in which the post-treatment EEG was recorded. We have 1 patient in which the family has reported seizures occurrence and we recorded GSW during the EEG therefore we classified this participant as a not responder. In 2 patients we recorded GSW in the EEG post-treatment but families reported a good improvement in the clinical situation. This complexity exemplifies the difficulty in defining a good outcome measure: is it seizure freedom or presence of GSW in the EEG? As we were not able to answer this question, we did not allocate them to a specific category but we considered them as responders based on family report and not responders from EEG recording. None of the patients with JME presented GSW in the EEG recorded post-treatment and they have all reported good treatment outcome.

Table 3.3 : Treatment outcome classification at post-treatment scan of drug naïve patients.

GROUP	ID	RESPONDER STATUS	GSW on EEG	SELF-REPORT
POST-TREATMENT AE	#3b	YES	NO	No seizures
	#5b	/	YES	No seizures noticed
	#6b	NO	NO	Family was reporting no seizures at 6 moths but now she is having seizures with the same treatment
	#7b	NO	NO	Dad said the treatment was going ok. He noticed few seizures
	#8b	YES	NO	No seizures
	#9b	YES	NO	Parents are concerns as patient had cardiac problem so they think it is the AED
	#11b	/	YES	No seizures
	#13b	YES	NO	No more seizures
	#14b	NO	YES	Mum was concerned about side-effects – impression she was not given AED
	#15b	NO	NO	Reported seizures
POST-TREATMENT JME	#47b	YES	NO	No seizures reported
	#50b	YES	NO	She did report no seizures
	#51b	YES	NO	No more seizures
	#52b	YES	NO	No more seizures

#54b	YES	NO	No more seizures
#56b	YES	NO	No more seizures
#57b	YES	NO	Seizures free

3.4 MRI acquisition

Data were acquired at 1.5 Tesla, Avanto, Siemens Healthcare GmbH, Germany, at GOSH and 3.0 Tesla, MR750, General Electric, USA at King's College Hospital.

The MRI protocol was first designed for the 1.5T Avanto at GOSH and then adapted to ensure consistency for the 3.0T MR750 at KCH. Previous studies demonstrated that the variability of a multicentre study providing MRI data from different manufactures, does not interfere with data quality and experimental designs (Schnack et al., 2004; Davids et al., 2014; Pugnaghi et al., 2014). Based on this, we are confident that our matching protocols would not interfere with data quality and data analysis across centres.

We acquired T1-weighted image for volumetric measurements, simultaneous video-EEG-fMRI to measure functional activation related to epileptic activity, diffusion tensor imaging (DTI) to measure white matter structures, and arterial spin labelling (ASL) to measure variability of blood perfusion due to AED. Imaging parameter specifications for each scanner are specified in Table 3.4.

T2 and FLAIR were acquired in the 3.0T at King's College Hospital as prescribed by the protocol used by the Centre for Neuroimaging Sciences (CNS), King's College London. These images are reported to the general practitioner in case of incidental findings but they will not be considered further in any of the empirical studies.

The data acquisition procedure involved first, the preparation of the MRI-compatible EEG cap (Brain Products, Germany). Baseline scalp EEG was recorded outside the scanner for 5-10 minutes and then participants were moved to the MRI room. The MRI recording was started after participants and the EEG MRI-compatible equipment were positioned into the MRI bed following standard safety guidelines (Ives et al., 1993; Lemieux et al., 1997; Laufs, 2012).

Next, we acquired T1 weighted image with no EEG recording and 4 times 10 minutes simultaneous video-EEG-fMRI. During simultaneous video-EEG-fMRI, participants were instructed to watch for two sessions video-clips of the cartoon "Tom and Jerry" (details are explained in Chapter 3 Paragraph 3.5) alternating with two sessions of rest-eyes-closed, allocating the first randomly. After EEG cap removal, DTI and ASL were acquired with a random order considering participant tolerability. All participants were instructed to remain still during the scanning.

Table 3.4 : Specifications of MRI sequence.

MRI SEQUENCE	PARAMETERS	SCANNER	
		1.5	**3T**
	COIL	12 channels received head coil	12 channels received head coil
T1-WEIGHTED	**SEQUENCE**	FLASH	MPRAGE
	TE	4.94ms	3.016ms
	TR	11ms	7.312ms
	MATRIX	224x224x176	256x256x196
	FOV	256mm	270mm
	VOXEL SIZE	1x1x1mm	1.05x1.05x1.2mm
EEG-fMRI	**SEQUENCE**	EPI	EPI
	FOV	210mm	211mm
	TR	2160ms	2160ms
	TE	30	25
	FLIP ANGLE	75	75

	NUMBER SLICES	30	36
	SLICE THICKNESS	3mm	2.5mm
	SLICE GAP	1mm	0.8mm
	MATRIX	64x64x30	64x64x36
	NUMBER OF VOLUMES	300	300
	VOXEL SIZE	3.3x3.3x4.0mm	3.3x3.3x3.3mm
ASL	**INVERSION TI**	1500ms	1525ms
	TR	3770ms	4834ms
	TE	18.82ms	11.08ms
	VOXEL SIZE	3.6×3.6×5.0mm	1.875x1.875x3.0mm
	MATRIX	64x56	512x8
	SLICE THICKNESS	5mm	3mm
	BOLUS LENGHT	700ms	1500ms
	FOV	230mm	24
DTI	**DIRECTIONS**	60	32
	RESOLUTIONS	2.5×2.5×2.5 mm	2.4x2.4x2.4mm
	FOV	240mm	256mm
	TE	81ms	75ms[4]
	TR	7300ms	Pulse gated
	NUMBER OF SLICES	60	66
	SLICE THICKNESS	2.5mm	2mm

3.5 Child-friendly approach

Given the young population we investigated and the length of the MRI protocol (90 minutes), a child-friendly approach was used. The usefulness of this approach for data quality purpose and feasibility has been demonstrated (Centeno et al., 2016). We

[4] Approximate value as TEs are optimised for each patient as slices are angled differently for each patient; the scanner does a per-scan optimisation of the echo time, to get the shortest possible (and thus the highest signal to noise).

performed all the data collection with no sedation. This decision was supported by problems related to sedation such as unknown effects on epileptic activity and related BOLD response, increased scanning complexity (due to the need for close medical supervision), risk of medical complications, limitation of comparison of methods/results to an adult population in whom sedation is not used, limitation of comparing group results within patients due to variation of level of sedation needed per individual, and between patients and controls as using sedation is rarely ethically possible in control subjects. Natural stimulation has been proposed as a way to improve compliance and reduce movement as well as to create a more comfortable experience in the scanner for paediatric populations (Barnea-Goraly et al., 2014). Natural stimulation aims to provide sensory (audio-visual) stimulation whilst minimally interfering with cognitive networks, provided that this stimulation has a low cognitive demand. A video clip of "Tom & Jerry" where there is no talking or writing (no language areas involved) but only background music in rhythms with the characters movements was chosen for this purpose. Two episodes of the cartoon "Tom & Jerry" were presented for 8 minutes. At the end of each episode, a 1.24 minutes of black screen with written "PLEASE WAIT" was played as pictured in Figure 3.1 .

Figure 3.1 : Task Paradigm

Youngest participants and, at their discretion for the adolescents/adults, choose a DVD to watch during EEG cap preparation and structural acquisition (T1-weighted, DTI and ASL). We fitted a mirror facing a TV screen inside the MRI bed on the patient's head coil to allow the chosen DVD to be seen, projected to a screen fitted at the end of the MRI room.

As expected, 90% (28 patients) of the JME groups underwent the full protocol. One patient (both for pre and post-treatment scan) did not tolerate the noise of the MRI. The other patient had braces implanted; therefore, we terminated the MRI protocol after the simultaneous EEG-fMRI for safety and data quality purposes. 90.4% (19 participants) of the adult healthy control group underwent full protocol. One participant did not tolerate extra time needed to acquire ASL; for the other participant, the noise of the EPI sequence was intolerable. 48.5% (17 patients) of the AE patients underwent the full MRI protocol. In the remaining 51.4% (18 patients) of patients we acquired enough good quality data to pursue empirical studies. Only 19.04% of the healthy control group has the full MRI protocol acquired because ASL sequence was designed after the beginning of the study from which we shared the healthy control group. Specifications of the data acquired per patient are listed in Table 3.5.

Table 3.5 : MRI protocol acquisition rate per patient.

GROUP	ID	T1-WEIGHTED	EEG-fMRI	ASL	DTI
DRUG NAÏVE AE	#1	Y	4/4	Y	Y
	#2	Y	4/4	Y	Y
	#3	Y	4/4	/	Y
	#4	Y	2/4	/	/
	#5	Y	2/4	/	Y
	#6	Y	4/4	Y	Y
	#7	Y	4/4	Y	Y
	#8	Y	3/4	/	Y
	#9	Y	3/4	Y	Y
	#10	Y	4/4	Y	Y
	#11	Y	4/4	Y	Y
	#12	Y	3/4	Y	Y
	#13	Y	3/4	Y	Y
	#14	Y	2/4	/	/
	#15	Y	2/4	/	Y
	#16	Y	4/4	/	Y
POST-TREATMENT AE	#3b	Y	4/4	Y	Y
	#5b	/	3/4	/	/
	#6b	Y	4/4	Y	Y
	#7b	Y	3/4	Y	Y
	#8b	Y	4/4	/	Y
	#9b	Y	4/4	Y	Y
	#11b	Y	4/4	Y	Y
	#13b	Y	4/4	Y	Y
	#14b	Y	4/4	/	Y
	#15b	Y	4/4	Y	Y

REFRACTORY AE	#17	Y	3/4	Y	Y
	#18	Y	4/4	Y	Y
	#19	Y	4/4	Y	Y
	#20	Y	4/4	/	/
	#21	Y	4/4	Y	Y
	#22	Y	4/4	Y	Y
	#23	Y	4/4	Y	Y
	#24	Y	3/4	/	/
	#25	Y	4/4	/	Y
HEALTHY CONTROL CHILDREN	#26	Y	4/4	Y	Y
	#27	Y	4/4	/	Y
	#28	Y	4/4	/	Y
	#29	Y	4/4	Y	Y
	#30	Y	4/4	/	Y
	#31	Y	4/4	/	Y
	#32	Y	4/4	/	Y
	#33	Y	4/4	Y	Y
	#34	Y	4/4	/	Y
	#35	Y	4/4	/	Y
	#36	Y	4/4	/	Y
	#37	Y	4/4	/	Y
	#38	Y	4/4	/	Y
	#39	Y	4/4	/	Y
	#40	Y	4/4	/	Y
	#41	Y	4/4	/	Y
	#42	Y	4/4	/	Y
	#43	Y	3/4	Y	Y
	#44	Y	4/4	/	Y
	#45	Y	4/4	/	Y
	#46	Y	4/4	/	Y

DRUG NAÏVE JME	#47	Y	4/4	Y	Y
	#48	Y	4/4	/	/
	#49	Y	4/4	Y	Y
	#50	Y	4/4	Y	Y
	#51	Y	4/4	Y	Y
	#52	Y	4/4	Y	Y
	#53	Y	4/4	Y	Y
	#54	Y	4/4	Y	Y
	#55	Y	4/4	Y	Y
	#56	Y	1/4	/	/
	#57	Y	4/4	Y	Y
	#58	Y	4/4	Y	Y
	#59	Y	4/4	Y	Y
	#60	Y	4/4	Y	Y
	#61	Y	4/4	Y	Y
POST-TREATMENT JME	#47b	Y	4/4	Y	Y
	#50b	Y	4/4	Y	Y
	#51b	Y	4/4	Y	Y
	#52b	Y	4/4	Y	Y
	#54b	Y	4/4	Y	Y
	#56b	Y	3/4	/	/
	#57b	Y	4/4	Y	Y
REFRACTORY JME	#62	Y	4/4	Y	Y
	#63	Y	4/4	Y	Y
	#64	Y	4/4	Y	Y
	#65	Y	4/4	Y	Y
	#66	Y	4/4	Y	Y
	#67	Y	4/4	Y	Y
	#68	Y	4/4	Y	Y
	#69	Y	4/4	Y	Y

	#70	Y	4/4	Y	Y
HEALTHY CONTROL ADULTS/ADOLESCENTS	#71	Y	4/4	Y	Y
	#72	y	4/4	/	Y
	#73	Y	4/4	Y	Y
	#74	Y	4/4	Y	Y
	#75	Y	4/4	Y	Y
	#76	Y	4/4	Y	Y
	#77	Y	4/4	Y	Y
	#78	Y	4/4	Y	Y
	#79	Y	4/4	Y	Y
	#80	Y	4/4	Y	Y
	#81	Y	4/4	Y	Y
	#82	Y	4/4	Y	Y
	#83	Y	4/4	Y	Y
	#84	Y	2/4	Y	Y
	#85	Y	4/4	Y	Y
	#86	Y	4/4	Y	Y
	#87	Y	4/4	Y	Y
	#88	Y	4/4	Y	Y
	#89	Y	4/4	Y	Y
	#90	Y	4/4	Y	Y
	#91	Y	4/4	Y	Y

3.6 Simultaneous video-EEG-fMRI setup

To record simultaneous scalp video-EEG-fMRI, participants were fitted with a 64 channels (62 EEG electrodes, 1 ECG electrode and 1 reference electrode) MRI compatible EEG cap (BrainCap, Germany). The electrodes were arranged accordingly to

the modified combinatorial nomenclature referenced to FCz electrode. The preparation time of the EEG cap varied between 20 to 40 minutes depending on the population. Two people (I and another member of Dr Carmichael's team) applied the EEG cap for the children whilst only I prepared the EEG cap for the adults/adolescents. Participants were then moved to the scanner room, they were fitted with ear plugs, ear phones and their head was immobiised using a vacuum cushion. EEG wires were straightened along the Z axis, immobiised and connected to 2x32 MRI-compatible Amplifiers (Brain Products, Germany) at the back of the scanner. EEG data were transmitted from the amplifiers to the recording computer located in the control room via fibre-optic cables. Scalp EEG was recorded simultaneously during fMRI with a sampling rate of 5000 Hz and was synchronised to the scanner's 20 KHz gradient clock. Other recording parameters for EEG were: resolution = 0.5 μV; digitization = 16-bit. ECG was recorded with a single electrode which was placed just below the left clavicle and connected to the same amplifier as for EEG electrodes.

Video was recorded via a MR-compatible camera (MR-Cam 12M, MRC Systems GmbH, Heidelberg, Germany) that was positioned inside the bore of the scanner focusing on the subject's face, recording facial expressions related to seizures and subject's motion. The video signal from the camera was transmitted to the recording computer placed outside the scanner room through shielded cable and low-pass filter (1MHz: MRC Systems GmbH, Heidelberg, Germany) to provide radio frequency (RF) shielding. The low-pass filter box was grounded to the scanner room shield.

Video and EEG were recorded synchronously using Brain Vision Recorder software (Brain Products, Munich, Germany). The recording was monitored using RecView software (Brain Products, Munich, Germany) which provides online artefact correction.

3.7 EEG pre-processing

MR gradient and pulse-related artefacts were removed off-line from the EEG recorded inside the MRI using template artefact subtraction (Allen et al., 1998; Allen et al., 2000) implemented in a commercial EEG processing package (Brain Analyzer, Brain Products). EEG was down sampled to 250 Hz. GSW were identified after visual inspection and manually marked on the EEG traces for each session. Because of the stereotypical shape of GSW, consensus with clinical neurophysiologist was not required. However, the EEGs were reviewed in both bipolar and referential montages to ensure accurate identification of epileptiform abnormalities.

3.7.1 GSW recording

As reported in Table 3.6, a total of 285 runs of GSW were successfully marked in the EEG. 55.51% (34 patients) of all the patients presented GSW during simultaneous EEG-fMRI recording. 73.52% (25 patients) of those patients belong to the AE groups and the remaining 26.5% (9 patients) belong to JME groups. Among the AE groups, 75% (12 patients) of the drug naïve group, 50% (5 patients) of the post-treatment group and 88.8% (8 patients) of the refractory group presented with GSW. Amongst the JME groups, 40% (6 patients) of the drug naïve group, 0% of the post-treatment and 33.3% (3 patients) of the refractory group presented GSW. AE patients had longer GSW mean duration compared to JME patients: 5.67 s ± 5.16 s (AE) versus 1.53 s ± 1.19 s (JME),

$t(75)= 4.017$, $p< 0.001$. We compared the mean duration of GSW from pre-treatment (M^5=6.87, SD^6=5.65) to post-treatment (M=2.51, SD=2.74) in the AE groups which has been found to be significantly decreased $t(36)=2.433$, $p=0.020$. As this comparison was not possible in the JME groups, we compared drug naïve JME (M=1.78, SD=1.33) with refractory JME (M=0.97, SD=0.5) and we did not find statistical differences between the length of GSW $t(24)=1.65$, $p=0.111$, although the mean length is less in the refractory group. This has been also the case for the drug naïve AE group (M=6.87, SD=5.65) compared to the refractory AE group (M=5.84, SD=4.81), $t(38)=0.57$, $p=0.572$. A trend was found between the GSW duration of the post-treatment AE group (M=2.51, SD=2.74) with the refractory AE group (M=5.8, SD=4.81), $t(22)=-2.02$, $p=0.055$.

Table 3.6: GSW incidence during simultaneous EEG-fMRI.

GROUP	ID	SESSION 1		SESSION 2		SESSION 3		SESSION 4	
		N	MD	N	MD	N	MD	N	MD
DRUG NAÏVE AE	#1	/	/	/	/	/	/	/	/
	#2	/	/	5	9.4032	6	15.816	13	3.7822
	#3	2	7.302	8	5.205	1	8.184	/	/
	#4	3	3.8667	17	3.0252	/	/	/	/
	#5	/	/	/	/	/	/	/	/
	#6	1	28.6756	/	/	/	/	1	5.672
	#7	1	5.34	2	6.84	10	1.5632	/	/
	#8			1	7.9505	3	6.8027	/	/
	#9	/	/	/	/	1	3.616	/	/
	#10	/	/	/	/	/	/	/	/
	#11	/	/	4	0.4969	/	/	2	1.8783

[5] Mean
[6] Standard deviation

	#12	3	5.46	14	5.1434	5	6.8776	/	/
	#13	1	10.728	3	8.6013	1	11.464	/	/
	#14			3	9.8853	/	/	/	/
	#15	3	0.984	2	1.1559	/	/	/	/
	#16	/	/	/	/	/	/	/	/
POST-TREATMENT AE	#3b	/	/	/	/	/	/	/	/
	#5b	/	/	/	/	1	0.712	/	/
	#6b	/	/	/	/	/	/	/	/
	#7b	/	/	/	/	1	5.0609	/	/
	#8b	/	/	1	7.924	3	6.78	/	/
	#9b	/	/	/	/	/	/	/	/
	#11b	1	1.7538	2	0.9853	1	2.116	3	0.2893
	#13b	/	/	/	/	/	/	/	/
	#14b	1	0.888	3	0.4853	1	0.6823	/	/
	#15b	/	/	/	/	/	/	/	/
REFRACTORY AE	#17	/	/	/	/	/	/	/	/
	#18	/	/	/	/	/	/	/	/
	#19	6	3.6107	6	5.2147	/	/	1	10.234
	#20	/	/	/	/	/	/	/	/
	#21	/	/	/	/	/	/	/	/
	#22	/	/	4	9.9431	/	/	3	7.3472
	#23	/	/	5	10.833	1	14.1793	6	10.0582
	#24	1	1.24	7	1.216	4	0.739	/	/
	#25	/	/	1	0.92	/	/	1	0.388
DRUG NAÏVE JME	#47	10	1.6721	6	0.9279	7	0.8858	4	1.9539
	#48	/	/	4	3.5081	/	/	2	2.5320
	#49	1	1.5280	/	/	/	/	/	/
	#50	/	/	/	/	/	/	/	/
	#51	/	/	/	/	/	/	/	/

	#52	3	3.3520	/	/	1	5.196	/	/
	#53	1	0.36	/	/	/	/	/	/
	#54	/	/	/	/	/	/	/	/
	#55	/	/	2	3.528	/	/	/	/
	#56	7	1.7331	/	/	/	/	/	/
	#57	/	/	/	/	/	/	/	/
	#58	4	0.606	3	0.8147	4	0.4	1	1.48
	#59	/	/	/	/	/	/	/	/
	#60	/	/	/	/	/	/	/	/
	#61	5	0.7	/	/	1	1.02	/	/
POST-TREATMENT JME	#47b	/	/	/	/	/	/	/	/
	#50b	/	/	/	/	/	/	/	/
	#51b	/	/	/	/	/	/	/	/
	#52b	/	/	/	/	/	/	/	/
	#54b	/	/	/	/	/	/	/	/
	#56b	/	/	/	/	/	/	/	/
	#57b	/	/	/	/	/	/	/	/
REFRACTORY JME	#62	/	/	/	/	/	/	/	/
	#63	/	/	/	/	/	/	/	/
	#64	/	/	/	/	/	/	/	/
	#65	/	/	/	/	/	/	/	/
	#66	/	/	1	0.4056	/	/	/	/
	#67	/	/	/	/	/	/	/	/
	#68	/	/	/	/	/	/	/	/
	#69	1	1.796	1	1.22	11	1.1549	11	1.3178
	#70	6	0.8540	3	0.7867	2	0.384	2	0.27

N=number of GSW per session. MD=mean duration of GSW per session in seconds.

3.8 MRI processing and statistical analysis

All fMRI data were analysed using the software package Statistical Parametric Mapping (SPM8) (http://www.fil.ion.ucl.ac.uk/spm) running under Matlab (Mathworks Inc., U.S.A.). After discarding the first four volumes to avoid T1-saturation effect, the EPI time series images were realigned to the first image, corrected with Functional Image Artefact Correction Heuristic (FIACH) (Tierney et al., 2016), normalised to MNI space and spatially smoothed using an isotropic Gaussian kernel of 8mm FWHM (Friston et al., 1995).

The fMRI data were analysed within the GLM framework to measure GSW related haemodynamic changes. GSW marked in the EEG were represented as blocks of variable duration depending upon the length of the discharge and considered effects of interest in the GLM. Details of GLM specifications are listed in experimental Chapters 5 and 6 as different models were used. For each effect of interest, SPM[T+] were used at the single subject-level. Images generated from SPM[T+] (con images containing the betas) for the effects of interests were used for group comparison at the second-level analysis where SPM[F] maps were generated. The presence of significant BOLD changes was assessed by applying a family wise error corrected threshold using extended threshold available in the random field theory framework in SPM. The resulting SPM[F] maps were overlaid on normalised T1-weighted MRI scans to evaluate the anatomical localisation of effects. BOLD time courses were plotted for BOLD clusters when required to classify the BOLD change as increases or decreases according to the sign of the peak change relative to baseline.

Structural data were analysed using FSL (http://fsl.fmrib.ox.ac.uk/fsl/fslwiki/FSL), free-surfer (http://freesurfer.net/) and locally-written Matlab scripts depending upon the research questions of interests. Specifications of these methods are found in Chapters 4 and 7.

SECTION 3: EXPERIMENTAL STUDIES

In this section I will introduce the experimental studies conducted on the recruited sample introduced in Chapter 3.

Firstly, we explored the effect of AED on structural grey matter and GSW related BOLD responses. Secondly, we studied differences in grey matter structures and cerebral blood flow using a longitudinal approach. With this, we aimed to identify markers of treatment outcomes by comparing grey matter volume and shape between drug naïve and post-treatment measures. Thirdly, we measured GSW BOLD response in different brain states to identify if BOLD deactivation in DMN during GSW is an epiphenomenon specific to resting state.

In Chapter 4 I will describe our investigation of structural abnormalities in grey matter volume and shape in drug naïve patients with early diagnoses of GGE. Via the application of the longitudinal approach, we will describe if grey matter measures can function as marker of treatment outcome. Chapter 5 contains the first simultaneous EEG-fMRI analysis in which we tested changes in BOLD response prior and related to the onset of GSW in the biggest group of drug naïve patients. Chapter 6 describes the second simultaneous EEG-fMRI study where we interrogated differences in BOLD changes related to GSW when patients are in different brain states. Chapter 7 contains the analysis on ASL where we compared blood perfusion parameters before and after treatment intake.

Chapter 4 : Volumetric analysis

4.1 Background

Patients diagnosed with GGE are expected to have a normal-looking brain when studied with a conventional clinical MRI scan (Berg et al., 2010). However, structural abnormalities in grey matter are supported by emerging evidence. For example, it is now well established that there are abnormalities in thalamic-cortical connections that might underlie disease manifestation (Bernasconi et al., 2003).

Previous studies have used standard measurements of T1-weighted image and grey matter volume to compare patients with GGE and healthy controls. Among all measures, voxel based morphometry (VBM) (Mechelli et al., 2005; Whitwell, 2009), volumetric measures and shape analysis (Kim et al., 2013) have been widely used. Studies to date have shown conflicting results with regard to the areas of abnormalities, whether they show increased or decreased GM volume in patients compared to healthy controls, and the effect that AED have had on the results.

The brain area that has shown most consistent results across studies is the thalamus. However, different nuclei of the thalamus have been reported to be atypical in GGE, together with different additional areas of the basal ganglia. For example, patients with GTCS revealed reduced grey matter ratio compared to healthy controls in the ventral anterior and lateral nuclei of the thalamus (Ciumas and Savic, 2006). Consistent with this study, a deflation of the thalamus, in addition to putamen and pallidum, was reported (Du et al., 2011). In a group of JME patients, shape analysis showed surface reduction in the medial and lateral nuclei of bilateral thalami together with hippocampi

(Saini et al., 2013). Decreased grey matter volume in anteromedial thalamus has also been found in a group of mixed GGE patients (Kim et al., 2014) and in JME patients (Kim et al., 2007). Similar abnormalities of grey matter volume reduction in bilateral thalami (Chan et al., 2006) were also reported in patients with AE.

While there is some consensus regarding basal ganglia changes, abnormalities in the cortical areas remain more controversial. For example, a decrease in volume was found in the frontal cortex of a group of JME patients (O'Muircheartaigh et al., 2011a). In addition, medial frontal gyrus and areas related with BOLD changes in the presence of GSW such as the precuneus, were found to have decreased grey matter volume (Chan et al., 2006) in groups of GTCS (Ciumas and Savic, 2006; Huang et al., 2011). However, contrasting evidence was reported in a group of JME in which increased grey matter volume was found in the superior mesial frontal cortex (Kim et al., 2007).

All the results currently reported are extracted from populations of patients having i) refractory GGE, ii) long-term AED treatment intake and iii) long disease durations. As such, controlled measures of disease duration are essential to understand the progression of structural abnormalities in the disease although it has been found that GM matter volume (cortical and subcortical) is negatively correlated with disease duration (Huang et al., 2011). However, concerns regarding the selection of refractory patients from tertiary centres might have biased the evidence. For example, one study used treated patients with different IGE syndromes who were seizure free and found no differences between grey matter volume between patients and controls neither in thalamus nor in the total grey matter volume. The only difference was found in the putamen (Seeck et al., 2005). This evidence raises questions: are the structural abnormalities caused by

seizures and/or AED treatment? Or are these debated structural abnormalities intrinsic in GGE patients? Or is this phenomenon the results of a combination of the three? As most of the available studies selected refractory patients and have samples of patients already on treatment, it has been difficult to separate the effects of these different factors. Almost all of the studies mentioned have been cross-sectional and measured the degree of modification of the grey matter in patients with GGE retrospectively to identify the aetiology and/or progression of structural abnormalities related to GGE. Only one study has investigated longitudinally to determine grey matter volume changes from maximum of 12 months after the diagnoses with a follow-up scan at 24 months after the diagnoses. However, all the patients were on treatment (Pulsipher et al., 2011), thus the potential confounding effect of medication could not be excluded. Although the antiepileptic drug effects on brain atrophy are unclear, some research has indicated that antiepileptic drugs can influence nerve morphology, causing changes such as pseudo-atrophy of the brain (Papazian et al., 1995) or neurogenesis (Hao et al., 2004). As such, removing the potential effect of medication when examining brain volumes is crucial. There is only one study that is currently available which reported decreased grey matter volume in a group of drug naïve CAE only (Wang et al., 2016). Therefore, it is essential to identify if results of this study are reproducible not only in CAE but in all the GGE syndromes.

This work aimed to measure, for the first time, structural abnormalities in a group of drug naïve patients diagnosed with GGE syndromes. We compared their structural brain scan acquired before starting treatment with a group of age-matched healthy controls to control for treatment effect biases. Also, as patients were longitudinally followed-up, we

were able to compare pre-treatment brain scans with post-treatment brain scans allowing us to measure any structural differences related to disease progression and the effect of treatment. Finally, in order to understand whether brain abnormalities were related to treatment outcome, we investigated if there were differences in our measurements of brain structure between patients responding to treatment and those considered refractory to treatment.

4.2 Methods

4.2.1 Subjects

The sample for this study consisted of 16 drug naïve patients with AE (mean age= 9.73, 5 F), 15 drug naïve patients with JME (mean age= 20.79, 8 F), 17 post-treatment patients from these 31 drug-naïve (AE: mean age= 10.5, 3F; JME: mean age= 21.9, 3 F), 9 refractory (long-term) AE (mean age=10.04, 5 F), 9 refractory (long-term) JME (mean age= 28.4, 4 F). In addition we studied 16 age-matched healthy controls (mean age= 10.38, 10 F) to compare with the drug naïve AE group and 15 age-matched healthy controls (mean age= 23.06, 10 F) to compare with the JME drug naïve group. A full list of the demographic characteristics of the participants is available in Table 4.1. For specification of the sample refer to Chapter 3.

We will refer to the drug naïve (DN) when we consider DN AE and JME together. Otherwise, we will specify if we refer to DN JME or DN AE. The post-treatment (PT) group will be divided in PT responders as those patients who presented good outcome at the PT scan and PT refractory as those patients who reported bad outcome to the PT

scan. We will refer to DN responding when we measure grey matter volume at the drug naïve stage but we know from PT that they subsequently responded to treatment. Similarly, DN refractory will refer to those patients who subsequently showed bad outcome at PT scan. We will refer to refractory long-term patients for those patients who are on treatment for more than 1 year and presenting seizures. We will refer to refractory when in the group we will include refractory long-term and PT refractory. Classification of PT responding and PT refractory was based on family report and EEG (Table 3.3).

Table 4.1: Sample selected for T1-weighted structural analysis

GROUP	CODE	GENDER	AGE
DRUG NAÏVE	#1	M	6.03
AE	#2	M	14.00
	#3	M	10.51
	#4	M	6.37
	#5	M	10.58
	#6	F	13.65
	#7	M	8.03
	#8	F	7.73
	#9	M	10.28
	#10	F	9.72
	#11	F	16.18
	#12	M	7.15
	#13	M	9.26
	#14	M	5.92
	#15	M	6.84
	#16	F	13.50

POST-TREATMENT AE	#3b	M	11.49
	#5b	M	11.30
	#6b	F	14.21
	#7b	M	8.54
	#8b	F	8.25
	#9b	M	10.77
	#11b	F	16.78
	#13b	M	9.78
	#14b	M	6.43
	#15b	M	7.56
REFRACTORY AE	#17	M	8.60
	#18	F	12.33
	#19	M	10.45
	#20	M	8.34
	#21	F	13.12
	#22	F	9.66
	#23	F	9.93
	#24	F	7.00
	#25	M	10.98
CONTROL CHILDREN	#26	M	14.08
	#27	F	9.72
	#28	F	13.62
	#31	M	8.34
	#33	F	8.32
	#34	F	9.08
	#35	M	6.61
	#36	M	12.00
	#37	F	12.14
	#38	F	9.08
	#39	M	10.32

	#40	F	8.85
	#42	M	7.50
	#44	F	14.22
	#45	F	12.67
	#46	F	9.58
DRUG NAÏVE JME	#47	M	21.71
	#48	M	16.75
	#49	F	16.58
	#50	F	13.64
	#51	F	20.11
	#52	M	35.98
	#53	F	15.38
	#54	F	17.69
	#55	F	26.04
	#56	M	14.44
	#57	F	25.94
	#58	F	31.23
	#59	F	16.46
	#60	M	20.86
	#61	F	19.18
POST-TREATMENT JME	#47b	M	22.95
	#50b	F	14.14
	#51b	F	20.78
	#52b	M	36.44
	#54b	F	18.26
	#56b	M	14.94
	#57b	M	26.48
REFRACTORY JME	#62	F	18.18
	#63	F	22.18
	#64	M	39.10

	#65	M	40.06
	#66	M	21.39
	#67	M	20.69
	#68	F	22.33
	#69	F	30.86
	#70	M	40.84
CONTROL ADOLESCENTS/ ADULTS	#71	F	23.89
	#72	F	20.28
	#73	M	24.98
	#74	F	25.64
	#76	M	23.00
	#77	F	25.14
	#78	F	23.34
	#79	F	22.85
	#80	F	20.47
	#82	M	21.28
	#84	F	27.00
	#85	M	24.00
	#88	F	17.10
	#90	M	24.00
	#91	F	24.00

4.2.2 MRI acquisition

Three-dimensional T1-weighted MPRAGE was acquired in the sagittal plane (echo time= 3.016ms, repetition time= 7.312 ms, acquisition matrix= 256 x 256 x 196 over a field of view of 27 cm3, voxel size 1.05 x 1.05 x 1.2 mm3) using a 3T 750 General Electric scanner. Inversion recovery spoiled gradient-recalled echo images were used for quantitative analysis in the JME drug naïve, JME post-treatment, JME refractory and

healthy control adults/adolescents participants (Table 4.1). A three-dimensional isotropic T1-weighted FLASH was acquired in a sagittal plane (echo time= 4.94 ms, repetition time= 11 ms, acquisition matrix= 192 x 256 x 176 mm over a field of view of 256 mm3, voxel size 1 x 1 x 1 mm3) using a 1.5T Siemens scanner in the AE drug naïve, post-treatment, refractory and children included in the healthy control sample (Table 4.1).

4.2.3 MRI processing

T1-weighted images were transformed from dicom to nifti format using the SPM8 dicom import tool. Nifti images were then imported into FSL software (http://fsl.fmrib.ox.ac.uk) and reoriented to match the Montreal Neurological Institution 152 (MNI152) (Mazziotta et al., 2001a; Mazziotta et al., 2001b) standard template so that they appear in the same orientation in FSLView by applying a 90, 180 or 270 degree rotations about the different axes as necessary to obtain the labels in the same position as the standard template using fslreorient2std (http://fsl.fmrib.ox.ac.uk/fsl/fslwiki/Fslutils).

4.2.4 MRI analysis

Using the extensive literature in the field we generated an a priori hypothesis that the following specific cortical and subcortical areas would show grey matter volume loss and abnormalities in: thalami, putamen, caudate, pallidum and hippocampi; and involvement in GGE manifestation of cuneus, prefrontal cortex, precentral cortex and cingulate.

4.2.4.1 Volumetric analysis (subcortical and cortical)

We used FSL-integrated registration and segmentation toolbox (FSL-FIRST) software, version 5.0 (http://fsl.fmrib.ox.ac.uk/fsl/fslwiki/first) for the automated segmentation of the subcortical structures of interest, which included the thalami and the major structures of the basal ganglia (putamen, caudate, and pallidum) and hippocampi. As described in detail elsewhere (Patenaude et al., 2011; Kim et al., 2013), FSL-FIRST automatically segmented the subcortical structures from the MR images and produced volumetric outputs (from which each structure's global volume was obtained using FSL statistical tools).

Grey matter volumes of the subcortical areas were extracted per hemisphere and the mean volume for each subcortical area across both hemispheres was calculated. To account for possible effects of global brain volume and head size, each region volume was corrected for global brain volume. To accomplish this, we made use of a widely-implemented method available through the FSL platform, SienaX (Smith et al., 2002; Smith et al., 2007). This method measures brain volume from a single MRI scan. This is achieved by normalising an individual's image to a standard template for both the skull and brain surface (both obtained using BET (Smith, 2002)) followed by tissue segmentation (including correction for partial volume effects) to yield a normalised brain volume (NBV). This methodological choice was supported by evidence showing that volumes of the subcortical areas of interest are positively correlated with the cranium size (Goodro et al., 2012) and that SienaX measures are an excellent surrogate for the intracranial vault volume (Fein et al., 2004). Thus NBV takes into account of both brain atrophy and global head size scaling. We divided each subject-specific

subcortical region volume by the subject-specific NBV, and compared each NBV-corrected subcortical region between groups. ANOVA as implemented in SPSS was used to compare the corrected bilateral volumes between DN and HC, AE DN and HC, JME DN and HC, DN and PT, DN and refractory, PT responders and refractory, refractory and HC, DN responders and DN refractory. Age, gender and scanner type were introduced as covariates in the univariate model. For each region, a *p*-value threshold adjusted for multiple comparisons using false discovery rate (FDR) was applied.

Measurements of the cortical volumes were calculated using Freesurfer software (http://freesurfer.net/) (Fischl, 2012). All images were processed using the standard 'recon-all' processing stream (https://surfer.nmr.mgh.harvard.edu/fswiki/recon-all), which supplies the surfaces and morphometry data for each subject. We used region-based analysis, based on the automated parcellation of the cortex into 34 regions. FSLstats (http://fsl.fmrib.ox.ac.uk/fsl/fslwiki/Fslutils) was used to extrapolate the grey matter volumes from the parcellated cortical regions. Differences in the volumes of cortical regions were calculated applying the same procedure as described for the sub-cortical regions. To account for possible effects of global brain volume and head size on cortical region volumes, each was corrected for global brain volume using the NBV from SienaX consistent with the procedure used for subcortical areas. Scanner type, age and gender (Sowell, 2002) were used as covariates of no interest. Comparison between the mean volume of bilateral cuneus, prefrontal cortex, precentral cortex and cingulate were made between DN and HC, JME DN and HC, AE DN and HC, DN and PT, DN and refractory, PT responding and refractory, refractory and HC, DN responding and

DN refractory. We selected these cortical areas as consistently reported in the literature as involved in GGE syndromes.

We performed a separated ANOVA with scanner type, age and gender as covariates, to measure differences in NBV between groups (DN and HC, JME DN and HC, AE DN and HC, DN and PT, DN and refractory, PT responding and refractory, refractory and HC, DN responding and DN refractory). This was calculated as a control measure to ensure that differences in sub-cortical and cortical grey matter were not driven by differences in NBV.

4.2.4.2 Shape analysis

FSL-integrated registration and segmentation toolbox (FSL-FIRST) software, version 5.0 (http://fsl.fmrib.ox.ac.uk/fsl/fslwiki/first) was also used for surface shape analysis of the subcortical structures of interest: thalami, putamen, caudate, pallidum and hippocampi. FSL-FIRST outputs parameterised volumetric labels (meshes) from surfaces of the selected structures after affine registration of raw T1-weighted images to MNI 152 standard space. Vertex-wise shape analysis along the surface of the segmented structures was then performed via the measures of differences in mean vertex position between groups (Patenaude et al., 2011; Kim et al., 2013). Registration to MNI space ensured that global brain volume effects were fully taken into account for the vertex-wise shape analysis. Comparisons of thalami, putamen, caudate, pallidum and hippocampi shapes were made between healthy control, drug naïve patient, and 'not-responders' patient groups.

For the shape analysis, permutation testing using 'randomise' was used to calculate statistics from surface meshes of the segmented structures, which were thresholded at

p<0.05 and corrected for multiple comparisons using False Discovery rate (FDR). Scanner type, age and gender (Sowell, 2002) were introduced as covariates in the model.

4.2.4.3 VBM

For voxel-based morphometry (VBM) preprocessing we used SPM12 software (Ashburner and Friston, 2000). In SPM12, the 'segment' procedure was used applying a new generation of tissue probability maps (TPM) with improved anatomical delineation of sub-cortical areas (Lorio et al., 2016). Unified tissue segmentation applies normalisation to MNI space, tissue segmentation and bias field correction within a single step to warp tissue probability maps to match the image (Ashburner and Friston, 2005). Next, Diffeomorphic Anatomical Registration Through Exponentiated Lie algebra (DARTEL) was used to account for more detailed shape variability in the population (Ashburner, 2007). The DARTEL registration involves alternating between computing a template, based on the average tissue probability maps of all subjects, and warping the GM and WM tissue maps of all subjects into increasingly good alignment with the template. A sample specific template was created selecting the best quality data per group (9 HC adults, 9 HC children, 9 JME DN and 9 AE DN). Images were spatially normalised to standard Montreal Neurological Institute (MNI) space, followed by a smoothing procedure with a Gaussian Kernel of 8 mm. A region of interest (ROI) mask of bilateral thalamus, caudate, pallidum and hippocampi was applied given a priori hypothesis. Scanner type, age and gender (Sowell, 2002) were introduced as covariates in the model consistent with the previous analysis. Two-samples T-tests were calculated and results at a primary threshold of p<0.05 FWE were explored.

4.3 Results

The quality of subcortical and cortical segmentation was inspected visually. All the participants included in the analysis were judged as good quality; participants, in which cortical and subcortical segmentation did not visually match the brain structures, were excluded. We excluded one refractory JME patient (#61) due to poor T1-weighted image quality. One refractory AE patient (#17) was excluded from cortical volume measures due to poor quality of cortical segmentation. Two patients from the AE drug naive group (#15, #14) and one healthy control (#35) were excluded from voxel based analysis due to misclassification of brain tissues because of motion artefacts.

4.3.1 Volumetric analysis (subcortical and cortical)

The results of volume analysis for bilateral thalami, putamen, pallidum, hippocampi and caudate are shown in Table 4.2. We found a trend of decreased grey matter volume in drug naive (DN) patients in all the subcortical areas considered compared with healthy controls (HC). Thalamus ($F(1,57)=6.591$, $p=0.013$) and pallidum ($F(1,57)=5.936$, $p=0.018$) were the areas surviving significant statistical threshold corrected for multiple comparisons (Figure 4.1). In the AE drug naïve group, thalamus, putamen and pallidum appeared to be smaller in volume compared with their age matched HC participants, although the value did not survive statistical threshold (Figure 4.2). Similarly, but surviving statistical significance threshold, JME drug naïve (DN JME) patients had smaller volumes than healthy controls (HC) in thalamus ($F(1,26)=5.334$, $p=0.029$), pallidum ($F(1,26)=6.598$, $p=0.016$) and hippocampus ($F(1,26)=5.334$, $p=0.029$) (Figure 4.3).

Eleven patients post-treatment were classified as responding and 4 as not responding to treatment. Two patients had discordant information from the EEG and from families. In one of them, a post-treatment T1-weighted image was not acquired due to the patient not tolerating the scan, therefore this individual was not included in the analyses; the second patient was alternatively assigned to PT responder and PT refractory groups in two separate alternative analyses. Independent of which category this individual was put into we found consistent results, therefore (in Table 4.2), we reported the results for when this patient is classified as PT refractory and DN refractory. We found no statistically significant differences between grey matter volumes of DN and refractory (Figure 4.5). However, we found lower mean values of grey matter volume in the sub-cortical areas in the refractory patients compared to the PT responding patients (Figure 4.7). We found statistically significant differences in thalamus ($F(1,49)=11.208$, $p=0.002$) and hippocampus ($F(1,49)=12.740$, $p=0.001$) comparing refractory patients and HC (Figure 4.4). We compared volumetric measures of drug naïve patients who were classified as responders (DN responder) with drug naïve patients who were classified as not responders (DN refractory). Although we found no statistically significant differences between the groups, patients who did not respond to treatment showed smaller mean values in grey matter volumes (Figure 4.8).

Table 4.2: Volumetric differences in subcortical areas

COMPARISON	THALAMUS	PUTAMEN	PALLIDUM	HIPPOCAMPUS	CAUDATE
DN (31) vs HC (31)	M=0.0047; 0.0050; *p*=0.013	M=0.0010; 0.0031; *p*=0.073	M=0.0010; 0.0011; *p*=0.018	M=0.0022; 0.0023; *p*=0.073	M=0.0022; 0.0023; *p*=0.431
AE DN (16) vs HC (16)	M=0.0045; 0.0046; *p*=0.228	M=0.0028; 0.0029; *p*=0.239	M=0.0009; 0.0010; *p*=0.423	M=0.0020; 0.0020; *p*=1	M=0.0021; 0.0021; *p*= 0.779
JME DN (15) vs HC (15)	M=0.0050; 0.0054; *p*=0.029	M=0.0032; 0.0033; *p*=0.218	M=0.0011; 0.0012; *p*=0.016	M=0.0024; 0.0026; *p*=0.029	M=0.0023; 0.0025; *p*=0.158
DN (31) vs PT (16)	M=0.0047, 0.0047; *p*= 0.635	M=0.0030, 0.0030; *p*= 0.804	M=0.0010, 0.0010; *p*= 0.353	M=0.0022, 0.0021; *p*= 0.778	M=0.0022, 0.0023; *p*=0.468
DN (31) vs refractory (22)	M=0.0047, 0.0047; *p*=0.626	M=0.0030, 0.0030; *p*=0.732	M=0.0010, 0.0010; *p*=0.339	M=0.0022, 0.0021; *p*=0.346	M=0.0022, 0.0023; *p*=0.440
DN (31) vs refractory (21)	M=0.0047, 0.0048; *p*=0.606	M=0.0030, 0.0030; *p*=0.728	M=0.0010, 0.0010; *p*=0.364	M=0.0022, 0.0021; *p*=0.374	M=0.0022, 0.0023; *p*=0.475

PT Responders (11) refractory (22)	M=0.0049, 00048; *p*=0.876	M=0.0031, 0.0030; *p*=0.769	M=0.0011, 0.0010; *p*=1	M=0.0023, 0.0021; *p*=0.52	M=0.0024, 0.0023; *p*=0.917
PT Responders (11) vs refractory (21)	M=0.0049, 0.0048; *p*=0.883	M=0.0031, 0.0030; *p*=0.774	M=0.0011, 0.0010; *p*=1	M=0.0023, 0.0021; *p*=0.526	M=0.0024, 0.0023; *p*=0.924
Refractory (22) vs HC (31)	M=0.0048, 0.0050; *p*=0.002	M=0.0030, 0.0031; *p*=0.055	M=0.0010, 0.0011; *p*=0.1	M=0.0021, 0.0023; *p*=0.001	M=0.0023, 0.0023; *p*=0.553
Refractory (21) vs HC (31)	M=0.0048, 0.0050; *p*=0.002	M=0.0030, 0.0031; *p*=0.073	M=0.0010, 0.0011; *p*=0.119	M=0.0021, 0.0023; *p*=0.002	M=0.0023, 0.0023; *p*=0.548
DN responders (25) vs DN refractory (6)	M=0.0048, 0.0044; *p*=0.288	M=0.0031, 0.0028; *p*=0.426	M=0.0010, 0.0009; *p*=0.169	M=0.0023, 0.0019; *p*=0.248	M=0.0023, 0.0021; *p*=0.381

Comparison of subcortical volumetric measures. DN= Drug Naïve, HC= Healthy Controls, PT= Post-treatment, M=mean (the first value corresponds to the first group specified in the comparison column). Number in parenthesis in the comparison column refers to the number of participants considered per group. Comparison resulted significantly different for multiple comparisons are highlighted in yellow. The last 3 comparisons were run twice using different patients' classification for responders/not responders.

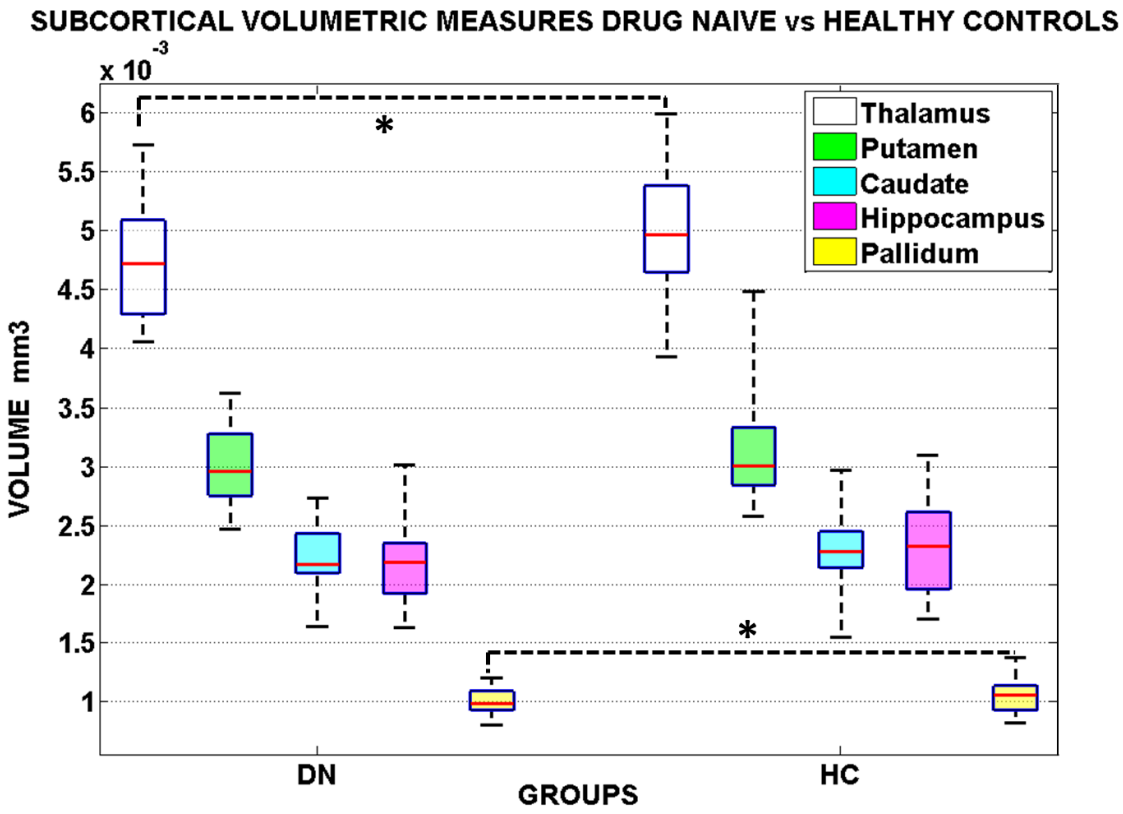

Figure 4.1: Volumetric measures in mm3 of Drug Naïve Patients (DN) vs Healthy Controls (HC). Thalamus and Pallidum are statistically significant (see text). * marks statistical significance surviving multiple comparisons between groups, upper limit of the box represents the upper quartile, lower limit represents the lower quartile, red line in the box is the median, error bars represent minimum and maximum values.

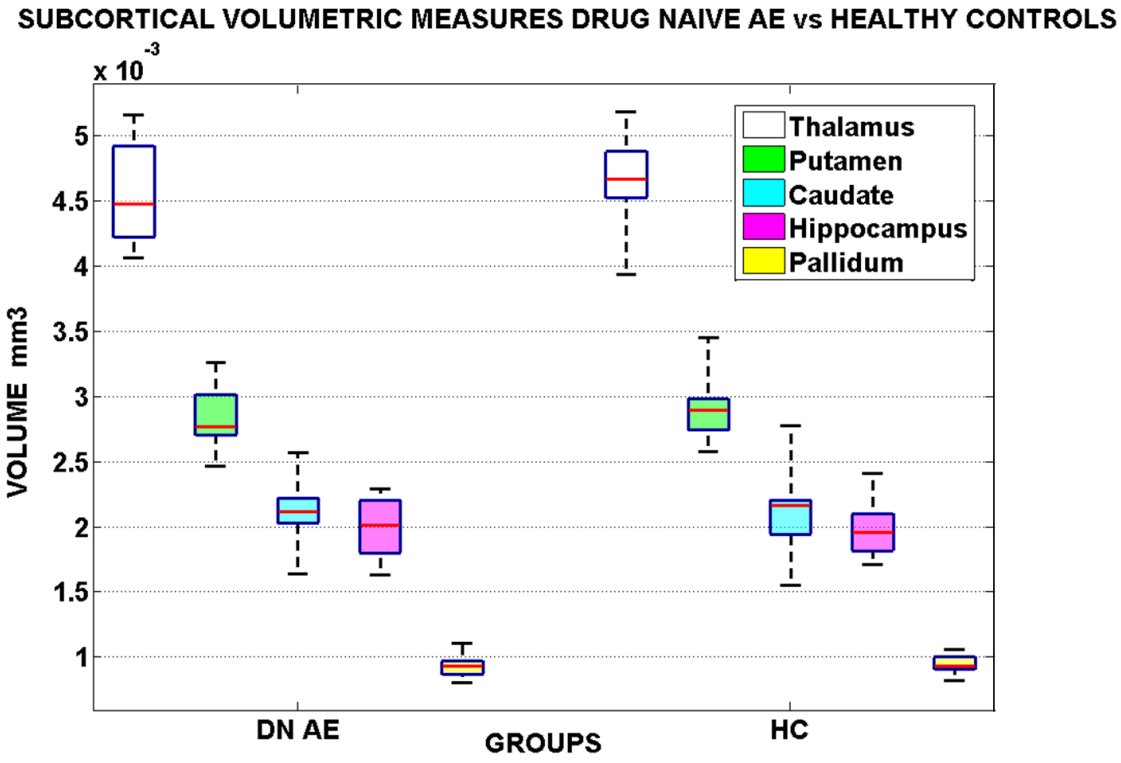

Figure 4.2: Volumetric measures in mm3 of AE Drug Naïve Patients (DN) vs Healthy Controls (HC). Upper limit of the box represents the upper quartile, lower limit represents the lower quartile, red line in the box is the median, error bars represent minimum and maximum values.

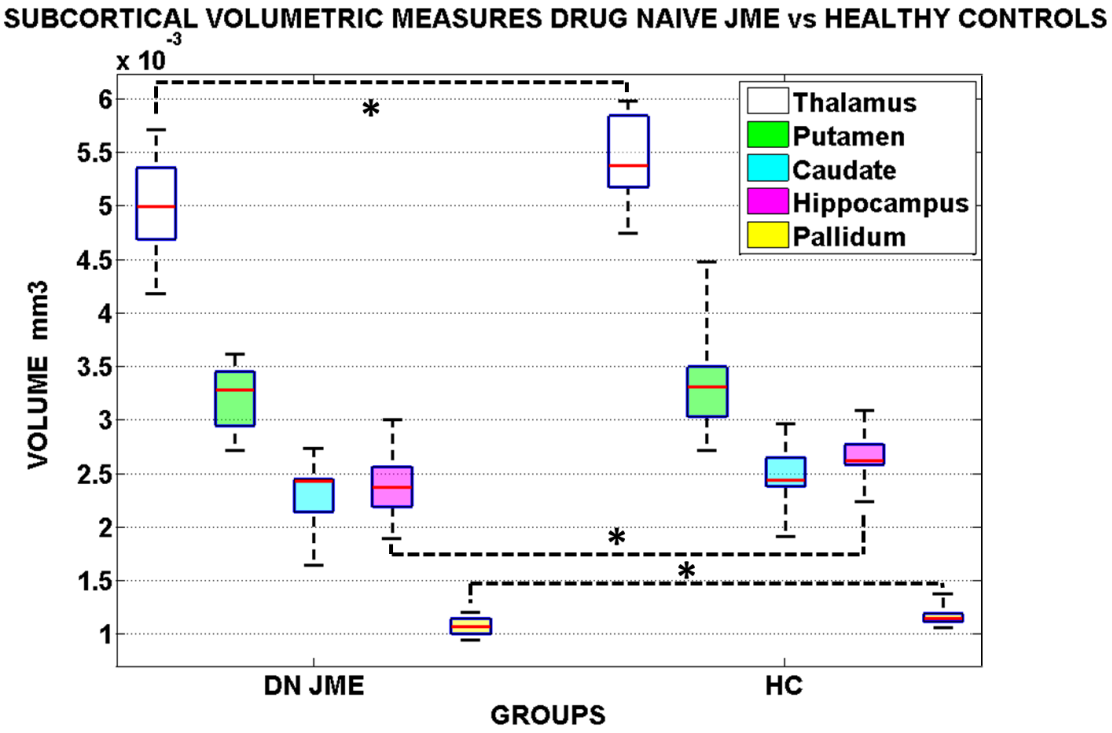

Figure 4.3: Volumetric measures in mm3 of JME Drug Naïve Patients (DN JME) vs Healthy Controls (HC). Thalamus, Pallidum and Hippocampus are statistically significant (see text); * marks differences between groups surviving statistical significance corrected for multiple comparisons. Upper limit of the box represents the upper quartile, lower limit represents the lower quartile, red line in the box is the median, error bars represent minimum and maximum values.

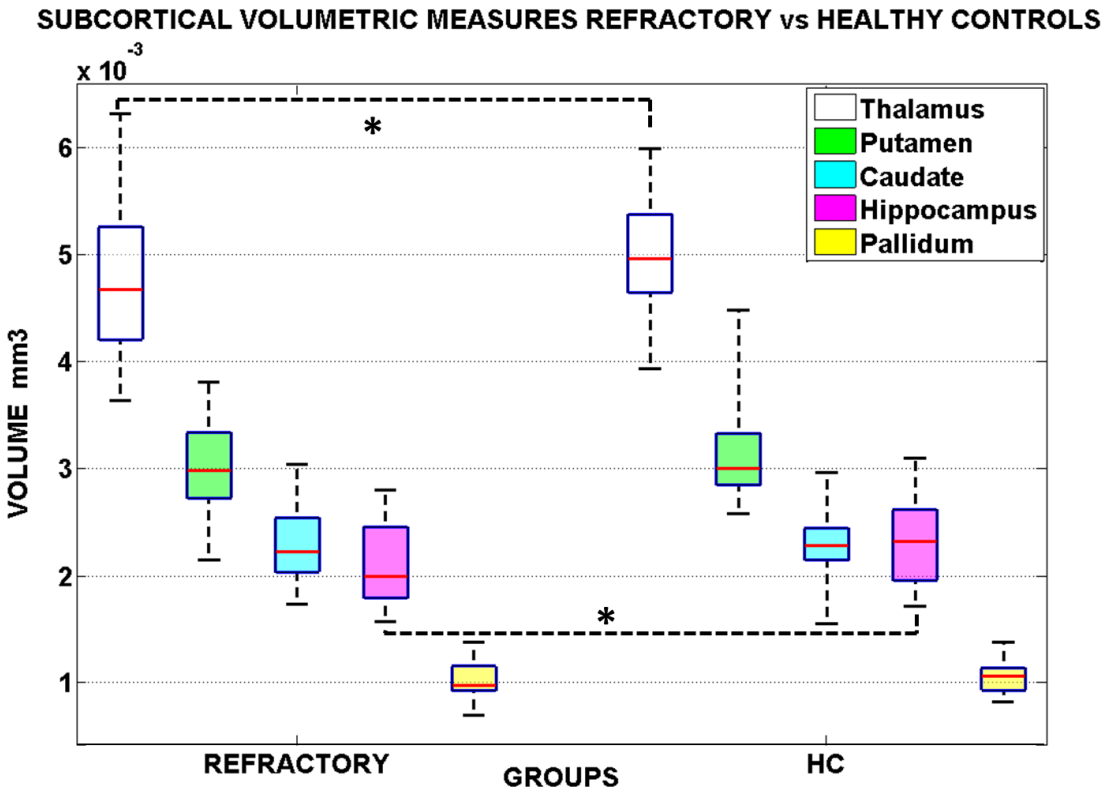

Figure 4.4: Volumetric measures in mm3 of Refractory Patients (post-treatment not–responders and Refractory) vs Healthy Controls (HC). Thalamus, Putamen and Hippocampus are statistically significant (see text); * marks differences between groups surviving statistical significance corrected for multiple comparisons. Upper limit of the box represents the upper quartile, lower limit represents the lower quartile, red line in the box is the median, error bars represent minimum and maximum values.

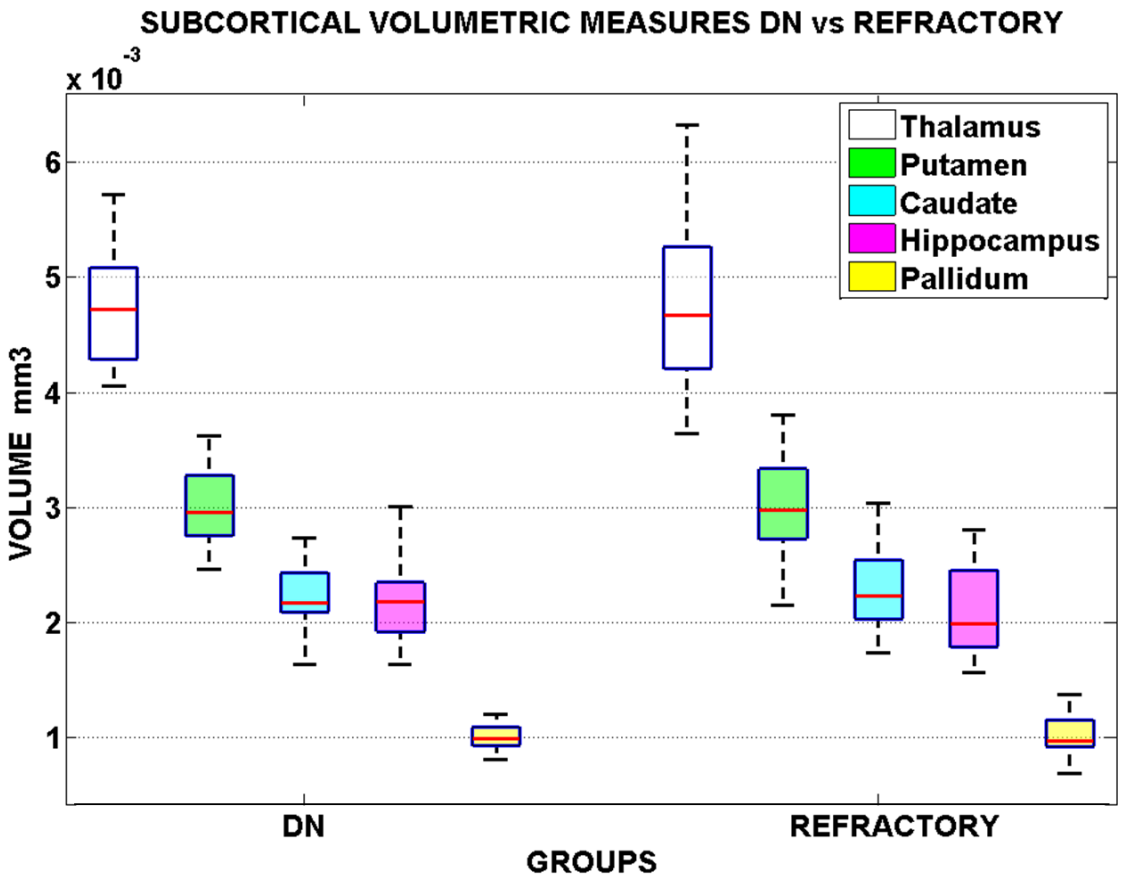

Figure 4.5: Volumetric measures in mm3 of Refractory Patients (long term Refractory and PT refractory) vs Drug Naive. Upper limit of the box represents the upper quartile, lower limit represents the lower quartile, red line in the box is the median, error bars represent minimum and maximum values.

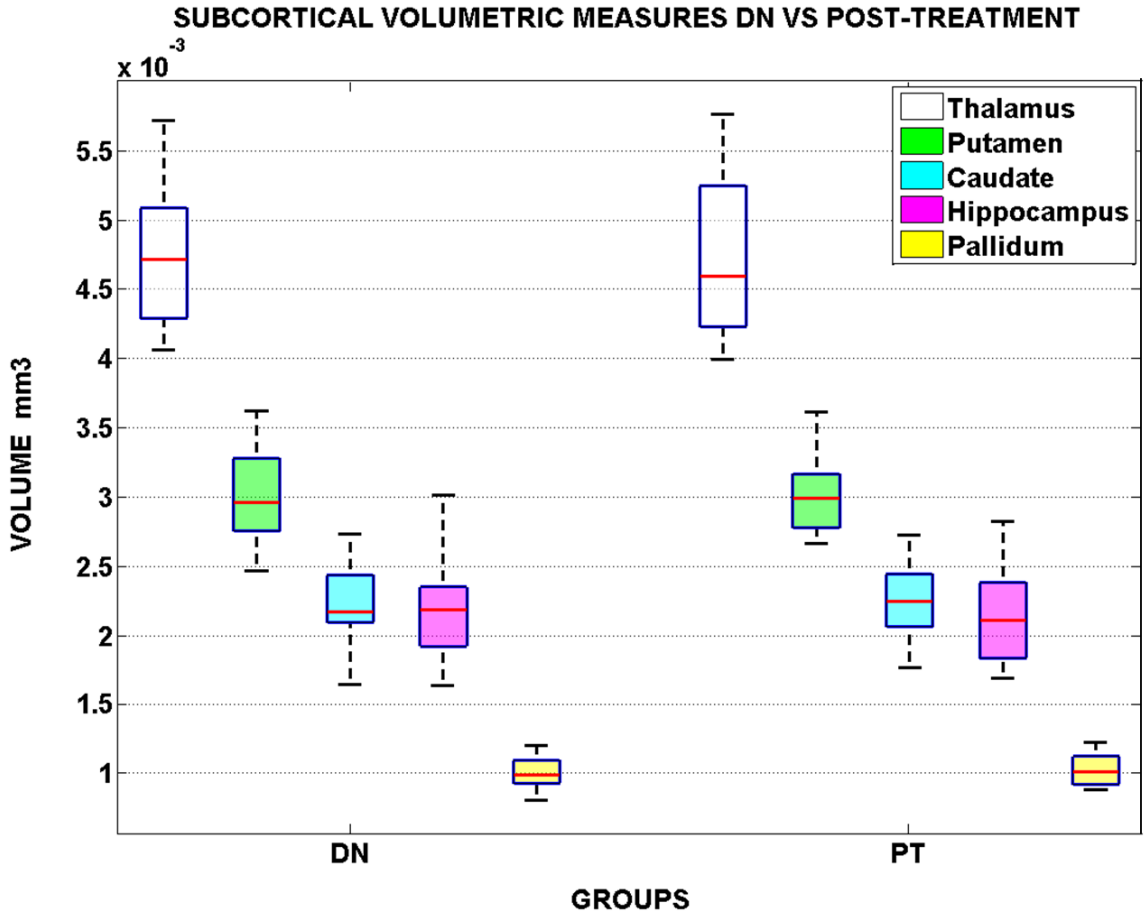

Figure 4.6: Volumetric measures in mm3 of DN vs Post-treatment (PT). Upper limit of the box represents the upper quartile, lower limit represents the lower quartile, red line in the box is the median, error bars represent minimum and maximum values.

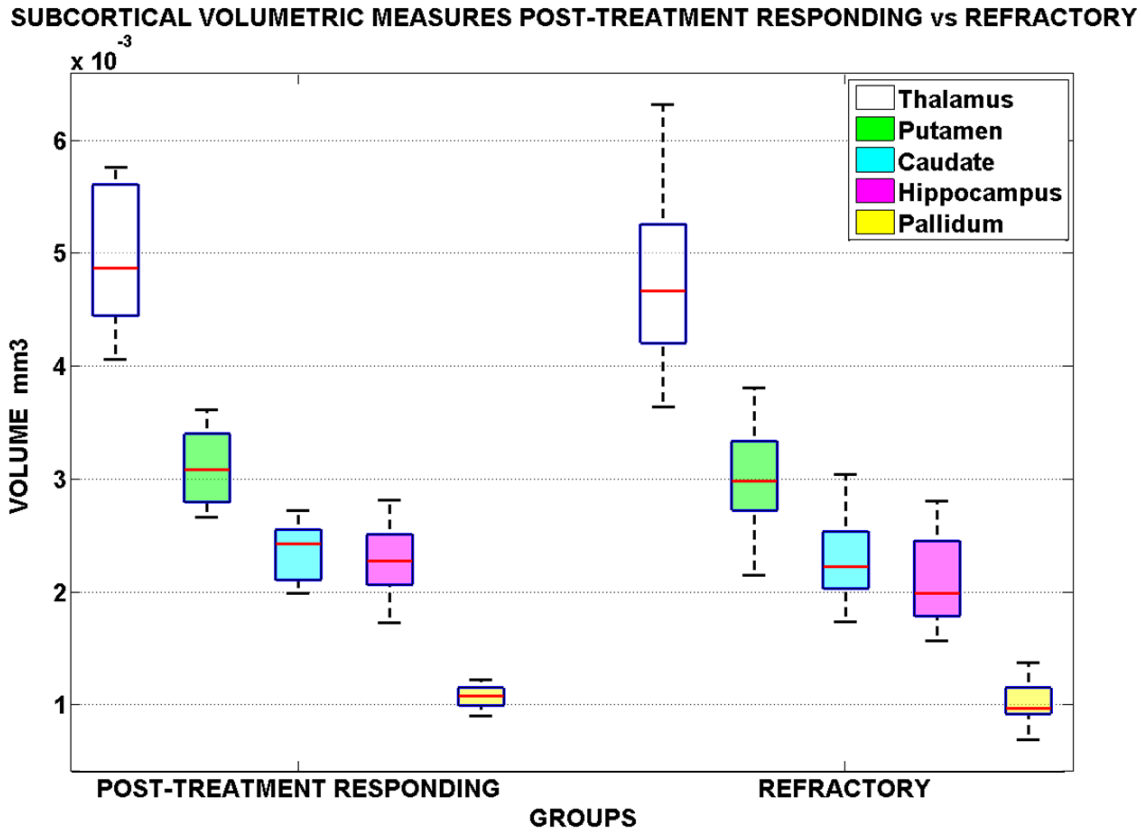

Figure 4.7: Volumetric measures in mm3 of Refractory vs post-treatment responding (PT responding). Upper limit of the box represents the upper quartile, lower limit represents the lower quartile, red line in the box is the median, error bars represent minimum and maximum values.

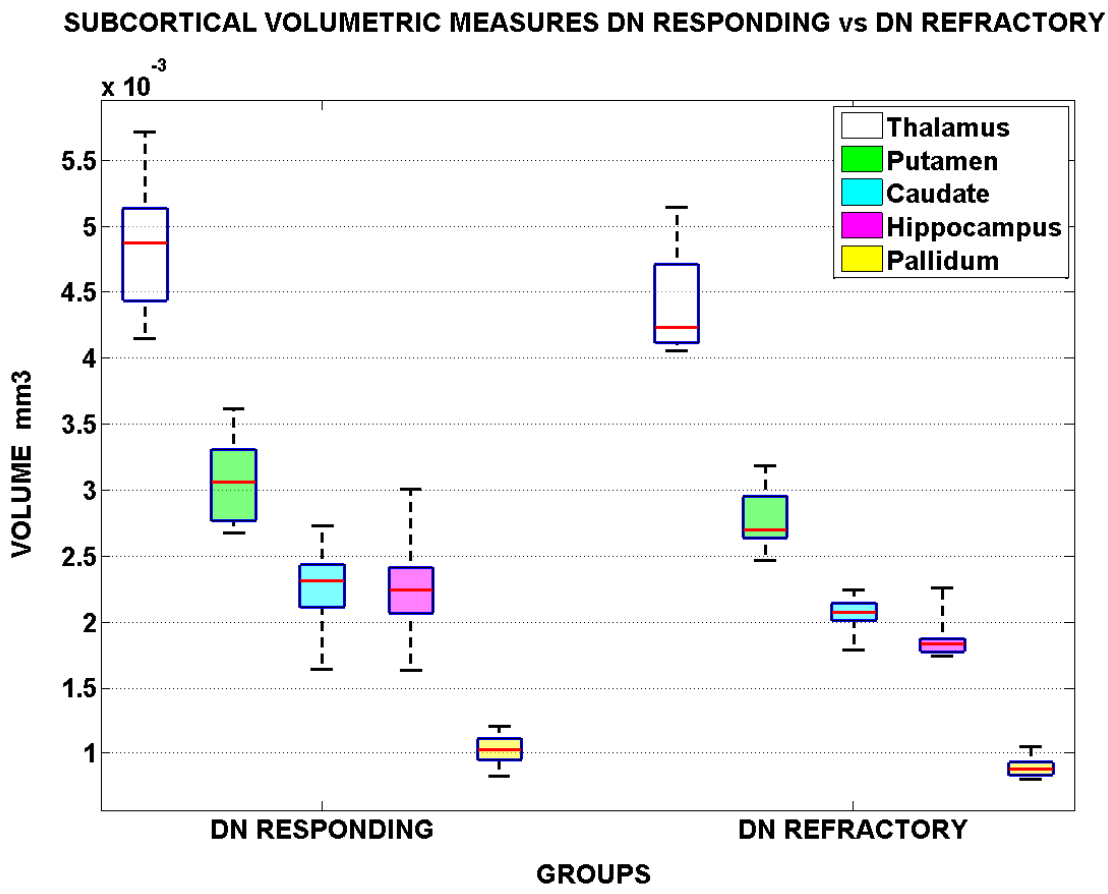

Figure 4.8: Volumetric measures in mm3 of Drug naïve patients with positive treatment outcome (DN responding) vs Drug Naïve patients with negative treatment outcome (DN refractory). Upper limit of the box represents the upper quartile, lower limit represents the lower quartile, red line in the box is the median, error bars represent minimum and maximum values.

We measured grey matter volume in the cortex to identify any differences in cortical structures (Table 4.3). We focused the comparison on specific cortical areas involved in the manifestation of GGE: prefrontal cortex, precentral cortex, cuneus and cingulate. We found that only the grey matter volume of the prefrontal cortex was significantly different between patients and HC participants if not correcting for multiple comparisons. The comparison of DN responders and DN refractory was not performed

due to the lack of numbers of not-responders (in 2 patients cortical parcellation was poor due to motion). Given the lack of differences in the volume of cortical areas, we focused the next analysis only on subcortical areas.

Table 4.3: Volumetric differences in cortical areas

Comparison	**PFC**	**PRECENTRAL**	**CUNEUS**	**CINGULATE**
DN (29) vs HC (30)	M=0.0508; 0.0528; *p*=0.033	M=0.0134; 0.0137; *p*=0.353	M=0.0027; 0.0027, *p*=0.97	M=0.0075; 0.0077; *p*=0.439
AE DN (14) vs HC (15)	M=0.0497; 0.0503; *p*=0.245	M=0.0128; 0.0126; *p*=0.963	M=0.0025;0.0025 ; *p*=0.770	M=0.0072; 0.0068; *p*=0.321
JME DN (15) vs HC (15)	M=0.518; 0.0553; *p*=0.08	M=0.0139; 0.0147, *p*=0.190	M=0.0028; 0.0028, *p*=0.9547	M=0.0078; 0.0085; *p*=0.130
DN (29) vs PT (16)	M=0.0508; 0.0502; *p*=0.366	M=0.0134, 0.0132; *p*=0.542	M=0.0027, 0.0026; *p*=0.259	M=0.0075, 0.0075; *p*=0.797
DN (29) vs refractory (21)	M=0.0508, 0.0515; *p*=0.783	M=0.0134, 0.0132; *p*=0.526	M=0.0027, 0.0026; *p*=0.735	M=0.0075, 0.0076; *p*=0.841
DN (29) vs refractory (20)	M=0.0508, 0.0517; *p*=0.834	M=0.0134, 0.0132; *p*=0.433	M=0.0027, 0.0026; *p*=0.701	M=0.0075, 0.0076; *p*=0.778
PT Responders (11) vs refractory (21)	M=0.0512, 0.0515; *p*=0.368	M=0.0136, 0.0132; *p*=0.625	M=0.0027, 0.0026; *p*=0.580	M=0.0077, 0.0076; *p*=0.940

PT Responders (11) vs refractory (20)	M=0.0512, 0.0517; *p*=0.373	M=0.0136, 0.0132; *p*=0.606	M=0.0027, 0.0026; *p*=0.583	M=0.0077, 0.0076; *p*=0.934
Refractory (21) vs HC (30)	M=0.0515, 0.0528; *p*=0.142	M=0.0132, 0.0137; *p*=0.245	M=0.0026, 0.0027; *p*=0.555	M=0.0076, 0.0077; *p*=0.643
Refractory (20) vs HC (30)	M=0.0517, 0.0528; *p*=0.14	M=0.0132, 0.0137; *p*=0.196	M=0.0026, 0.0027; *p*=0.533	M=0.0076, 0.0077; *p*=0.581

Comparison of cortical volumetric measures. DN= Drug Naïve, HC= Healthy Controls, PT= Post-treatment, M=mean (the first value corresponds to the first group specified in the comparison column). Number in parenthesis in the comparison column refers to the number of participants considered per group. Comparison resulted significantly different if not corrected for multiple comparisons are highlighted in green. The last 3 comparisons were run twice using different patients' classification for responders/not responders.

We compared the NBV across all the groups and we did not find any significant differences between DN and HC, JME DN and HC, AE DN and HC, DN and refractory, PT responding and refractory, refractory and HC, DN responding and DN refractory. NBV was found to be statistically significantly bigger in DN (M=1687323.122, SD=115370.1020) compared to PT (M=1639581.737, SD=116283.7651) ($F(1,42)=4.28$, $p=0.045$).

4.3.2 Shape analysis

Surface shape analysis indicated that drug naïve patients (DN) showed significant localised inward surface deflation of right and left thalami, right and left pallidum and bilateral hippocampi compared to healthy controls (HC), corrected for multiple

comparisons. Left thalamus showed differences between DN and HC in a continuum strip that connects anteriorly to posteriorly, whilst the right thalamus presented two different localised regions of differences, one anterior and one posterior. Left pallidum showed a deflection on its superior part which crosses from the anterior to the posterior part of the structure. The deflection of the right pallidum showed a difference in deflection only in its anterior part. Left and right hippocampi show a similar deflection in the more anterior part of the structures (Figure 4.9). No significant deflections were seen in the bilateral caudate or putamen (Table 4.4). No significant differences were found between AE DN and HC. Right pallidum was found statistically significant between JME DN and HC in the more anterior part of the structure (Table 4.4, Figure 4.10). No significant differences were found between DN and PT, between DN and refractory, between PT responders and refractory (Table 4.4). A significant difference was found between DN responder compared with DN refractory in the lateral part of the left pallidum (Figure 4.11).

Table 4.4: Shape analysis subcortical areas

Sub-cortical areas	DN vs HC	AE DN vs HC	JME DN vs HC	DN vs PT	DN vs refractory	Responders vs refractory	DN Responder vs DN refractory
THALAMUS	R and L	/	/	/	/	/	/
PUTAMEN	/	/	/	/	/	/	/
PALLIDUM	R and L	/	R	/	/	/	L
HIPPOCAMPUS	L and R	/	/	/	/	/	/
CAUDATE	/	/	/	/	/	/	/

DN=Drug Naïve, HC=Healthy Controls, PT=Post-treatment, R=right, L=left.

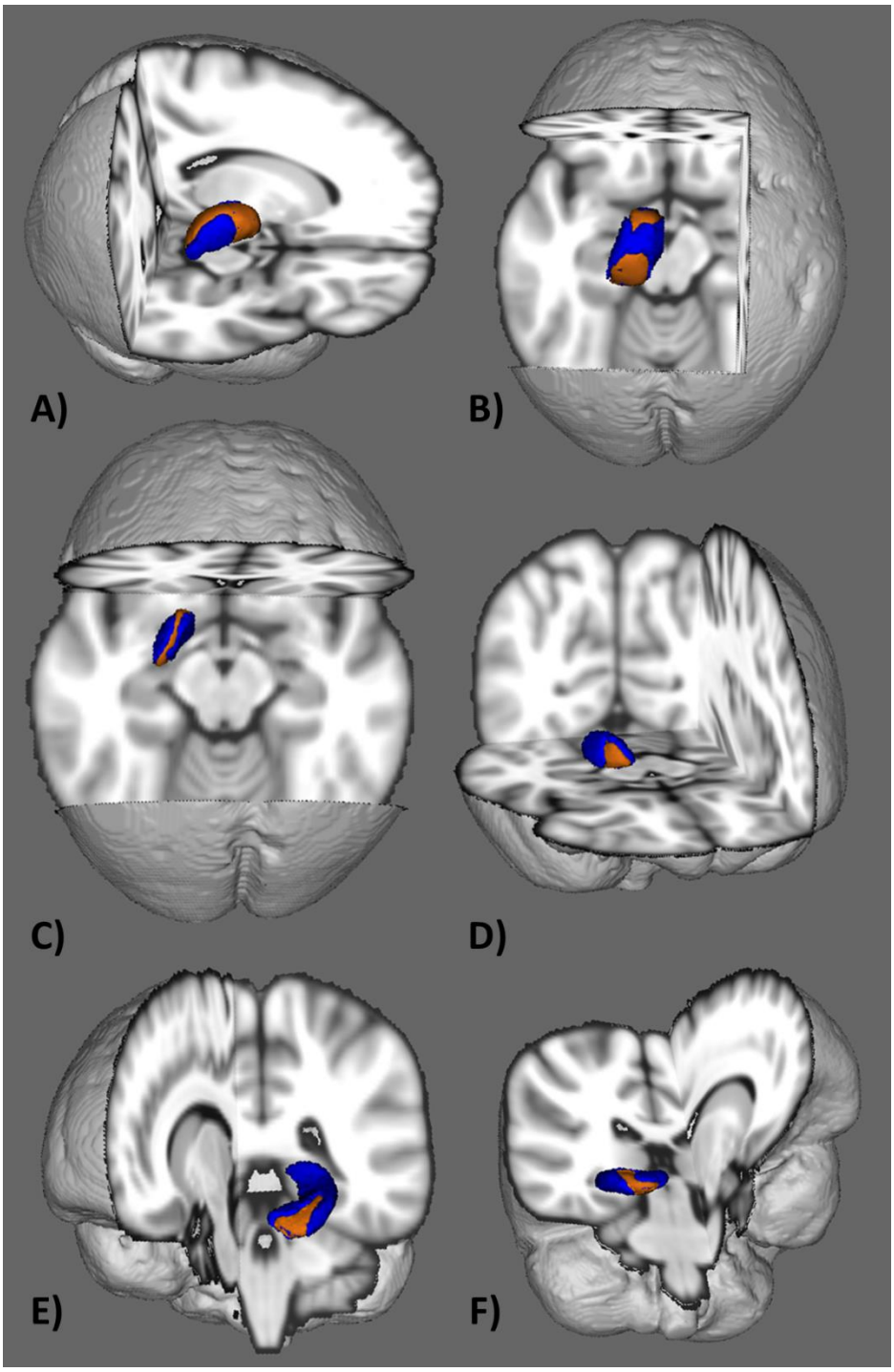

Figure 4.9: Shape differences between Drug naïve patients (DN) and healthy controls (HC). A) Left thalamus; B) right thalamus; C) left pallidum; D) right pallidum; E) left hippocampus; F) right hippocampus. Orange surfaces are the area of differences between drug naïve patients and healthy controls.

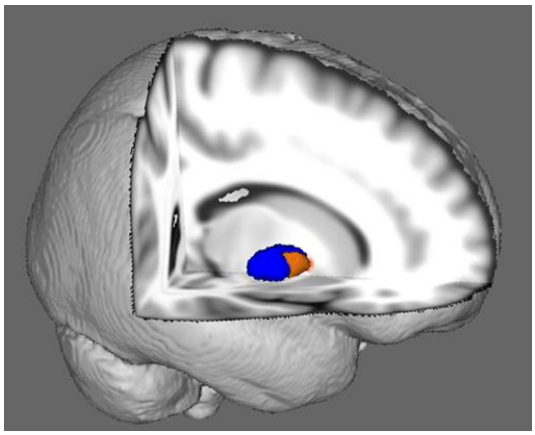

Figure 4.10: Shape differences between JME drug naïve (DN JME) and healthy controls (HC) in the right pallidum. Orange surface is the area of difference between JME drug naïve patients and healthy controls.

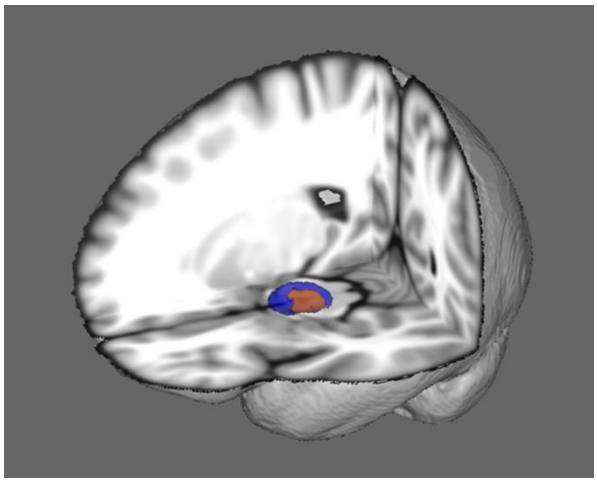

Figure 4.11: Shape differences between drug naïve patients responding to the treatment (DN responding) vs Drug naïve patients not responding to the treatment (DN refractory) in the left pallidum. Orange surface is the area of difference between drug naïve patients responding to the treatment vs drug naïve patients not responding to the treatment.

4.3.3 Voxel-based Morphometry

No statistically significant differences at a threshold of p=0.05 FWE were found between drug naïve patients and healthy controls using VBM. We explored the data below this threshold and found differences in bilateral thalamus and right hippocampus between DN and HCs at p=0.05 (uncorrected). Although this is not statistically significant, it suggests that there were changes in these regions in accordance with volumetric analysis and shape analysis results that our study was insufficiently powered to detect these using VBM.

4.4 Discussion

For the first time, we measured structural abnormalities in a drug naïve population diagnosed with GGE. Our unique sample of drug naïve patients followed-up longitudinally, allowed us to separate grey matter structural abnormalities and any potential influences of treatment; a subject of debate in this field of research.

We found that thalamus and pallidum were smaller in volume in the entire drug naïve group compared to healthy controls. Dividing the subjects between AE and JME, we found no significant volume differences comparing AE patients with matched controls. Wang et al., (2016) reported reduced thalamic volumes in a group of 20 drug naïve CAE (4 more than us). Although it is possible that the amount of patients made differences in the statistical power, we argue that the patients from Wang et al., (2016) had longer disease duration (1.86 years) than our sample (Table 3.1); therefore this difference in the syndrome specific group may have driven the differences. Contrary to AE, thalamus, pallidum and, additionally hippocampus were smaller in the JME group compared to

matched controls. Also, shape analysis showed that thalamus, pallidum and hippocampus had significant regional deflation in the entire drug naïve group compared to healthy controls. When the patients were split into their specific syndromes (AE and JME), most of these effects were not large enough to be detected; the only area of difference was the right pallidum being smaller in the JME group compared to controls. Our results are concordant with previous literature reporting reduction the grey matter volume in subcortical areas like thalamus (Saini et al., 2013) and pallidum (Du et al., 2011). In addition, we found differences in bilateral hippocampi confirming previous findings (Saini et al., 2013). Therefore, we have shown that thalamus, pallidum and hippocampus show volumetric differences in GGE patients before starting treatment, and that these are not related to AED. This was supported also from the lack of differences between volumes measured at drug naïve and post-treatment stages. On the contrary, cortical grey matter volumes calculated in prefrontal cortex, pre-central gyrus, cingulate and cuneus did not show statistical significant differences between drug naïve and healthy controls. Therefore, it is possible that the volumes of the cortical areas are influenced by AEDs. However, the prefrontal cortex did show a trend towards reduced volume in GGE compared to controls which may point to a difference that was not large enough to be detected with the statistical power in our study. Therefore, although this is the largest group available, given the complexities of the recruitment, this trend needs to be interpreted carefully and awaits replication.

The longitudinal data allowed the examination of changes in relation to disease progression. We did not find any difference between the volumes of subcortical and cortical areas before and after treatment. This suggests that changes in region volume

over the time period we used to follow-up (6 months) either do not occur or are too small to be detectable in our data. However, this is in accord with the negative correlation found between volume and disease durations (Woermann et al., 1998; Kim et al., 2013). Also our results are in accordance with previous results that suggested that structural abnormalities are present even before the onset of first seizure and they are possibly developmental in origin (Pulsipher et al., 2011). As 93% of our patients were diagnosed within 1 week from the pre-treatment scan, this suggests that structural abnormalities are present at the point of receiving the diagnoses. However, the real point of disease onset may be substantially different to the average point of diagnosis which is very difficult to establish given how subtle some epileptic features such absence seizures can be, particularly early in life. This was reflected in some parental reporting that was vague regarding the first seizures and the actual start of the condition.

For the first time, we also explored the relationship of volumetric abnormalities and treatment outcome. We observed differences in the shape of left pallidum between drug naïve patients who will respond to treatment and those who will not. In addition to this, a trend of decreased grey matter volumes in sub-cortical areas in patients not responding to treatment (including refractory post-treatment and refractory long-term) compared to patients responders to treatment was found. In particular, these reductions in subcortical grey matter volumes were found at the drug naïve stage. Overall, our results suggest that there may be an underlying difference in grey matter volume between patients responding and not responding to treatment. Further analysis with a bigger sample size of post-treatment not responders is needed to confirm this effect as it is only with

longitudinal data that is possible to gain unbiased information. In practice this is difficult to achieve given that we recruited over 11 sites for 3 years.

In addition, we reported no differences between NBV across groups supporting the idea that all differences in grey matter volumes found were not influenced by differences in the ratio between cortical/subcortical grey/white matter volumes. However, we found bigger NBV in DN compared to PT patients suggesting an influence of AED on NBV. This group did not show any differences in subcortical and cortical areas raising the question about the possible influence of the ratio between not only grey matter, but also white matter as an effect of AED. Further analyses are needed to explore this point in more detail.

Considering the reduced grey matter volume found in DN not responders compared to DN responders, we can speculate that this may also be a marker of treatment outcome.

4.4.1 Syndrome related differences

In this study we chose to consider all the drug naïve patients in one group given that similar studies suggested that there may be common factors shared between syndromes (Kjeldsen et al., 2003). Further evidence in support of this possibility comes from genetic studies that have identified the same recurrent chromosomal microdeletions in all the common GGE syndromes, showing substantial genetic overlap between syndromes (Dibbens et al., 2009; de Kovel et al., 2010). In these studies, the most frequently identified microdeletions have been reported in three of the four common GGE syndromes included in our study (de Kovel et al., 2010): microdeletions 15q11.2 were identified in patients with JME, JAE, CAE and GTCSO; microdeletions at 16p13.11 were found in JME and CAE and microdeletions at 15q13.3 were found in

JME, JAE, and CAE. In addition, previous studies looking at EEG (Chowdhury et al., 2014a), neuropsychological (Chowdhury et al., 2014b) and transcranial magnetic stimulation (Chowdhury et al., 2015) in the same subject group found endophenotypes shared across GGE syndromes.

We also decided to explore each syndrome separately given that there is also evidence suggesting that GGE syndromes are phenotypically similar but may be genetically and mechanistically more distinct (Berkovic et al., 1987; Andermann and Berkovic, 2001).

Our results showed differences only in the JME group compared to healthy controls when we separated the GGE sub-syndromes. Indeed, we found that the difference in GM volume and shape survived statistical threshold only in the JME group compared to healthy controls but not in the AE group. These results might suggest that most of the differences were contributed by the JME group. This is in accordance with previous findings that showed that the majority of patients with volumetric alteration were JME (Woermann et al., 1998) suggesting different patterns of cortical abnormalities in GGE sub-syndromes (Betting et al., 2006). However, there is also greater variability due to age variance within the AE group which can only be partially accounted for in a linear model. Therefore an alternative possibility is that the CAE group would require therefore a larger group to find a significant effect.

We did not look at white matter differences. It might be possible that further important information will be extracted by exploring the underlying white matter structures in both AE and JME drug naïve patients. Future work will aim to address this possibility.

4.4.2 Thalamo-cortical network

The involvement of subcortical structures in the pathogenesis of GSW, the hallmark of GGE has been well established. Thalamocortical circuits are thought to play an important role in the pathogenesis of GGE in experimental animal models (Blumenfeld, 2005a). In humans, electrophysiological studies demonstrate that the thalamus is integral to seizure generation (Crunelli and Leresche, 2002); EEG-fMRI studies have shown synchronous thalamic activation and cortical deactivation during GSW (Gotman et al., 2005; Hamandi et al., 2006); brain connectivity studies indicate thalami-cortical circuit abnormalities in patients with GGE (Richardson, 2012). Subcortical areas are well connected with the neocortex and depending on which connections are abnormal, different behavioural manifestations can occur (Haber and Calzavara, 2009). For example, some executive dysfunction observed in the patients with JME seems to be related with volume loss in the anterior thalamic nucleus projecting to the frontal lobe (Hughes et al., 2012).

Our results reveal areas of abnormalities that are related with functions linked to GGE, such as deflation and volume loss in thalamus and pallidum. Although our approach did not allow us to parcellate the subcortical areas in nuclei, we note that the anterior, dorsal and posterior parts of the thalamus were different in shape in the drug naïve group. These areas connect to frontal, SMA, post-central cortex and occipital cortex (O'Muircheartaigh et al., 2011b), all cortical areas found associated with GGE and possibly involved in the manifestation of myoclonic jerks (Vollmar et al., 2011). The globus pallidus communicates to the thalamus directly and is involved in the regulation of voluntary movement. A lesion of the pallidum can cause jerks amongst other

movement disorders. Atrophy of the hippocampi was reported in patients with JME (Lin et al., 2013) and its involvement in GGE might be related via connection to the thalamus (Irle and Markowitsch, 1982) and indirectly with frontal areas (Bird and Burgess, 2008). In addition, the hippocampi are often considered part of the DMN (Raichle et al., 2001) and this network has often been reported as being part of the GSW related BOLD response (Chapter 5).

4.5 Conclusion

For the first time we have demonstrated that subcortical abnormalities are present in very early onset GGE patients when drug naive. As 93% of our patients were diagnosed within 1 week from the drug naive scan, we also suggest that structural abnormalities are present since the beginning of the diagnosis given the limits of the definition of disease onset. Our data suggest that there is no rapid progression of volume loss with duration from disease diagnosis as the same pattern of differences was seen in pre-treatment, post-treatment and refractory patients. We also identified that there is an interesting trend of volumetric measures differences between patients responding to treatment compared to those not responding to treatment. Having established these differences in structural measures, in the following chapter functional MRI and EEG will be used to acquire a more comprehensive picture of the diseases and look at the functional networks in GGE drug naïve patients.

Chapter 5 : Core network in GGE part I: Spatio-temporal characterisation of the network associated with GSW in drug-naïve patients

5.1 Background

The network associated with GSW activity has been studied extensively using simultaneous EEG-fMRI (Gotman et al., 2005; Kay and Szaflarski, 2014; Pugnaghi et al., 2014). Overall agreement has been reached in the community that the fMRI response associated with GSW consists of a sub-cortical activation, particularly in the thalamus and deactivation of cortical areas including frontal and default mode brain regions (Gotman et al., 2005; Kay and Szaflarski, 2014). The suppression of the default mode network, found active during rest in healthy controls (Raichle et al., 2001), has been interpreted as central for seizure generation (Carney et al., 2010) setting against theories that the thalamic-cortical network is principally involved in the generation of GSW (Meeren et al., 2005). Since the last century, an open debate regarding the origin of GSW from the cortex (Luders et al., 1984; Holmes et al., 2004) or from the thalamus (Jasper HH, 1947) has been ongoing suggesting that generalised epilepsies may have a focal origin.

Recent evidence points towards the thalamus as the originating point for GSW formation given a particular interaction with the cortex (McCormick, 2002). However, another hypothesis regarding the origin of GSW points towards the cortex; and cortex and thalamus form a unified oscillatory network in which both structures drive each other only after the oscillation has been set into motion form the cortex (Meeren et al.,

2002). Several studies have attempted to understand which mechanism was more likely in humans by exploring the temporal sequence of events. Therefore, using the temporal resolution of fMRI, previous studies have tried to determine which brain regions drive GSW onset by studying brain activity prior to GSW (here called "pre-GSW activity"). Up to date, contrasting results have been reported. For example, studies in GGE patients using EEG-fMRI have reported that cortical regions show an increase in BOLD activity several seconds before GSW onset. In fact, this activity was found in posterior cortical regions, especially precuneus (Bai et al., 2010; Benuzzi et al., 2012; Masterton et al., 2013), as well as in frontal cortical regions such as orbital and medial frontal cortex (Bai et al., 2010; Benuzzi et al., 2012). Cortical regions then switch to a prolonged decrease in BOLD activity during GSW which lasts for several seconds after the discharge (Bai et al., 2010; Benuzzi et al., 2012). Thalamic activity has typically not been observed until GSW onset, although one study found thalamic activity several seconds before GSW onset (Moeller et al., 2008b). While another did not observe cortical changes prior to GSW (Moeller et al., 2008a); therefore, it remains unclear whether the cortex is driving the emergence of seizure activity or if the activity changes in cortex reflect a seizure-permissive (but otherwise normal) brain state.

Studies applying source imaging in MEG data have shown that the earliest activity related to GSW onset was in medial frontal and precuneus regions (Westmijse et al., 2009; Sakurai et al., 2010; Gupta et al., 2011; Miao et al., 2014), with thalamus possibly involved in propagating activity between these cortical sites (Miao et al., 2014); although MEG data may not accurately capture the activity of deep grey matter sources. However, a study using distributed source imaging of EEG data suggested that the

thalamus drives cortical regions at GSW onset (Moeller et al., 2013) and another study using MEG showed thalamic and frontal cortical sources simultaneously active at GSW onset (Tenney et al., 2013). Similarly, EEG distributed source analysis of GSW exclusively in JME showed that the precuneus was functionally most connected to other regions at GSW onset, suggesting that this region facilitates GSW onset (Lee et al., 2014), a finding supported by causal modelling of fMRI data during GSW (Vaudano et al., 2009); conversely, other studies found that the onset of discharges was localised to orbitofrontal and medial frontal sources (Holmes et al., 2010; Braga et al., 2014).

The variability of the results presented may be related to different factors. Indeed, the majority of the studies reported, have used mixed populations of patients who were under anti-epileptic medication (Gupta et al., 2011; Benuzzi et al., 2012) or who were previously on treatment (Carney et al., 2010; Masterton et al., 2013) . This will prevent unbiased comparisons between studies as treatment effects might interfere with the results. Up to date, we are aware of only two studies (Moeller et al., 2008a; Li et al., 2009) which have used drug naïve patients to detect BOLD changes related to GSW using simultaneous EEG-fMRI and two studies which recorded MEG data (Tenney et al., 2013; Miao et al., 2014). Moeller et al. (2008a) and Li et al. (2009) had limited number of subjects (6 and 12, respectively), therefore group comparison needs to be interpreted carefully (Friston K.J., 1999). Tenney et al. (2013) and Miao et al. (2014) had intrinsic spatial configuration problems of the neuronal activity due to the inverse problem limiting the interpretation of MEG results (Hamalainen et al., 1993). Therefore, the current state of the field is such that all the studies have some limitations related to

the potential influence of AED in the results, sample size and/or spatial resolution and no definitive conclusion can be reached.

Here we tried to circumscribe these limitations by studying the largest group of drug naïve patients diagnosed with GGE using simultaneous EEG-fMRI to date. This sample will allow exploring spatial and temporal characteristics of brain activity associated with GSW events. In addition, given the use of fMRI, we gained a better spatial resolution and capability to measure changes in deep grey matter regions than MEG or EEG alone.

We measured BOLD changes related to GSW onsets to identify if the pattern of activation/deactivation of thalamic-cortical network and default mode network is present in drug naïve patients as well as in treated patients (Kay and Szaflarski, 2014). In addition, we investigated BOLD changes occurring before GSW electrophysiological onset. Although most of the studies reported above focused on absence epilepsy patients, there is evidence that there is little difference between sub-syndromes of GGE in terms of the network generating the GSW (consistent with their electrophysiological similarity) (Pugnaghi et al., 2014). Therefore, the analysis presented here does not aim to distinguish between different syndromes but will concentrate on commonalities to answer the following questions: what are the BOLD changes related to GSW in a large group of drug naïve patients diagnosed with GGE? Are there region specific BOLD changes occurring before GSW electrophysiological onset?

5.2 Methods

5.2.1 Subjects

Drug naïve patients who underwent simultaneous video-EEG-fMRI and presented GSW during the recording were selected for this study. The sample included 16 drug naïve patients with AE (mean age=9.7 years), and 15 drug naïve patients with JME (mean age=20.7 years). A full list of the demographic characteristics of the participants is available in Table 5.1. For specification of the sample refer to Chapter 3.

Table 5.1: Sample selected for EEG-fMRI pre-GSW BOLD response analysis

GROUP	CODE	GENDER	AGE	GSW during EEG-fMRI
DRUG NAÏVE AE	#1	M	6.03	/
	#2	M	14.00	Y
	#3	M	10.51	Y
	#4	M	6.37	Y
	#5	M	10.58	/
	#6	F	13.65	Y
	#7	M	8.03	Y
	#8	F	7.73	Y
	#9	M	10.28	Y

	#10	F	9.72	/
	#11	F	16.18	Y
	#12	M	7.15	Y
	#13	M	9.26	Y
	#14	M	5.92	Y
	#15	M	6.84	Y
	#16	F	13.50	/
DRUG NAÏVE JME	#47	M	21.71	Y
	#48	M	16.75	Y
	#49	F	16.58	Y
	#50	F	13.64	/
	#51	F	20.11	/
	#52	M	35.98	Y
	#53	F	15.38	Y
	#54	F	17.69	/
	#55	F	26.04	Y
	#56	M	14.44	Y
	#57	F	25.94	/
	#58	F	31.23	Y
	#59	F	16.46	/
	#60	M	20.86	/
	#61	F	19.18	Y

5.2.2 Simultaneous video EEG-fMRI acquisition

Details of simultaneous video EEG-fMRI acquisition are described in the common methods (Chapter 3).

5.2.3 EEG-fMRI pre-processing

MR gradient and pulse-related artefacts were removed off-line from the EEG recorded inside the MRI using template artefact subtraction method (Allen et al., 1998; Allen et al., 2000) implemented in a commercial EEG processing package (Brain Analyser, Brain Products). EEG was down sampled to 250 Hz. GSW were identified after visual inspection and manually marked on the EEG traces for each session. GSW were marked in runs with onset and duration (length of the run).

All fMRI data were analysed using software package Statistical Parametric Mapping (SPM8) (http://www.fil.ion.ucl.ac.uk/spm) running under Matlab (Mathworks Inc., U.S.A.). After discarding the first four volumes to allow for T1-saturation effects, the EPI time series images were realigned to the first image, corrected with FIACH (Tierney et al., 2016), normalised to MNI space and spatially smoothed using an isotropic Gaussian kernel of 8mm FWHM (Friston et al., 1995). A more detailed specification of the pre-processing pipeline can be found in Chapter 3 Paragraph 3.8.

5.2.4 EEG-fMRI analysis

The fMRI data were analysed within the GLM framework to measure haemodynamic changes occurring before and during the electrophysiological onset of GWS.

5.2.4.1 Single subject analysis

For each subject, we created a nested model of GSW responses with two parts. In the first part we measured pre-GSW BOLD changes. We used a similar approach to Bagshaw et al. (2004). We defined a set of time points from 12s prior to the GSW, every 3s until GSW onset (0s) (i.e. -12s, -9s, -6s, -3s, 0s from GSW onset). These were convolved with gamma functions with window length of 10 and order of 1 that result in a peak response ~3s after the effect of interests selected points (i.e. -9s, -6s, -3s, 0s, 3s from GSW onset). This was set to account for variability in the onset and shape of possible pre-GSW BOLD responses (Bai et al., 2010). The duration of pre-GSW onsets was set to be instantaneous (0s) as we assumed that any changes prior to the GSW onset would be independent from the subsequent electrophysiological duration of GSW.

In the second part of the model we wanted a biophysically constrained but flexible model that could account for GSW duration. This is necessary because the duration of GSW events has a known influence on the BOLD response (Pugnaghi et al., 2014). We therefore convolved GSW with HRF, time and dispersion derivatives using GSW events defined by their EEG onset and duration.

The full model was then able to fit effects of interest peaking at -9s, -6s, -3s, 0s and +3s with gamma functions; and from +6s with the canonical HRF, time and dispersion derivatives (Figure 5.1). Six inter-scan realignment parameters from image pre-processing, 6 extra noise regressors from FIACH (Tierney et al., 2016) and the cartoon blocks were included in the GLMs as confounds. A high-pass filter of 128s was included to remove slow scanner drift unrelated to physiological BOLD changes.

SPM[T+] contrasts were generated at the single subject level to create con images that were used at the second level analysis to measure commonalities across patients.

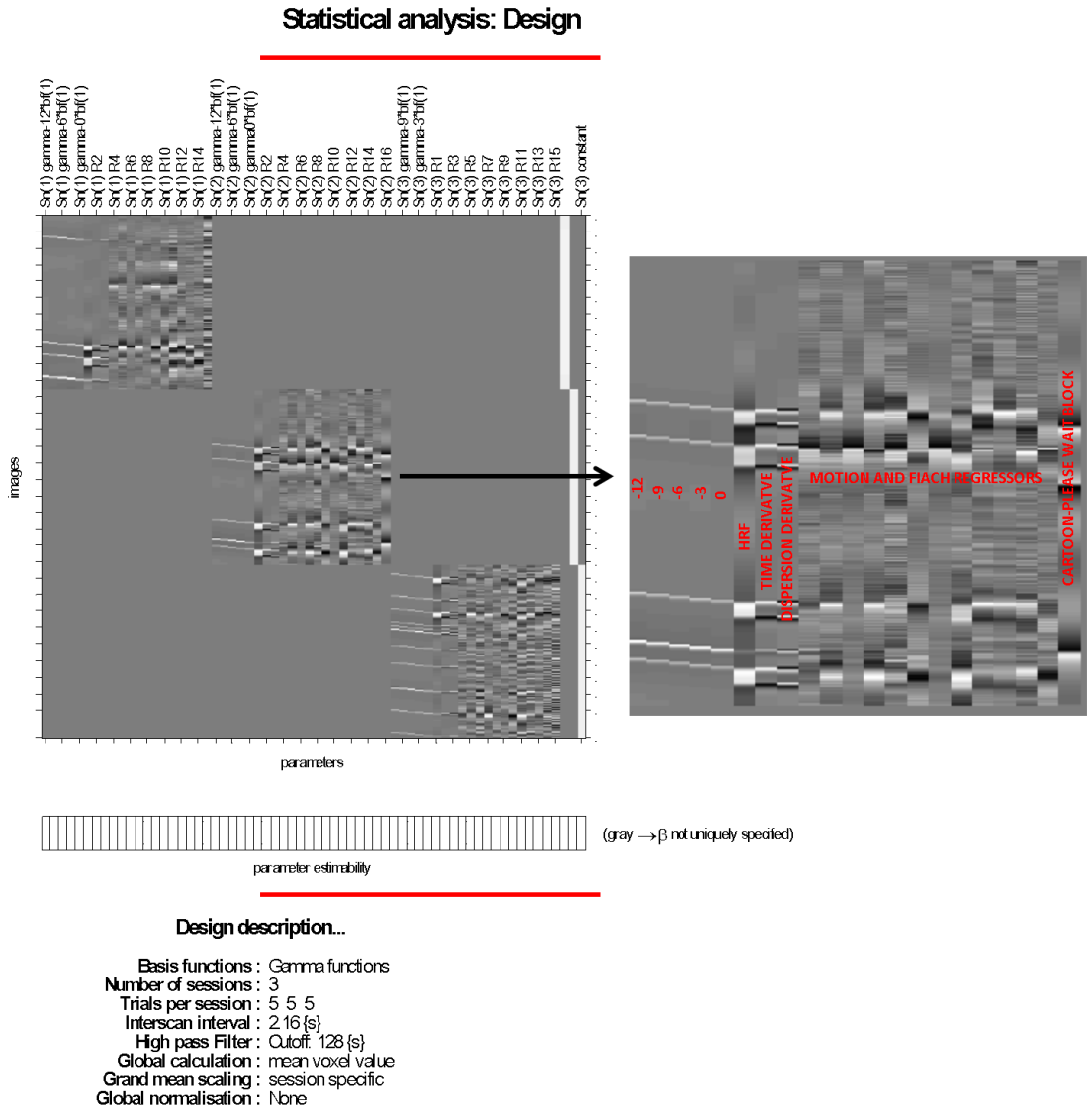

Figure 5.1: Single subject level design matrix. In the zoomed section of the model, from left to right, there are: numbers from -12 to 0 representing effects of interest convolved with gamma functions (first 5 columns); HRF+Time+Dispersion derivatives represents effects of interests convolved with HRF, time and dispersion derivatives (columns 6, 7 and 8); columns numbers 8-20 include noise; last column includes the task regressor.

5.2.4.2 Group level analysis

We calculated common areas of BOLD changes across patients using a 3x2 full factorial design at the second level. The first factor, "Basis functions", had 8 levels, one for each effect of interest explaining GSW BOLD responses: gamma functions with onsets at -12s, -9s, -6s, -3s, 0s, (instantaneous duration) and canonical HRF and its time and dispersion derivatives (onset 0s, duration based on GSW marking). The second factor was "Syndrome" having 2 levels, patient with AE and patients with JME (Figure 5.2). Con images derived from the single subject level contrasts were entered in this second level model. SPM[F] contrasts were calculated to identify pre-GSW and post-GSW related BOLD signal changes (Ashburner J, 2012b). A statistical threshold of $p<0.05$ FWE cluster level correction (which corresponds to $p<0.001$ uncorrected with extent threshold k=102 at voxel level) was used to determine significant results.

SPM[F] contrasts were built to explore the temporal evolution of BOLD changes related to GSW. We explored pre-GSW BOLD responses by constructing one SPM[F] contrast per effect of interest (onset times at -12s, -9s, -6s, -3s and 0s convolved with gamma functions). An SPM[F] representing all pre-GSW changes was calculated to test for regions with any pre-GSW changes. Correspondingly the spatial region of activation/deactivation related with electrographic GSW onset was calculated by performing an SPM[F] contrast across the post-GSW model (i.e. the GSW onsets convolved with HRF, time and dispersion derivatives).

5.2.4.3 Group level regional response extraction

As we were interested in the direction and dynamics of the BOLD response from 12s before GSW onsets up to their electrophysiological onsets, we wanted to visualise the

average fitted temporal response to GSW in regions exhibiting a significant response in the SPM[F] contrasts calculated from gamma functions (Paragraph 5.2.4.2). Also, as we were interested in the spatial location of main networks related with GSW, we wanted to visualise the average fitted temporal response to GSW in regions exhibiting a significant response in the SPM[F] contrasts calculated from HRF, time and dispersions derivatives (Paragraph 5.2.4.2). The results of the group level model give the betas for every voxel in the brain. The fitted response is therefore the product of the basis set described in Paragraph 5.2.4.1 and the group level betas taken from the second level model estimation. To achieve this, we created a design matrix containing the basis set used in the model described in Paragraph 5.2.4.1 with higher temporal resolution (0.2s) than the repetition time used for fMRI acquisition (2.160s). The mean temporal responses of the voxels within the clusters of interest were plotted with +/- the standard deviation of the response across the cluster.

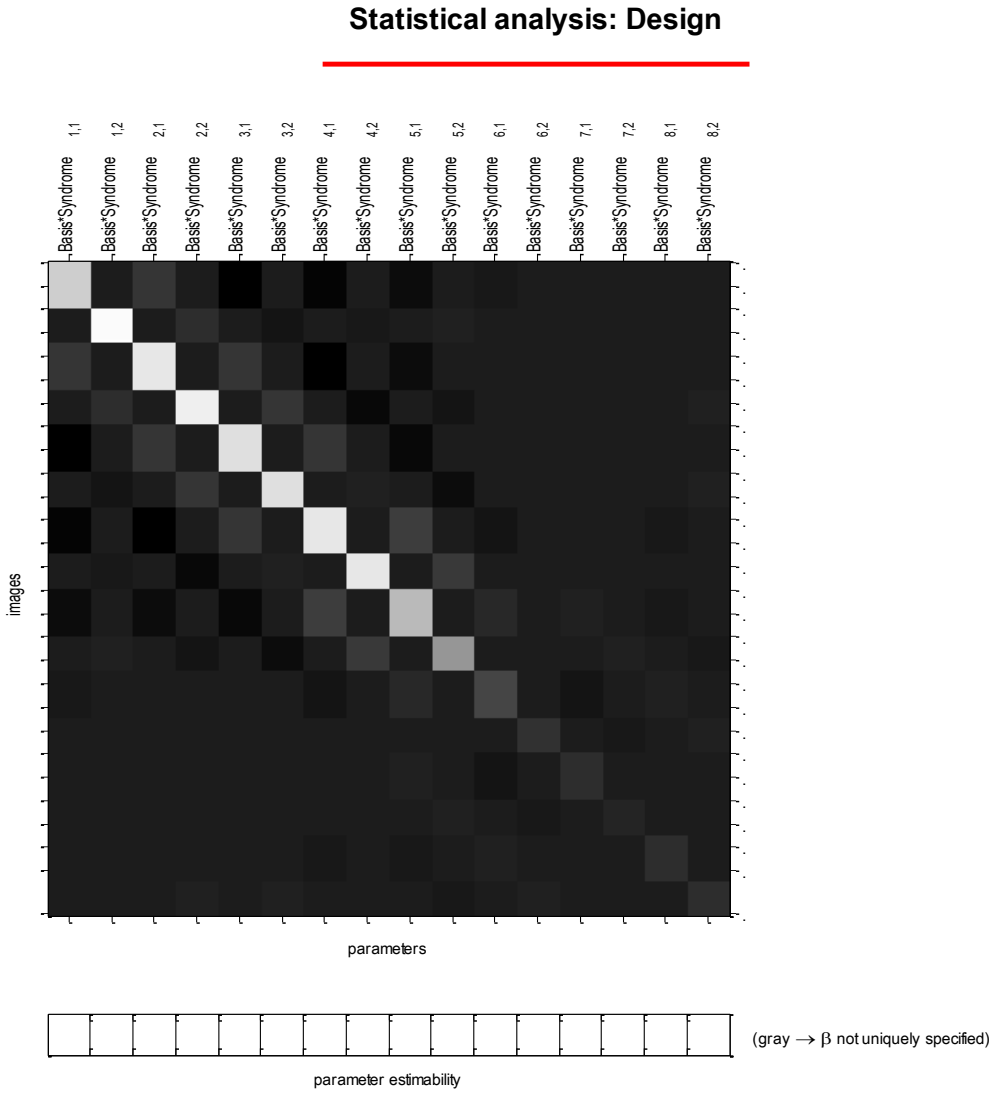

Figure 5.2: Group level analysis full factorial design matrix.

5.3 Results

We recorded GSW during simultaneous video-EEG-fMRI in 21 patients. We excluded 12 patients from our analysis; in one patient the MRI was corrupted by artefacts and in 11 patients we did not record GSW events. We included 12 drug naïve patients diagnosed with AE and 8 patients diagnosed with JME. We recorded a total of 119 runs of GSW in the AE patients group (mean duration= 6.87s, SD=5.65) and 60 runs in the JME patients group (mean duration=1.41s, SD=1.15).

5.3.1 GSW-related BOLD response at GSW-onset using canonical HRF, Time and Dispersion derivatives

The GLM presented in Figure 5.2 allowed us to explore BOLD responses pre and post-GSW onset. The post-GSW model was created via the convolution of the onsets with canonical HRF and its time and dispersion derivatives to allow for variability of response shape. The directionality of the BOLD response for the time and dispersions derivatives cannot be meaningfully assessed using t-tests (the derivative estimates depend on the size (and sign) of the HRF estimate (Ashburner J, 2012a)). Therefore the network associated with GSW events was assessed using an SPM[F] contrast across the combination of the HRF, time and dispersion derivatives and information about the directionality and shape was extrapolated from the fitted response.

SPM[F] maps showed changes in mesial frontal cortex, bilateral parietal cortices, posterior cingulate and bilateral caudate. Other areas of activity were found in the bilateral dorso-lateral middle frontal cortices, occipital cortex, unilateral fusiform gyrus,

unilateral insula, superior and middle temporal gyri and inferior frontal gyrus (Figure 5.3, Table 5.2).

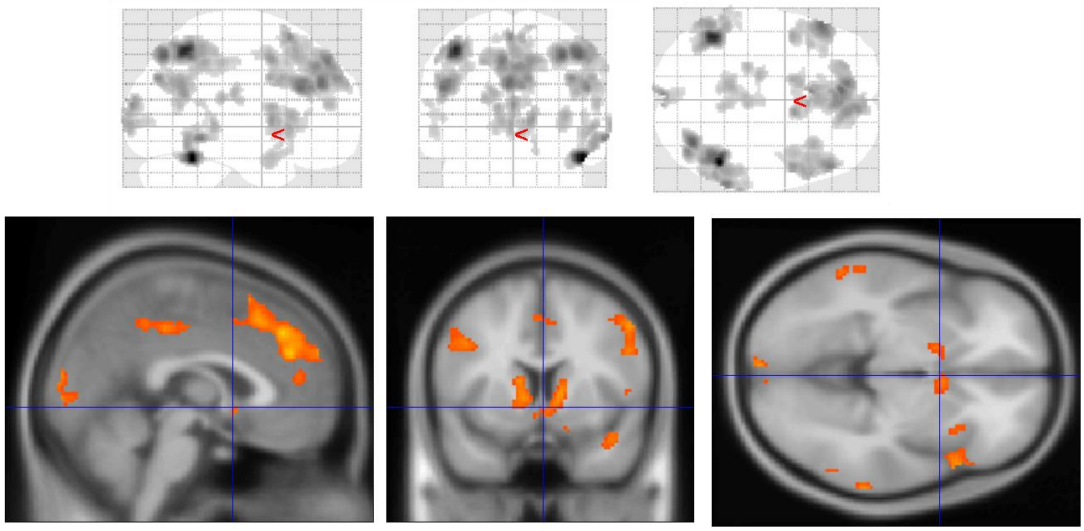

Figure 5.3: SPM[F] maps of post GSW-related BOLD response (onsets and durations convolved with canonical HRF, Time and Dispersion derivatives).

5.3.2 Fitted response of GSW "classical" core network

GSW SPM[F] maps of the HRF time and dispersion derivatives showed areas of activity which included the "classical" GSW-related networks: sub-cortical areas such as caudate; and cortical regions such as bilateral parietal cortex, PCC and mesial frontal cortex. We plotted the fitted response for these areas to explore the directionality of the BOLD response following canonical HRF and its time and dispersion derivatives (therefore peaking at about +6s from onset). Parietal cortex (most prominently left) and PCC showed a negative BOLD response whilst mesial frontal cortex and bilateral caudate showed a positive BOLD response (Figure 5.4).

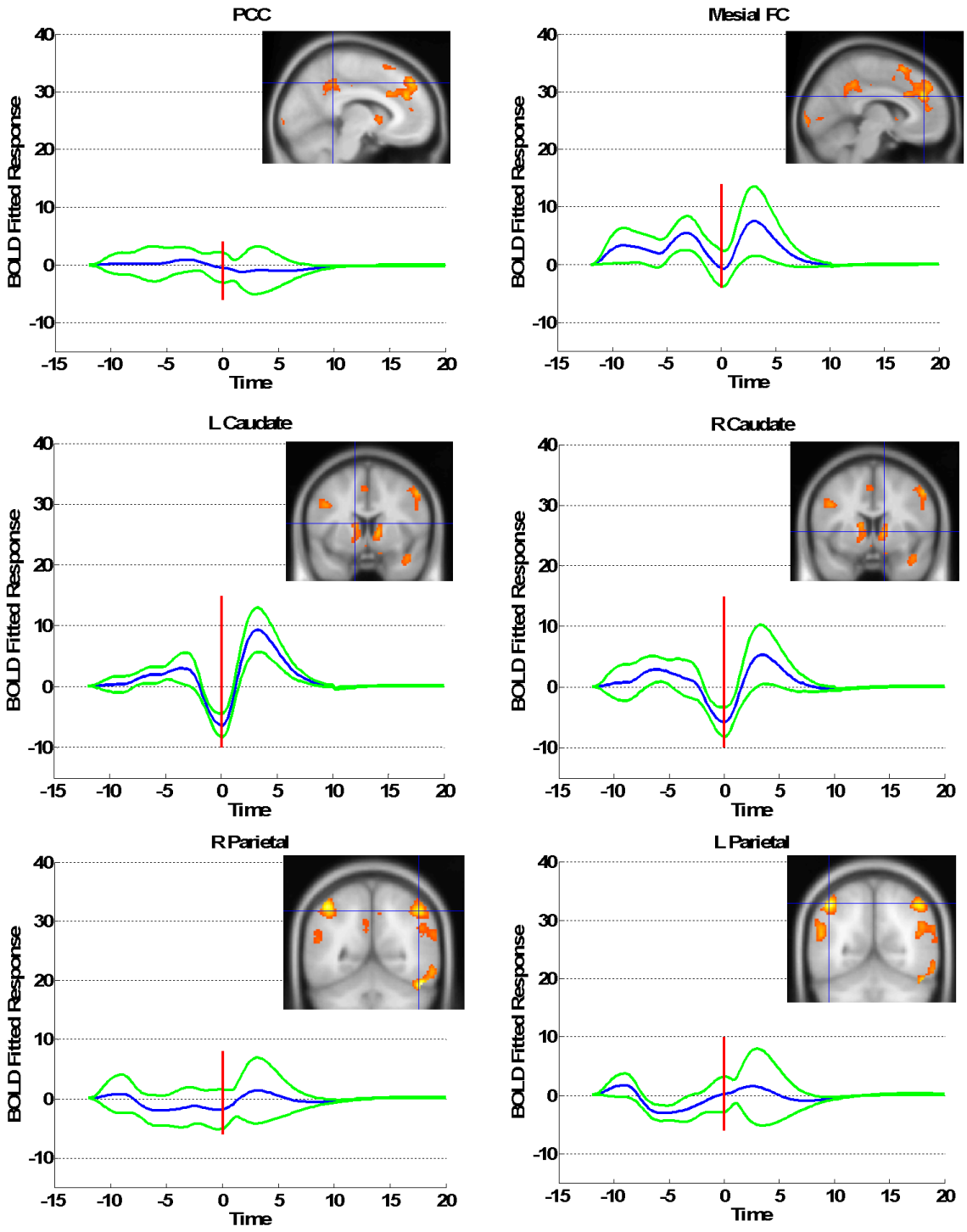

Figure 5.4: Group level BOLD fMRI response calculated with SPM[F] maps for selected cluster representing the "classical" network related to GSW convolved with HRF, time and dispersion derivatives. The mean cluster BOLD fitted response (blue) is plotted with +/- standard deviation (green). Red line marks the

electrophysiological onset of GSW. R=right, L=left, FC=frontal cortex, PCC=posterior cingulate cortex.

5.3.3 GWS-related BOLD response pre-GSW using gamma functions

A basis set of gamma functions was used pre-GSW to look for early BOLD signal changes that cannot be captured by the canonical HRF and derivatives. SPM[F] maps showed no changes surviving the statistical threshold of $p<0.05$ FWE corrected, cluster level, at onsets of 12s and 9s before electrophysiological recording of GSW. A significant BOLD response was found in the mesial superior frontal cortex at 6s before GSW electrophysiological onset and caudate/thalamus at 3s before GSW onset. Bilateral caudate was found significant at the onset of GSW together with bilateral insula, right inferior frontal gyrus and right superior temporal and middle frontal gyri (Figure 5.5, Table 5.2).

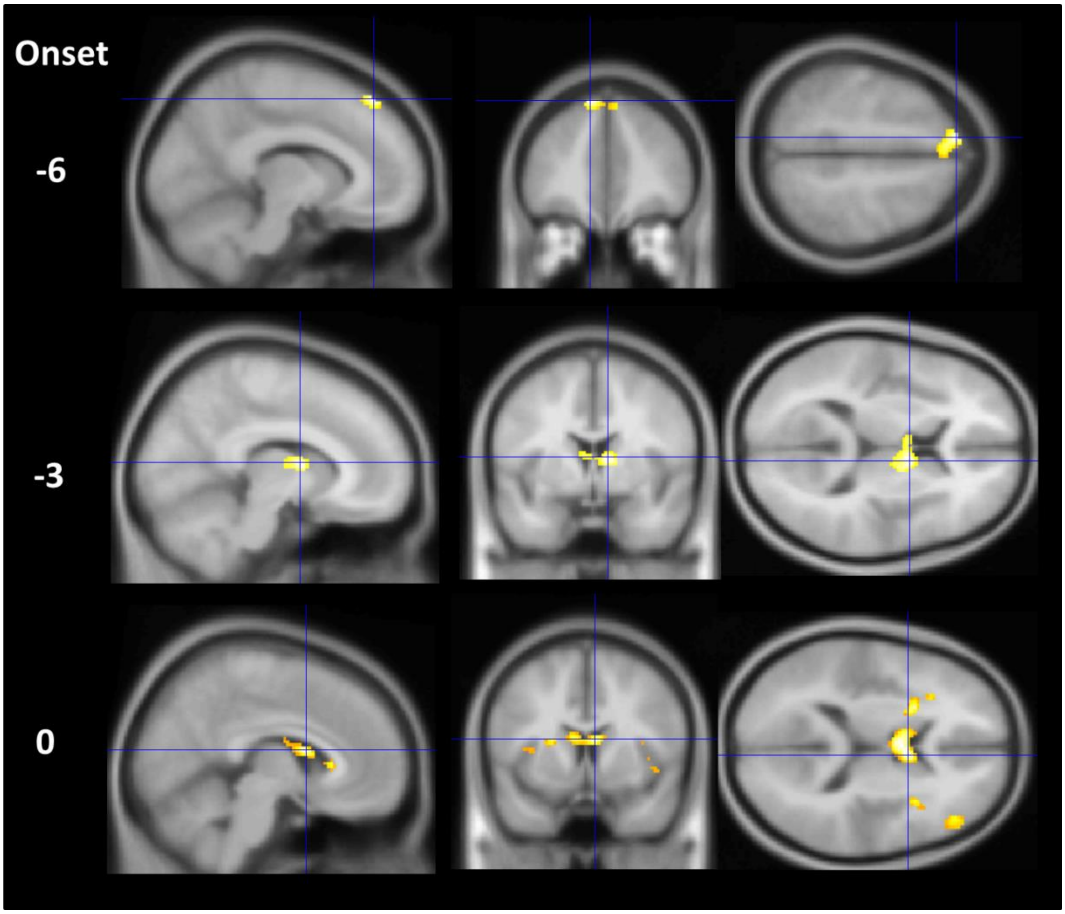

Figure 5.5: BOLD response changes 6s and 3s before and at onset of GSW using gamma functions (peak of the function at -3s, 0s and +3s).

Table 5.2: GSW-related BOLD response for each effect of interest.

SPM[F] contrast	AE+JME	x, y, z
-12	/	
-9	/	
-6	S MESIAL FC	-10 40 54
-3	R THALAMUS/ L CAUDATE	-10 2 10
0	BILATERAL CAUDATE	6 8 14
	L INSULA	-26 12 12
	R STG/R INSULA	50 14 6
	R IFG/MFG	48 36 12
-12+-9+-6+-3+0	BILATERAL CAUDATE	6 8 14
HRF+Time+Dispersion	R FUSIFORM GYRUS	48 -52 -24
	L INFERIOR PARIETAL	-44 -58 52
	R INFERIOR PARIETAL	46 -54 48
	MESIAL FC	-6 42 28
	L DORSO-LATERAL MFG	-2 26 26
	R DORSO-LATERAL MFG	52 32 26
	OCCIPITL CORTEX	-2 -96 14
	L STG	-52 -58 22
	R CAUDATE	12 6 4
	R IFG	56 18 -2
	L CAUDATE	-12 6 12
	PCC	-8 -44 42
	R INSULA	36 20 6
	L MTG	-58 -50 -4

GSW-related BOLD changes (p<0.05 FWE corrected, cluster level). R=right, L=left, PCC=posterior cingulate cortex, FC=frontal cortex, ITG=inferior temporal gyrus, MFG=middle frontal gyrus, STG=superior temporal gyrus, IFG=inferior frontal gyrus.

5.3.4 Early BOLD changes associated with GSW

SPM[F] maps showed significant pre-GSW and GSW-onset related BOLD responses at statistical threshold of $p<0.05$ FWE corrected, cluster level as implemented in the random field theory framework in SPM (Figure 5.3, Figure 5.5). However, for all the

areas, BOLD response at the second level is a static map related to the particular effect of interest with no time information (Ashburner J, 2012a). Therefore, fitted responses across time of the clusters resulted significant in the SPM[F] contrasts of each gamma functions and across all 5 gamma functions were plotted (Figure 5.6). We found that caudate, thalamus, right inferior frontal gyrus and right superior temporal gyrus showed a positive BOLD response from 12s to 3s before GSW onset; negative BOLD response was measured during GSW onset and a positive BOLD response was measure 2s after GSW onset. Different was the mean BOLD response found in the left insula cluster that showed a very low amplitude positive BOLD response prior to GSW onset, a settled negative BOLD response at GSW onset and a positive BOLD response changes after GSW onset. Mesial frontal cortex showed positive BOLD response 10s and 3s before GSW onset, negative BOLD response around 7s prior to GSW onset and at GSW onset following positive BOLD response after 3s since GSW onset (Figure 5.6).

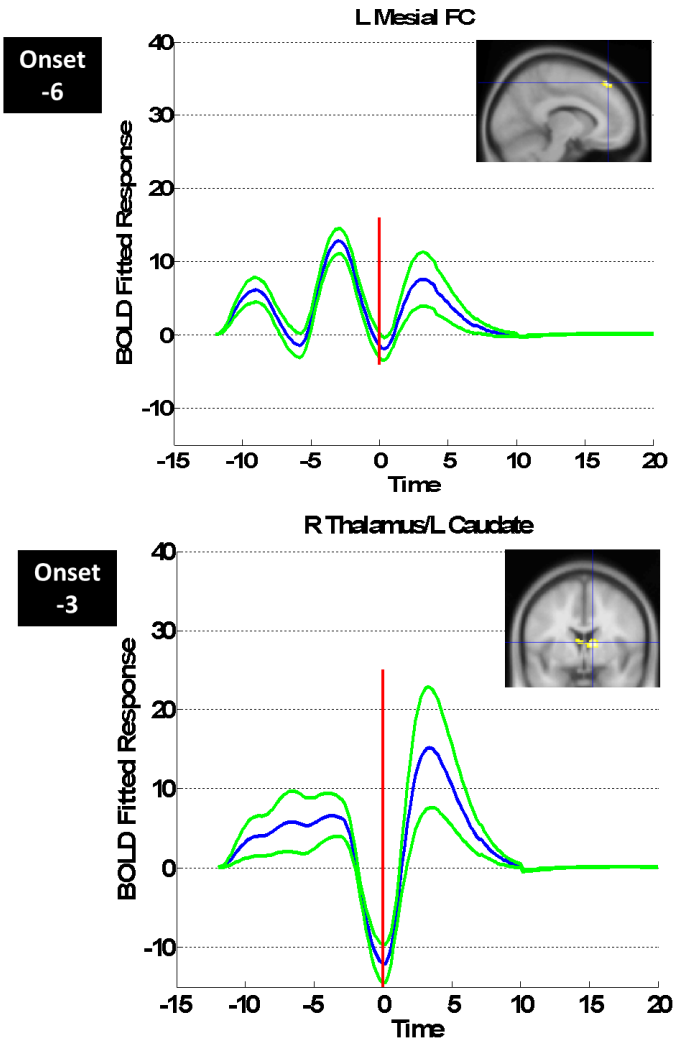

(Figure 5.6 continues in the following page)

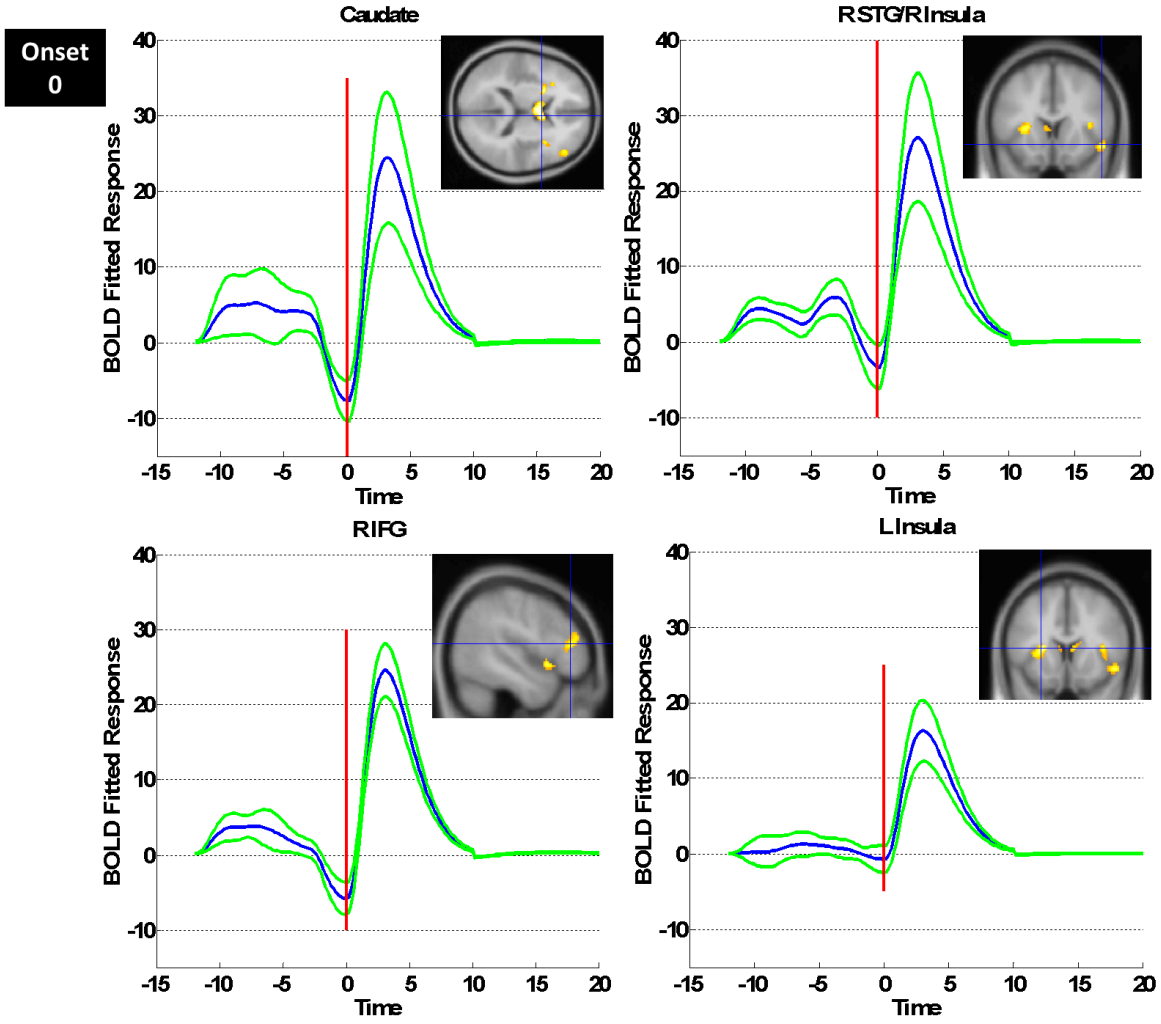

Figure 5.6: Group level BOLD fMRI response calculated with SPM[F] maps for each and all onsets time (-6s, -3s, 0s) convolved with gamma functions. The cluster mean BOLD fitted response (blue) is plotted with +/- standard deviation (green). Red line marks the electrophysiological onset of GSW. Selected visualisation of the cluster plotted is on the left. R=right, L=left, FC=frontal cortex, IFG=inferior frontal cortex, STG=superior temporal gyrus.

5.4 Discussion

In this study we measured GSW-associated BOLD responses in the biggest group of drug naïve patients diagnosed with GGE studied to date. We measured BOLD response

changes at the onset of the GSW to identify if drug naïve patients showed the same pattern of activation and deactivation of the thalamic-cortical network and DMN found in treated patients. We also measured changes before GSW onset to understand early BOLD changes that might relate to seizure initiation.

We found that DMN and the thalamic-cortical network were involved in GSW BOLD response changes in drug naïve patients, as in patients already treated with AEDs. Selecting the BOLD responses peaking 6 seconds after GSW onset following HRF and its time and dispersion derivatives shape, the DMN was found deactivated during GSW while caudate was found being activated. Therefore, we are confident to conclude that the same pattern of activation/deactivation of the thalamus/cortex is found in drug naïve patients as has been previously described in patients on AED treatment (Gotman et al., 2005; Hamandi et al., 2006; Laufs et al., 2006)

We also measured BOLD responses in brain areas prior to GSW onset. The earliest BOLD response changes we found were at about 6s before GSW onset in the frontal cortex. This suggests a role for this area in first generating GSW. BOLD changes in the thalamus were found later on, starting about 3s before GSW onset, suggesting a secondary role in the generation of GSW.

5.4.1 Drug naïve GSW BOLD changes

Significant BOLD responses in the thalamic-cortical network and in the default mode network were found at the electrophysiological onset of GSW in the largest group of drug naïve patients diagnosed with GGE available in literature. This suggests that the pattern of activity in the functional networks is independent of AED intake. Additional

areas were seen at GSW onset: bilateral insula, occipital cortex, fusiform gyrus and temporal cortex. These areas were found inconsistently across studies. For example, insula was reported only in one study (Gotman et al., 2005) while occipital and temporal cortices were reported more frequently (Aghakhani et al., 2004; Gotman et al., 2005; Hamandi et al., 2006; Laufs et al., 2006). Considering that some studies have relied on previous findings and used regions of interest analysis (Moeller et al., 2008b; Moeller et al., 2008a), in which only specific brain regions related to the thalamic-cortical network and DMN were targeted, it is possible that additional areas were neglected from the results. For this reason, we decided not to use ROIs. In addition, exploring whole brain activity has given the opportunity to fully interrogate the unknown GSW BOLD response of drug naïve patients.

The insula is a region of convergence of multisensory inputs that has recently been implicated in focal seizures (Isnard et al., 2004) but not in generalised discharges. However, the insula has widespread thalamic connections (Mufson and Mesulam, 1984; Cho et al., 2013), and connection with cortical areas involved with GSW such as frontal cortex and dorsal-posterior cingulate (Cauda et al., 2011), which may explain its activation during GSW found in our study. The activity of the visual cortex can be interpreted as a brain network that somehow interacts with the ictal onset mechanisms to allow GSW onset. Hints that pre-ictal cortical changes seen in fMRI studies might represent a seizure-permissive brain state have been found. For example, the rare syndrome of eyelid myoclonia with absences (EMA, Jeavons Syndrome) shows abnormally increased BOLD signal in visual brain regions during eye closure, suggesting that a hyperexcitable network has been activated by eye closure, from which

seizures might emerge (Vaudano et al., 2014). Patients with photoparoxysmal response on EEG (an abnormal response to stroboscopic light, which can evolve into GSW) showed activity in a set of visual cortical regions during the photoparoxysmal response, which additionally engages thalamus if a GSW arises (Moeller et al., 2013). This is reflected in a study of white matter connectivity using DTI, which showed abnormalities in visual regions in subjects with photoparoxysmal response alone, but also in thalamic connections in subjects with photoparoxysmal response and GGE (Groppa et al., 2012; Bartolini et al., 2014).

No functional or structural connection exists between the fusiform gyrus and areas of thalamic-cortical network of DMN. Therefore, we hypothesise that the activity found in the right fusiform gyrus relates to the cartoon task we are presenting during simultaneous EEG-fMRI recording. Although we account for the effect of the cartoon in our model, it is possible that a different state of the brain, not being at rest but watching a carton, will lead to additional BOLD responses. In fact, this area has been found related with face processing (Rossion et al., 2003) as well as active during our cartoon task (Shamshiri, 2016). In addition, given the strong connection between the fusiform gyrus with the occipital cortex (Catani et al., 2003), it is also possible that the activity of the occipital cortex found is related to the cartoon effect.

Given the importance of understanding the effect that GSW have on cognitive functions (Berman et al., 2010), we explored the effect that cartoon has in relation with GSW. This analysis has been presented in Chapter 6.

5.4.2 Directionality of pre-GSW BOLD signal changes

As SPM[F] maps do not allow the identification of the directionality of the BOLD response, we plotted the mean fitted response of each cluster.

We measured early changes in the mesial frontal cortex and then in thalamus and caudate. In particular, we found that the mesial frontal cortex BOLD response changed from positive to negative around 6s before GSW onset while thalamus and caudate did not change BOLD responses until about 3s before GSW onset. Particularly, thalamus and bilateral caudate were found switching BOLD response from positive to negative 2s before up to 2s after GSW onset.

In addition, although BOLD responses were not found in any SPM[F] contrasts using gamma functions, results of the effects of interest convolved with HRF showed a potential pattern of positive and negative BOLD changes prior to the onset of GSW in the parietal cortices.

Overall, these results suggest that there is an early activity in the cortex preceding GSW onset. These results replicate previous findings identifying the mesial frontal cortex as the area of first activation prior to GSW onset (Gupta et al., 2011; Miao et al., 2014). Given the later BOLD response changes of subcortical areas, we hypothesise that thalamus together with caudate appear to behave physiologically and reactively to the onset of epileptiform activity and play a critical role in facilitating and sustaining seizures as it has been previously reported (Meeren et al., 2002; Carney et al., 2010). These sub-cortical areas show a striking and very strong bi-phasic haemodynamic response around GSW onset on EEG. This suggests that they are essential to the generation of this activity and have a strong change in their activity from being

inhibitory (negative BOLD) to excitatory (positive BOLD) that this is concomitant with GSW generation.

5.4.3 Methodological considerations

We decided to use the canonical HRF together with time and dispersion derivatives (Friston et al., 1998) to measure GSW-related BOLD responses at event onset time to capture the higher degree of variability of the BOLD response. There is a debate regarding the accuracy of the HRF in capturing the effective response to GSW in adult (Grouiller et al., 2010) and in a paediatric populations (Jacobs et al., 2008). Previous studies have demonstrated the usefulness of modelling the event-related response with a canonical HRF and its partial derivatives, and assessed the contribution of the different basis functions by a series of SPM[F]-contrasts. Significant variability was captured by both the temporal derivative and dispersion derivative, confirming that different regions exhibited different shaped responses and the canonical HRF and its two partial derivatives were sufficient to capture the majority of experimental variability at stimulus onset (Henson, 2001). Similarly, in patients with epilepsy comprehensive responses of epileptic-type activity were captured in patients with epilepsy using HRF and its derivatives (Chaudhary et al., 2012b; Pugnaghi et al., 2014).

We captured differences in the BOLD response to prior and at the electrophysiological onset of GSW using gamma functions peaking at -9s, -6s, -3s, 0s and +3s. Considering the overall inconsistency regarding the activity prior GSW in the literature (Hawco et al., 2007; Moeller et al., 2008a; Amor et al., 2009), and the unknown shape of the HRF response in pathological situations (Bai et al., 2010) we decided to use an exploratory

approach based on nested HRF models with different latencies that could locate areas of activation that were previously undetected and or clarify the BOLD response as was demonstrated in focal (Bagshaw et al., 2004) and generalised (Aghakhani et al., 2004) epilepsies. Importantly by including the regressors within the same model statistical inference can be made to determine responses relative to each other via the nature of an SPM[F]-test being analogous to a model comparison.

5.5 Conclusion

Drug naïve patients diagnosed with GGE showed a spatial-temporal pattern of activation and deactivation of subcortical areas and DMN, respectively; suggesting that these networks, reported by previous literature, are GSW-related networks associated to GGE independent of AED effects. Early changes in the cortex followed by changes in subcortical areas supported the theory that generalised epilepsy may have a focal onset. However, given that evidence of causality is still insufficient, we concluded that the cerebral cortex and thalamus, together, can form cyclical loops of activity that may contribute to some forms of epileptic seizures.

Chapter 6 : Core network in GGE part II: Brain state dependence of GSW associated networks

6.1 Background

Previous EEG-fMRI studies have looked at GSW related BOLD changes where subjects were typically asked to lay in the scanner with eyes closed without performing any specific engaging task (Gotman et al., 2005; Hamandi et al., 2006; Moeller et al., 2008a; Kay and Szaflarski, 2014). In epilepsy studies this was chosen to increase the yield of epileptic discharges. However, the healthy brain has been shown to have measureable spontaneous fluctuations in large-scale brain networks in the so called 'resting state'. One of the most observed networks is the default mode network in which, from both PET and fMRI studies, increased metabolic activity at rest or a relative decrease in comparison to any other cognitive task was measured (Raichle et al., 2001; Fox and Raichle, 2007).

The deactivation of the DMN has been consistently found during GSW by group level studies in patients diagnosed with GGE (Kay and Szaflarski, 2014). This phenomenon has been interpreted as an interruption of the conscious state in this patient population (Gotman et al., 2005; Hamandi et al., 2006; Laufs et al., 2006), given the functional role of DMN in consciousness (Cavanna and Trimble, 2006). However, an alternative explanation is that the DMN deactivation is simply the perturbation of the ongoing brain activity by the GSW event; at rest this would be the DMN.

Evidence suggesting the latter argument is related to the fact that not all the patients have shown this pattern of DMN deactivation at the single subject level (Gotman et al.,

2005) and additional cortical activity was found outside of the DMN brain areas (Aghakhani et al., 2004).

A pattern of activation of the thalamic-cortical network was found more consistently across patients. This may suggest that the thalamo-cortical BOLD activation represents the key brain regions associated with GSW (Gotman et al., 2005) and the level of DMN deactivation is specific to the individual or their state during the GSW.

Indeed, a possible explanation about the inconsistency of DMN during GSW may be due to differences in the inter-burst baseline that might modify the BOLD response during GSW. Given that different a state of drowsiness changes the activity of DMN (Maquet, 2000) and that the border between resting state and drowsiness is slight (Tagliazucchi and Laufs, 2014), there are open questions related to the role of DMN deactivation that might not be specific for or causally related to GSW.

Taking into account the necessity to model the level of vigilance (Hamandi et al., 2006; Tagliazucchi and Laufs, 2014), some studies have investigated brain structures involved in the interaction between GSW and cognitive task using reaction time measures under continuous attention (Bai et al., 2010; Berman et al., 2010; Moeller et al., 2010a) and under a more cognitive demanding working memory task (Chaudhary et al., 2013). Although the first studies found that the pattern of activation and deactivation of the cortex and subcortical areas was replicated during resting state and tasks, Chaudhary et al. (2013) additionally found that during the task, active areas were deactivated in association with GSW. This supports the idea that GSW may perturb the networks which happen to be activated at the moment when GSW occur rather than the disruption of specific functional brain networks (Blumenfeld, 2005b).

However, none of these studies compared the response of GSW in different brain states. In addition, the neuropsychological tests used may suppress interictal discharges and/or change GSW amount or length of the discharges (Binnie et al., 1987; Binnie, 2003), preventing the detection of GSW on the EEG and/or leading to fMRI reduced signal changes (Hamandi et al., 2006; Chaudhary et al., 2013). Therefore, there is the need to explore GSW BOLD responses between different brain states using a different task which would not strongly alter GSW occurrence rates.

We hypothesised that GSW would deactivate whichever network was active in a particular brain state and that the DMN was therefore not an important part of the core network necessary to generate GSW. To test this, we used simultaneous recordings of EEG-fMRI in GGE patients during periods of rest and during a low level attention task involving watching a cartoon. The aim of this was to provide a different pattern of active brain areas in each period without dramatically affecting epileptic discharge rate (Centeno et al., 2016). We expected a greater deactivation associated with GSW in the key nodes of the DMN during rest than during the cartoon and correspondingly a greater deactivation associated with GSW in the key nodes of the task active network during the cartoon compared to rest.

6.2 Methods

6.2.1 Subjects

We selected 16 patients (mean age (Y)=15.26, 6 F) who had GSW during at least one session of rest and at least one session of cartoon during simultaneous video-EEG-fMRI. We have previously demonstrated GSW-related networks are similar in drug naïve patients recently diagnosed with GGE to those found in patients already on treatment

(Chapter 5). Therefore, in this analysis, we could reasonably include drug naïve, post-treatment and refractory patients and compare their results and how they were affected by brain state.

The list of patients selected for this analysis is in Table 6.1 further details of the patients are found in Chapter 3, Table 3.1.

Table 6.1: Sample information

GROUP	CODE	GENDER	AGE	"Cartoon" GSW	"Rest" GSW	"Please Wait" GSW
DRUG NAÏVE AE	#2	M	14.00	4 (10.9867)	5 (9.40)+13 (3.78)	2 (4.8293)
	#3	M	10.51	1 (6.4960)+1 (8.18)	8 (5.2)	1 (8.1080)
	#4	M	6.37	2 (2.4367)	17 (3.02)	1 (4.2960)
	#6	F	13.65	1 (28.67)	1 (5.67)	/
	#7	M	8.03	1 (5.34)+10 (1.56)	2 (6.84)	/
	#12	M	7.15	1 (0.4560)+3 (4.2464)	14 (5.14)	2 (5.308)+2 (2.6312)
	#13	M	9.26	1 (10.728)	3 (8.6)	1 (11.46)
POST-TREATMENT AE	#11b	F	16.78	1 (0.4375)	1 (1.75)	1 (1.5331)
	#14b	M	6.43	/	3 (0.48)+1 (0.68)	1 (0.8)

REFRACTORY AE	#19	M	10.45	5 (3.5592)	6 (5.21)+1 (10.23)	1 (0.309)
	#24	F	7.00	2 (0.3707)+6 (1.0549)	4 (0.839)	4 (0.8693)+1 (1.128)
	#23	F	9.93	/	5 (10.8)+6 (10.05)	1 (14.18)
DRUG NAÏVE JME	#47	M	21.71	5 (0.8847)+3 (1.275)	10 (1.67)+7 (0.88)	1 (0.26)+1 (2.716)
	#58	F	31.23	2 (0.3373)+1 (1.48)	4 (0.6)+4 (0.4)	1 (1.432)
REFRACTORY JME	#69	F	30.86	1 (1.79)+6 (0.6069)	1 (1.22)+11 (1.32)	5 (0.548)
	#70	M	40.84	2 (0.4813)	6 (0.85)+2 (0.382)+2 (0.27)	1 (0.916)

Age is in years; number of GSW per session for each patient is listed; in brackets there is the mean duration of GSW in seconds.

6.2.2 Simultaneous video-EEG-fMRI acquisition

Details of simultaneous video EEG-fMRI acquisition are described in the common methods (Chapter 3).

6.2.3 EEG-fMRI pre-processing

MR gradient and pulse-related artefacts were removed off-line from the EEG recorded inside the MRI using template artefact subtraction method (Allen et al., 1998; Allen et al., 2000) implemented in a commercial EEG processing package (Brain Analyser, Brain Products). EEG was down sampled to 250 Hz. GSW were identified after visual

inspection and manually marked on the EEG traces for each session. GSW were marked in runs with onset and duration (length of the run).

All fMRI data were analysed using software package Statistical Parametric Mapping (SPM8) (http://www.fil.ion.ucl.ac.uk/spm) running under Matlab (Mathworks Inc., USA). After discarding the first four volumes to avoid T1-saturation effect, the EPI time series images were realigned to the first image, corrected with FIACH (Tierney et al., 2016), normalised to MNI space and spatially smoothed using an isotropic Gaussian kernel of 8mm FWHM (Friston et al., 1995).

Specification of the pre-processing pipeline can be found in Chapter 3.

6.2.4 EEG-fMRI analysis

The fMRI data were analysed within a mass univariate GLM framework as implemented in SPM8 to measure haemodynamic changes related to GSW recorded during rest and during cartoon periods.

6.2.4.1 Single subject analysis

For each subject, a model was built that would enable us to test and compare the differences between GSW-associated responses during rest and during the cartoon brain states. To achieve this, GSW events were separated into those which occurred during rest and those occurring during cartoon watching using a full factorial design. It should be noted that cartoon had two short periods where the subject was asked to wait for the next cartoon segment (Figure 3.1). Therefore, the experimental design had 2 factors: GSW and task. GSW had 1 level: presence of GSW. Task had 3 levels: as first level we had “Cartoon”, the second level “Rest” and the third level is “Please Wait” calculating

the presence of GSW during break time in between episodes of the cartoon. Any GSW during this please wait period were treated as effects of no interest. This is because the 'please wait' epochs were short and therefore insufficient GSW occurred to evaluate the GSW-associated network in this state (which is different from rest and from cartoon). Effects of interests were convolved with the canonical HRF and its time and dispersion derivatives, resulting in 3 regressors for each combination of levels. The block of the task (rest, cartoon, please wait), six inter-scan realignment parameters from image pre-processing and 6 extra regressors from FIACH (Tierney et al., 2016) were included in the GLM as confounds. To enable a test for differences between GSW events in the cartoon and rest periods all the sessions were concatenated together; an extra regressor was introduced to account for any inter-session differences in the mean signal (Figure 6.1). A high-pass filter of 500s was included to remove slow scanner drift related BOLD effects (Ashburner J, 2012a) taking into account the low frequency of the task. SPM[T+] contrasts were used to generate T-maps (con images) revealing patient-specific BOLD changes for each effect of interests convolved with HRF, time and dispersion derivatives that were transported at the group level analysis. This was performed to allow variable response shapes to GSW (as observed in Chapter 5) where significant explanatory power is found in the canonical response and its derivatives.

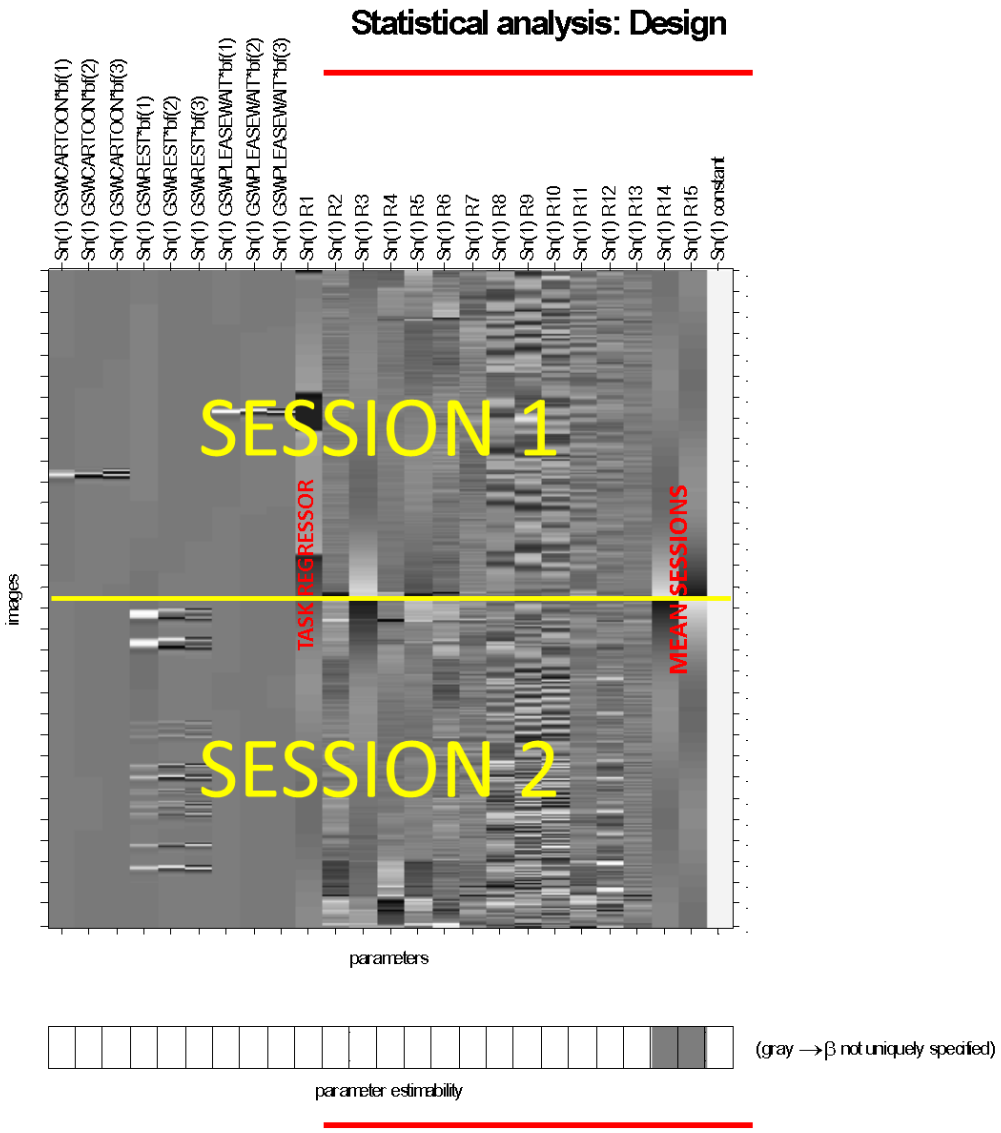

Figure 6.1: Single subject level GLM

6.2.4.2 Group level analysis

We wanted to discover the common and different regional group level BOLD changes associated with GSW while allowing for flexibility in the haemodynamic response. To achieve this, we used a 3x2 full factorial design, random effect at the second level of analysis. The first factor "task" had 2 levels; cartoon and rest. The second factor "Basis functions" had 3 levels; canonical HRF, time derivative and dispersion derivative. Scanner type was included in the model as covariate to remove any influence of the two scanning centres from the analysis (Figure 6.2). For each level, we entered the relevant Con images generated by the SPM[T+] contrast for each individual at the single subject level. An inclusive mask of the areas of interests was applied. We set out to test for differences in the response within brain regions that showed GSW associated response. We therefore confined our analysis to bilateral thalami, hippocampi, caudate, pallidum, putamen, frontal cortex, precuneus, occipital cortex and fusiform gyri (Figure 6.3) taken from the results in Chapter 5 showing the GSW-associated network. Amongst these areas, areas belonging to the cartoon network as defined by Shamshiri et al., (2016) were included (Figure 6.4, Figure 6.5). SPM[F] contrasts across the HRF, time and dispersion derivatives (Ashburner J, 2012b) were calculated to identify BOLD changes (with flexible shape) related to GSW occurring firstly during rest, secondly GSW occurring during the cartoon and thirdly the brain regions exhibiting differences in the GSW-associated response during rest and cartoon. SPM[F] maps will have a threshold set at $p<0.05$, FWE corrected cluster level as implemented by the random field theory, corresponding to $p<0.001$ uncorrected, k=194. Conjunction analysis implemented in

SPM8 (Friston et al., 2005) was performed to detect common areas between GSW during rest and GSW during cartoon.

Given our a-priori hypothesis, coordinates of precuneus and fusiform gyrus were selected from Hamandi et al., (2006) and Shamshiri et al., (2016). BOLD fitted responses of these core areas of DMN, thalamic-cortical network and cartoon watching were plotted during rest and task periods to identify differences in BOLD responses during different brain states.

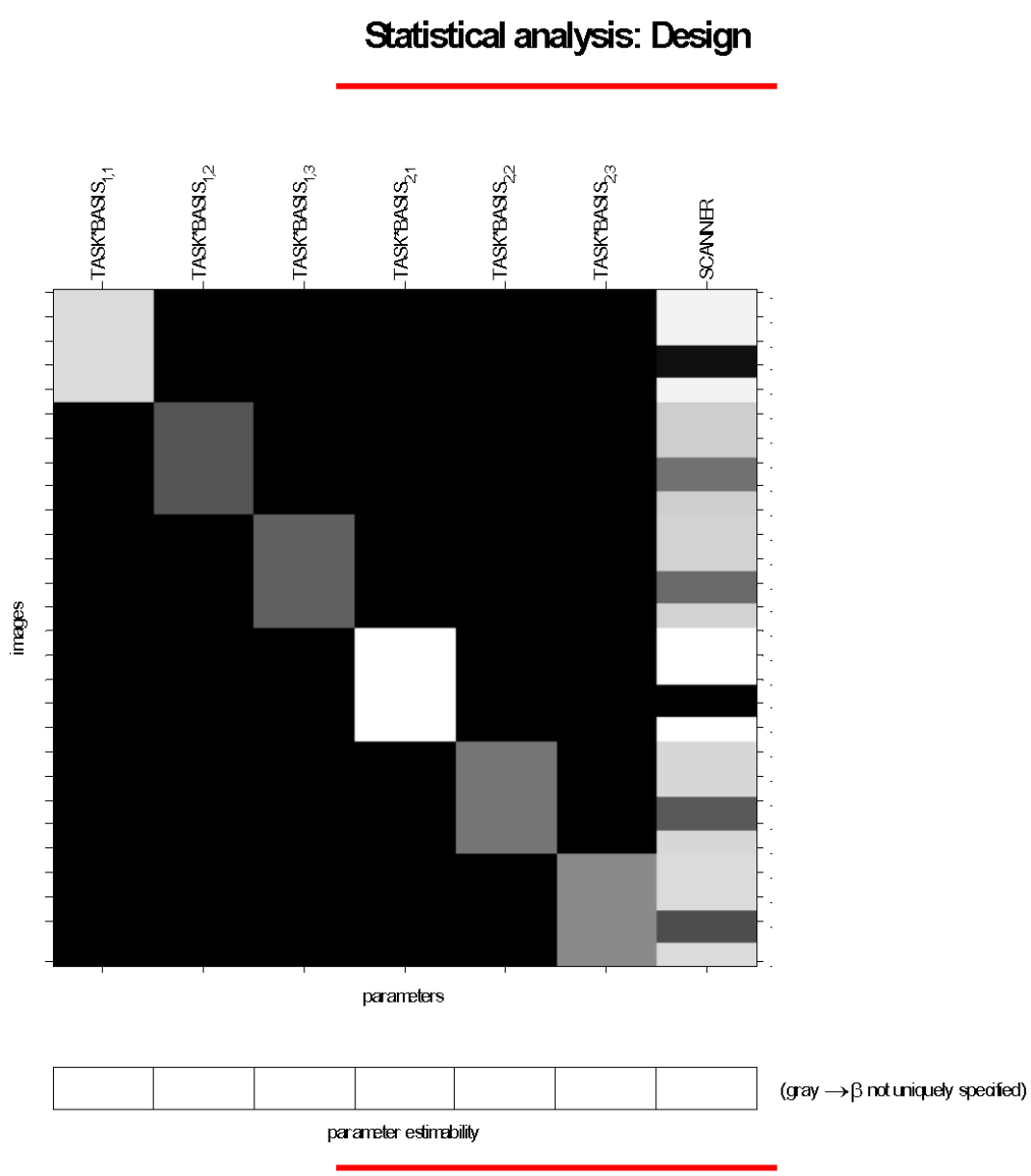

Figure 6.2: Full factorial design group level analysis GLM

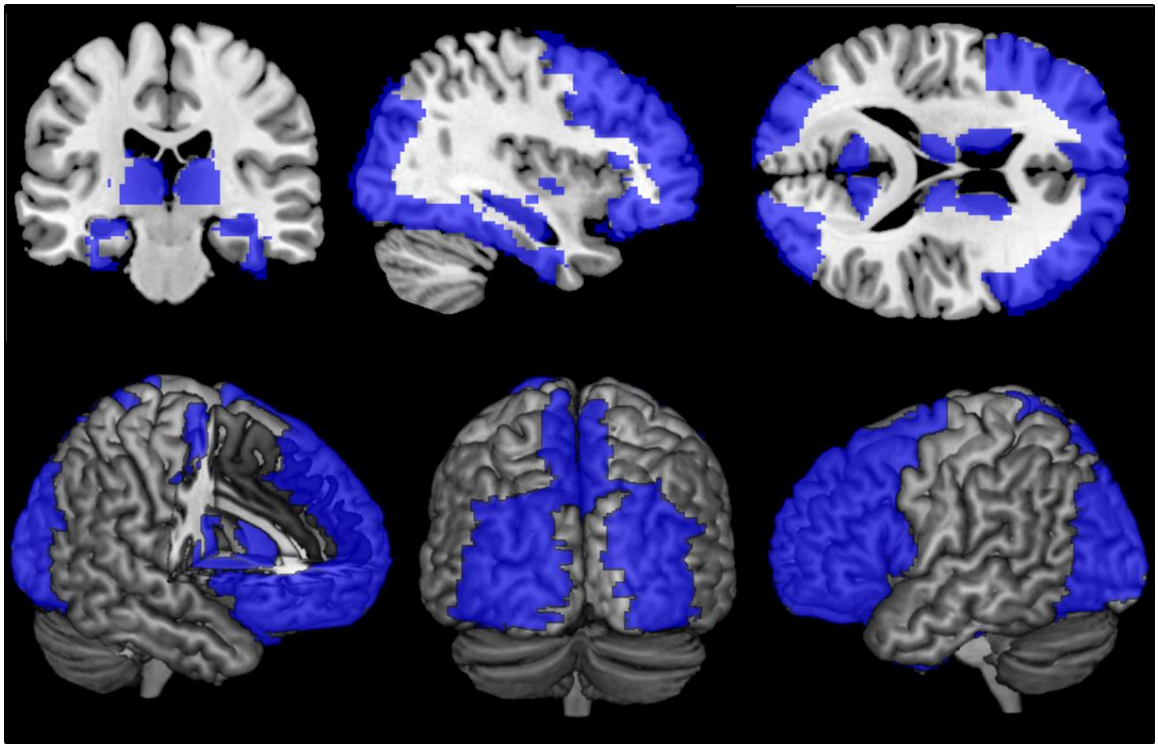

Figure 6.3: Regions of Interests mask.

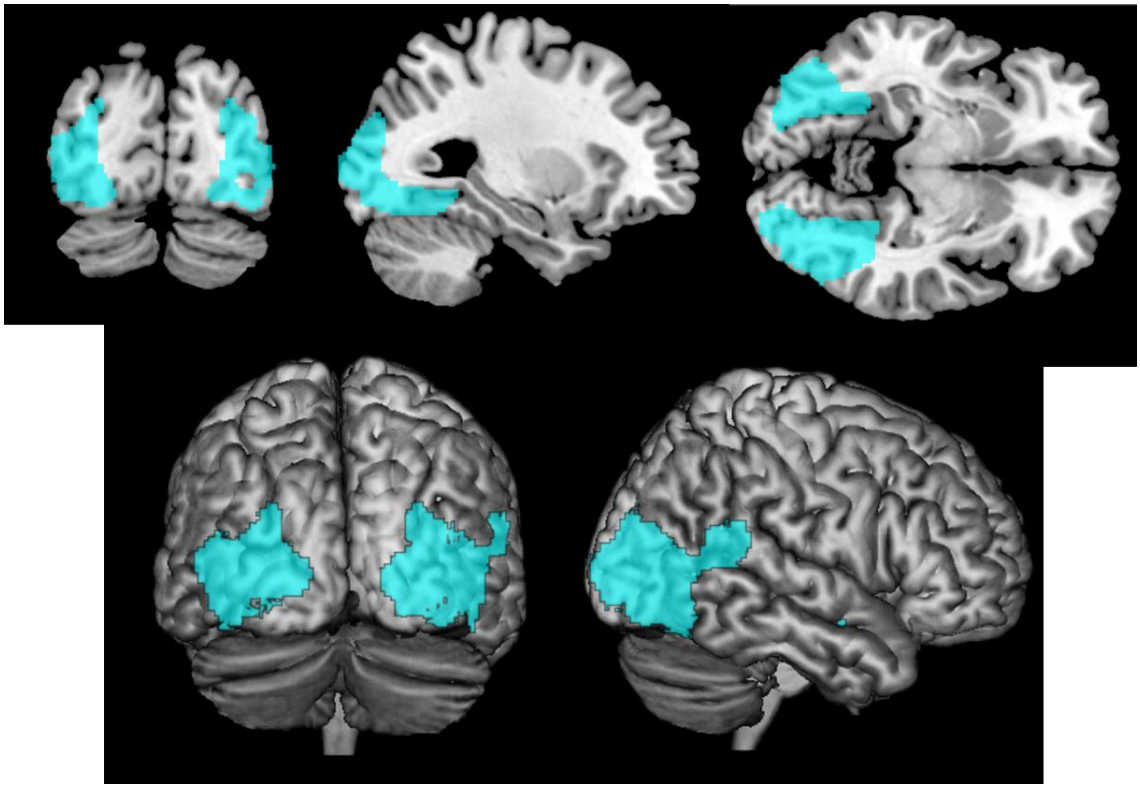

Figure 6.4: Cartoon network from Shamshiri et al. (2016). We extracted the cartoon network from Shamshiri et al. (2016) who reported SPM maps activated in a group of 17 healthy controls children during cartoon watching. Activity was found in the bilateral fusiform gyrus, bilateral middle occipital cortex with extensions in middle temporal regions (Shamshiri, 2016).

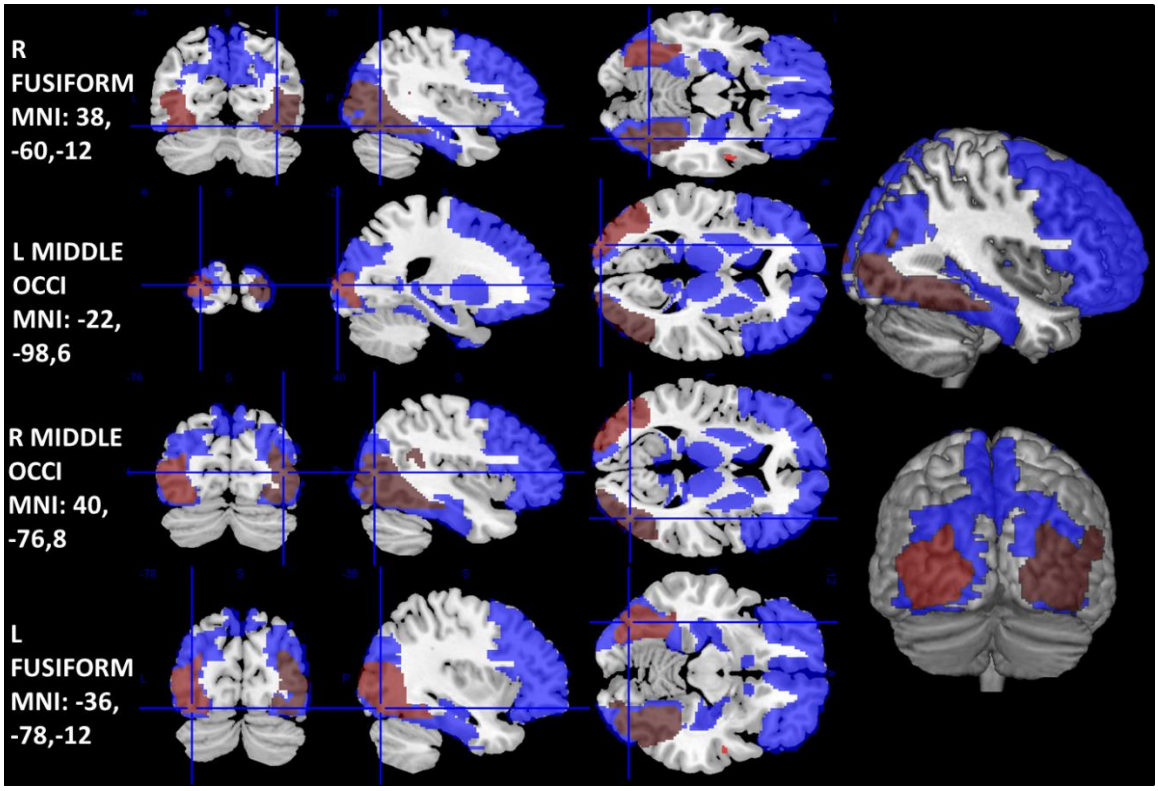

Figure 6.5: Overlay of cartoon network from Shamshiri et al. (2016) in red, ROI mask used in this analysis (Figure 6.3) in blue. This overlaid displays the inclusion in our mask of the main clusters of the cartoon network: right fusiform, left middle occipital cortex, right middle occipital cortex, left fusiform. R=right, L=left, Occi=occipital, MNI=Montreal National Institute coordinates.

6.3 Results

Fourteen patients were included in the analysis. Two patients were excluded as the GSW were only recording during the period of "Please Wait". One session of one patient was discarded due to the presence of a-typical epileptiform events occurring only in the frontal EEG electrodes. Although this is a feature seen in GGE patients (Seneviratne et al., 2014), we decided to discard it from the analysis to allow more consistency in the type of GSW discharge for comparison between states.

We included a total of 58 runs of GSW recorded during the cartoon period and a total of 113 runs of GSW recorded during rest. 25 runs of GSW were included as effects of no interest as they were recorded during "Please Wait" periods. There was no significant statistical differences between the number of GSW recorded during cartoon and during rest U=57.5, p=0.062. No differences were found in duration between GSW runs during rest and GSW runs during cartoon U=81.0, p=0.454. This suggests that stereotypical electrophysiological events of 3 Hz GSW are characterised in both conditions although there is a trend in reduction in GSW during cartoon.

6.3.1 GSW associated BOLD map during rest

SPM[F] map of HRF, time and dispersion derivatives of GSW during rest showed that right inferior frontal cortex, left precuneus and left middle occipital cortex survived p<0.05, FWE corrected at cluster level (Figure 6.6, Table 6.2).

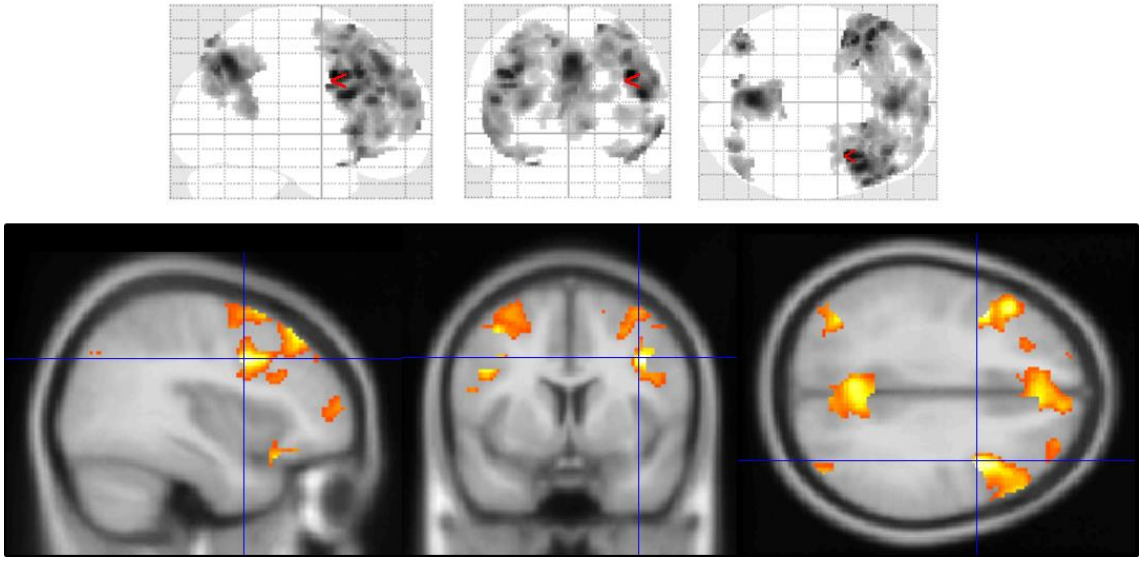

Figure 6.6: SPM[F] map of GSW during rest. The map had a threshold set at p<0.05 FEW, cluster level. List of significant clusters is included in Table 6.2.

6.3.2 GSW associated BOLD map during the cartoon

SPM[F] map of HRF, time and dispersion derivatives of GSW during cartoon showed that right inferior frontal gyrus and right middle occipital cortex survived $p<0.05$, FWE at the cluster level (Figure 6.7, Table 6.2).

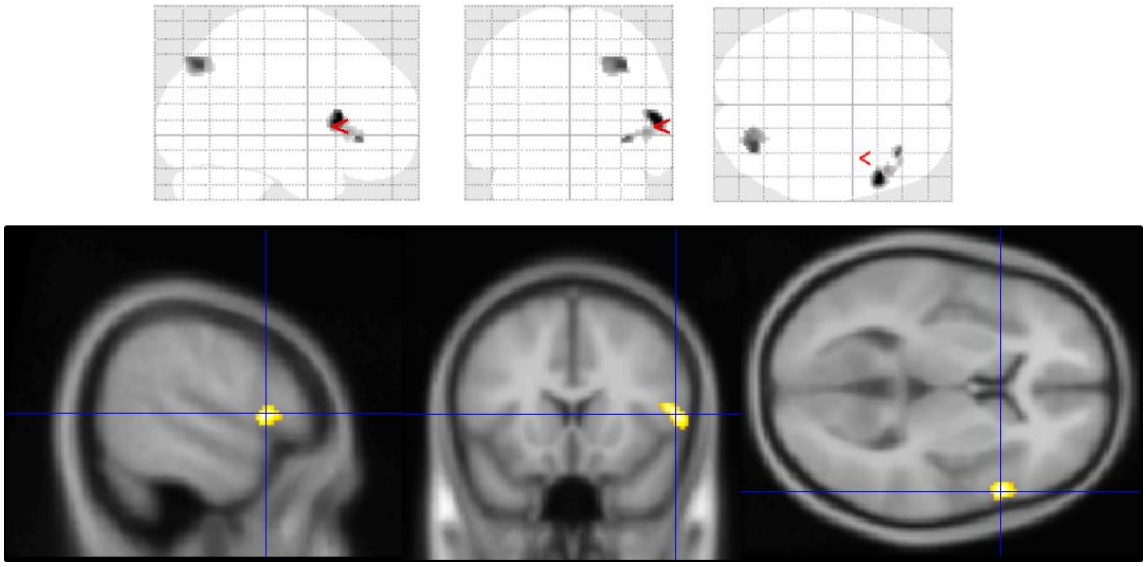

Figure 6.7: SPM[F] map of GSW during cartoon. The map had a threshold set at $p<0.05$ FWE corrected, cluster level. List of significant clusters is included in Table 6.2.

6.3.3 Cartoon vs Rest in a priori coordinates

Differences were not found between cartoon and rest surviving a statistical threshold of $p<0.05$ in precuneus and right fusiform, the key nodes of the DMN and cartoon network using the coordinates from Hamandi et al., (2006) and Shamshiri et al., (2016), following our spatial hypothesis.

However, BOLD responses were plotted for precuneus and fusiform gyrus (Figure 6.8) for exploratory purposes. We found that the right fusiform gyrus showed a positive

BOLD response and subsequent negative undershoot during rest whilst a negative BOLD response was seen during cartoon periods. The precuneus was found to have a negative BOLD response during cartoon and rest with a more negative change to GSW during rest (as expected), although this is not statistically significant.

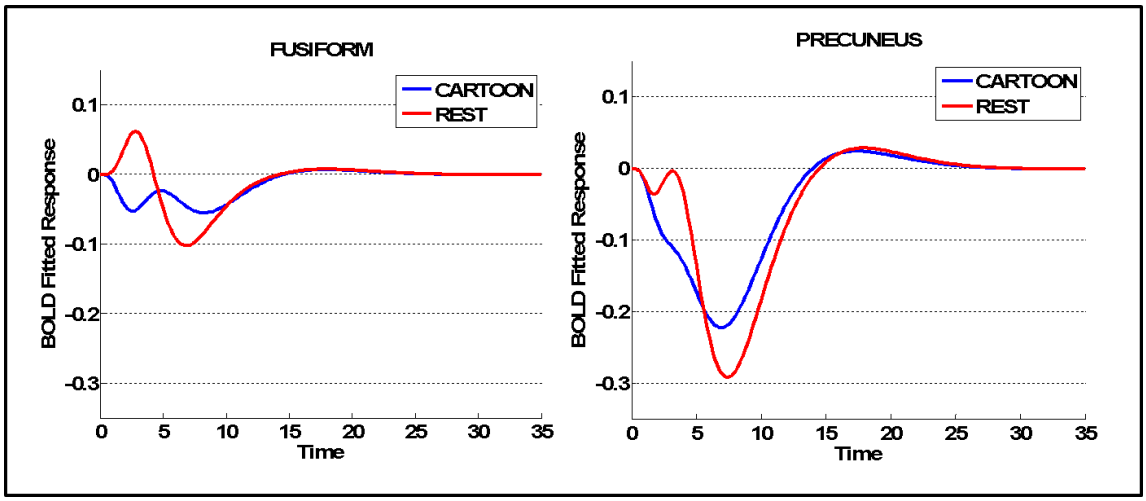

Figure 6.8: BOLD fitted responses during cartoon and rest using a priori ROI coordinates from previous studies: right fusiform (38, -60, -12) on the left; precuneus (6, -48, 17) on the right.

6.3.4 BOLD maps comparison between rest and cartoon

Conjunction analysis between GSW during rest and cartoon did not show any areas of overlapping that were statistically significant.

Under the assumption that differences between cartoon and rest in the a priori coordinates were not statistically significant and that the SPM[F] maps during rest and cartoon appeared spatially diverse, we decided to explore the variation in the GSW BOLD response between rest and cartoon across a wider range of areas included in the brain mask (Figure 6.3).

SPM[F] contrast of the difference in activity between GSW during rest and during cartoon has showed no results at a statistical threshold of $p<0.05$, FWE corrected at cluster level. Clusters of differences were found setting an exploratory statistical threshold at $p<0.05$, uncorrected. We found that bilateral occipital cortex, bilateral inferior frontal gyri, bilateral hippocampi, bilateral fusiform gyri, bilateral thalami, bilateral caudate, bilateral superior frontal gyri, mesial frontal cortex and left precuneus were the areas marking BOLD differences between GSW recorded during rest and cartoon sessions (Figure 6.9, Table 6.2).

Amongst these areas, we found cortical areas from which a priori coordinates were selected such as right fusiform gyrus and precuneus. In addition, we found left and right middle occipital cortex and left fusiform gyrus which were considered main clusters of the cartoon network (2^{nd}, 3^{rd} and 4^{th} clusters) by Shamshiri et al. (2016) (Figure 6.5). Therefore, we exploratory measured the nearest locations from the a priori coordinates showing a difference between rest and cartoon GSW responses. We found that different coordinates, very close to those reported by Shamshiri et al. (2016) and Hamandi et al. (2006), within the right fusiform gyrus (34, -34, -26) and precuneus (16, -54, 20) did show state related differences (Figure 6.10). Similarly, we found that close coordinates to those reported by Shamshiri et al. (2016) in right middle occipital cortex (38, -76, 10) and left middle occipital cortex (-18, -88, 22) did show differences between GSW during rest and cartoon. We found a closed cluster to the left fusiform gyrus from Shamshiri et al. (2016) which was on the border with left fusiform gyrus but falling on the inferior occipital cortex (-36, -76, -10). Therefore, the nearest coordinates we found

in the left fusiform gyrus (-16, -38, -16) were not as closed as Shamshiri et al. (2016)'s (Figure 6.10).

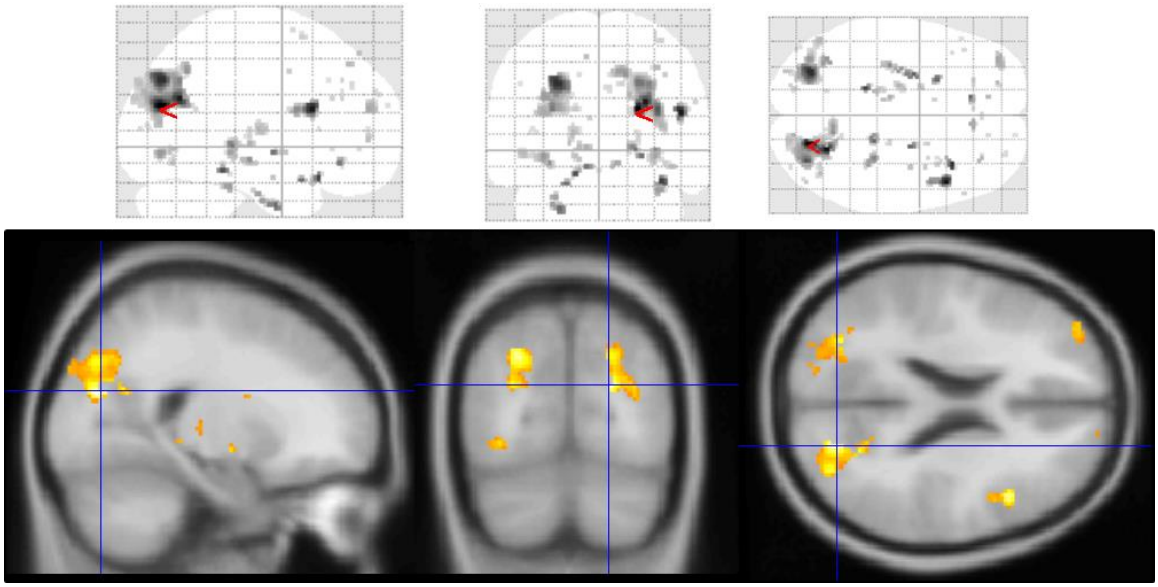

Figure 6.9: SPM[F] map of the difference between GSW during cartoon and GSW during rest (*p*<0.05 uncorrected).

Table 6.2: List of significant cluster from SPM GLM

CONTRAST	STATISTICAL THRESHOLD		Coordinates x, y, z
	p<0.05 FWE, cluster corrected	*p*<0.05, uncorrected	
GSW during CARTOON	R IFG	/	56 16 6
	R MIDDLE OCCIPITAL	/	32 -74 42
GSW during REST	R IFG	/	38 6 34
	L PRECUNEUS	/	0 -64 44
	L MIDDLE OCCIPITAL	/	-36 -70 40

	R IFG (triangular)	/	58 20 0
GSW during CARTOON vs GSW during REST	/	R OCCIPITAL	22 -74 22; 42 -68 12; 48 -78 14; 38 -88 8
	/	R IFG	48 16 20; 36 20 -20
	/	L OCCIPITAL	-28 -74 38; -36 -76 -6; -36 -64 28; -16 -86 22; -42 -84 10; -44 -82 8
	/	L FUSIFORM	-16 -38 -16; -26 -6 -36; -28 -20 -28
	/	R HIPPOCAMPUS	32 -32 -2; 38 -8 -20
	/	L CEREBELLUM	-10 -32 -12
	/	L HIPPOCAMPUS	-32 -22 -10; -14 -30 -8
	/	L IFG	-22 10 -22; -42 28 -4; -40 20 8
	/	R PALLIDUM	24 -8 -6
	/	R FUSIFORM	34 -34 -26
	/	L SFG	-36 50 20; -20 50 2; -22 34 26
	/	L THALAMUS	-18 -16 8
	/	R MFG	34 38 46; 38 2 42; 36 10 62; 30 56 28
	/	MESIAL FC	8 34 -10; -10 44 52; 12 34 36; 2 40 34; -2 34 -14; 16 44 -4
	/	L PALLIDUM	-16 0 -6

	/	R CAUDATE	22 4 20
	/	R THALAMUS	20 -22 8
	/	L CAUDATE	-8 8 16
	/	R SFG	32 4 66; 32 10 64; 16 62 22
	/	L PRECUNEUS	-14 -64 42
	/	L MFG	-50 26 36

List of significant clusters for each SPM[F] contrasts. L=left, R=right, IFG=inferior frontal gyrus, MFG=middle frontal gyrus, SFG=superior frontal gyrus, FC=frontal cortex.

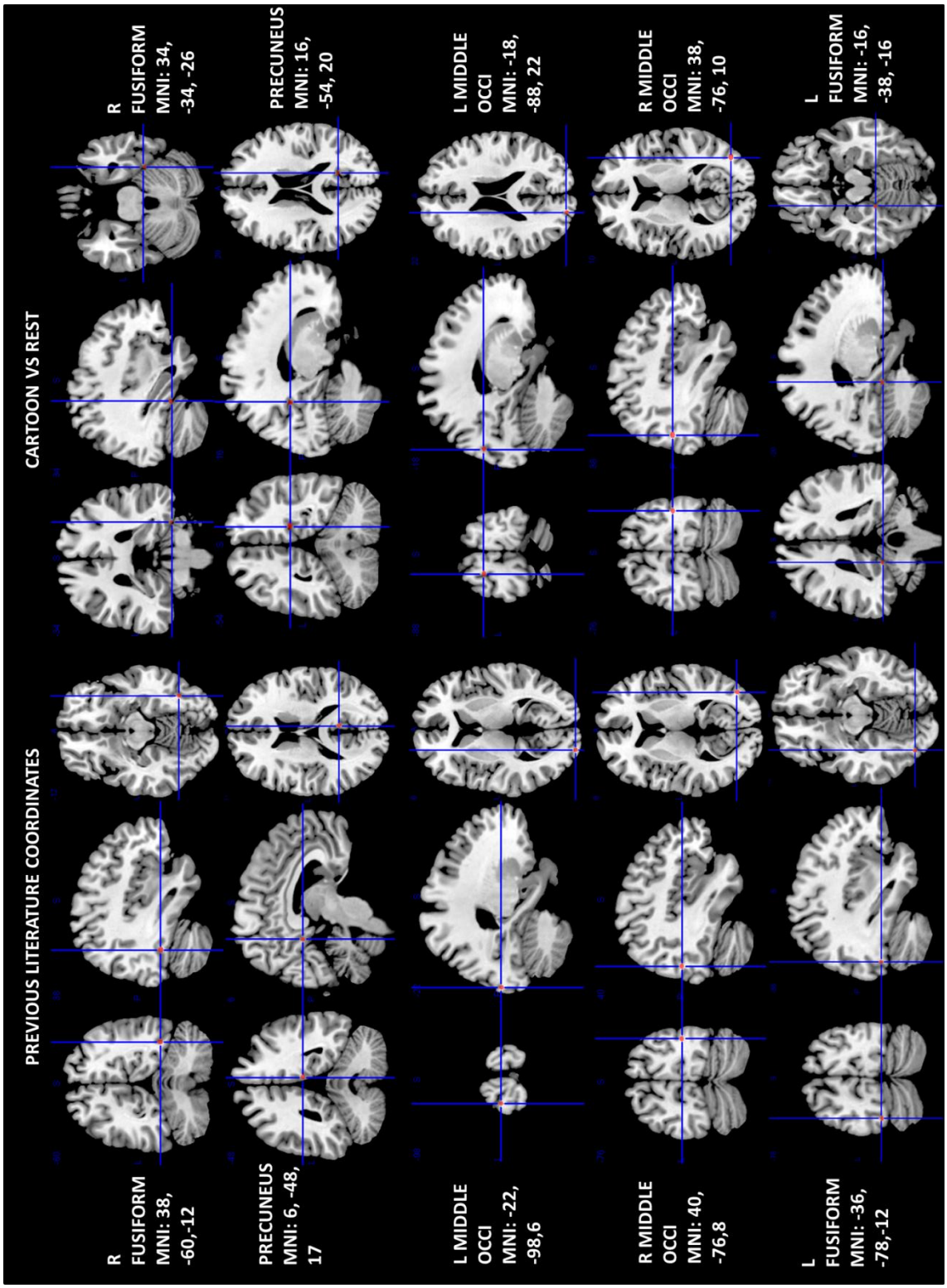

Figure 6.10: MNI coordinates from Shamshiri et al. (2016) and Hamandi et al. (2006) (on the left) and MNI coordinates of the nearest subthreshold cluster within the same cortical area resulted from SPM[F]contrast of GSW during cartoon vs

GSW during rest (on the right). R=right, L=left, Occi=occipital, MNI=Montreal National Institute coordinates.

6.4 Discussion

For the first time, we explored the relationship between GSW and functional brain networks in different brain states in a group of patients diagnosed with GGE. We tested differences and commonalities in the GSW-related BOLD response during rest and during a low demanding cognitive task.

We found that the SPM[F] map during rest was different from the SPM[F] map during cartoon. Indeed, the first map showed the typical spatial pattern of the DMN, whilst the map of GSW during cartoon exhibited only right inferior frontal gyrus and right middle occipital cortex. The conjunction analysis between the two GSW-related maps did not show common brain areas. This suggested that the functional correlates of GSW may be brain state specific.

All the BOLD responses to GSW found were related to the brain regions most active during the state in which the GSW occurred. In fact, the right inferior frontal gyrus, found during cartoon and during rest has been reported to be associated with attention processes (Collette and Van der Linden, 2002; Derrfuss et al., 2004; Hedden and Gabrieli, 2006; Hampshire et al., 2010) and during video watching (Anderson et al., 2006). Middle occipital cortex was found in both conditions as well. This is in accordance with Berman et al. (2010) and Aghakhani et al. (2004) who found a similar pattern of activation during attentional tasks in 6 patients with AE and during rest in 2

patients, respectively. In addition, the precuneus was found in our BOLD map, signalling a strong link with GSW during rest.

We measured differences in the BOLD response in the core areas of the cartoon and rest networks. We plotted the fitted responses in the coordinates of the right fusiform gyrus from Shamshiri et al. (2016) and the precuneus from Hamandi et al. (2006). Shamshiri et al. (2016) found that the fusiform gyrus was the global maximum in a group of healthy control children during cartoon watching. Hamandi et al. (2006) tested GSW activation during rest and found the precuneus to be the fourth most significant cluster. Although we did not find significant BOLD changes at these coordinates, interestingly, we found an early opposite direction of the BOLD response between rest and cartoon in the right fusiform gyrus (Figure 6.8) pointing towards the hypothesis that activity in the network in use at the time of the occurrence of the GSW may be impaired. This would support also the results of Chaudhary et al. (2013) who found perturbation of the active network in a working memory task in one patient. In addition, the precuneus showed a negative BOLD response both during rest and cartoon with a greater negative BOLD response during rest than during cartoon.

Given that we did not find BOLD changes at the a priori coordinates as we hypothesised, we performed an exploratory search for the nearest locations showing a difference between rest and cartoon GSW responses. We found that different coordinates, very close to those reported by Shamshiri et al. (2016), within the fusiform gyrus (34, -34, -26), middle occipital cortex (38, -76, 10; -18, -88, 22) and precuneus (16, -54, 20) did show state related differences. However because they were not preselected any activity surviving $p<0.05$ uncorrected for multiple comparisons may be

due to insufficient control of false positives. Further, we also exploratory investigated SPM[F] maps of the difference in activity between GSW during rest and GSW during cartoon. Although the SPM[F] map did show changes in the fusiform gyrus, an area involved in watching video (Anderson et al., 2006; Shamshiri, 2016) as well as areas of the DMN such as precuneus (Raichle et al., 2001), in addition changes were noted in the thalamic-cortical network as thalamus. Thus, these differences were only seen at a threshold of $p<0.05$ uncorrected for multiple comparisons, and due to the chance of false positives at the low statistical threshold used to reveal these clusters, the relationship between differences in BOLD maps related to GSW during cartoon and rest need further exploration in order to draw any strong conclusions.

Taken together, these results do not allow us to confirm that GSW deactivates the DMN more during rest than during cartoon or that GSW deactivated the areas of the cartoon network during task. However, considering the dissimilarities in the BOLD maps of GSW during rest and during cartoon, and the variations in the shape of fitted BOLD responses, results suggest that there could be an influence of different brain states on GSW networks derived from EEG-fMRI.

6.4.1 Effects of cartoon on DMN and limitations

In this study, a cartoon task was used for the first time in GGE patients by us. Also, this is the first investigation which explored the relationship between the baseline of brain states and their interaction with GSW BOLD response. Therefore, there are some considerations that require attention as they may have led us to reject our hypothesis.

First of all, consideration about the sensitivity of our task is needed. In contrast to any other study (Bai et al., 2010; Chaudhary et al., 2013), was our use of a low demanding task. It is possible that during the cartoon, the DMN activity may be too close to rest and therefore, not able to provide a large enough baseline difference against which the GSW perturbations can be measured. However, Shamshiri et al. (2016) and Anderson et al. (2006) found a clear activity in fusiform gyrus and occipital cortex, areas involved during video watching. Similarly, we also found activity in the occipital cortex, suggesting the involvement of the same visual component associated with cartoon watching in our results. Therefore, we consider this alternative unlikely as GSW BOLD changes related with the cartoon were found.

Another explanation may be related to GSW and functional connectivity. In fact, substantial differences were found in the functional connectivity of DMN and cartoon network in relation to IED (Shamshiri, 2016). Therefore, we can hypothesis that connectivity measures will reveal significant differences within rest and cartoon networks during GSW. Future analysis will address this question.

6.4.2 Effects of cartoon on GSW

We found that watching cartoon did not alter the average length of GSW, allowing BOLD related changes of stereotypical epileptic activity. However, we noticed that the number of GSW runs was larger during rest than during the cartoon. Although this did not reach statistical significance, it did approach significance ($p<0.062$). In addition, it is important to note that the selection criteria for this study required that the same patient showed GSW during rest and cartoon. This does not include all those patients who showed GSW during cartoon or rest only. Seven patients were excluded because GSW

only occurred during the cartoon and 6 were excluded because GSW only occurred during rest. Therefore, although there is evidence that IED rate is unaffected by cartoon watching in focal epilepsy (Centeno et al., 2016), it is difficult to confirm the same in generalised epilepsy. Indeed, even though there is not a very strong effect in the influence of cartoon on GSW rates, this needs to be confirmed in more patients.

6.4.3 Brain state baseline

SPM[F] maps of the differences between GSW recorded during rest and during cartoon were found at the statistical threshold of $p<0.05$, uncorrected for multiple comparisons. Although we are aware of the limits of this threshold, we wanted to present these results given the interesting exploratory information we gained. This is the first study that has looked at the effect of differences in brain states on GSW with the largest group of subjects with GGE. With these results we wanted to demonstrate that there are differences in GSW related BOLD response dependent on the cognitive state of the patients. Although outcomes need to be replicated and further analysis is needed, our results do suggest that baseline brain state and level of consciousness may be important.

6.5 Conclusion

In this study we tested if GSW-related BOLD responses were dependant on brain state. We found that BOLD maps of GSW during rest was spatially similar to the DMN while the BOLD map of GSW during cartoon consisted of mainly visual cortex suggesting contradistinction in activation across brain states. However, the statistical differences between the brain states did not reveal clear results. Although our results may point towards variation in the GSW responses during rest and task, we did not have a

statistically significant difference in the brain locations selected a priori and so cannot confirm our hypothesis. Therefore, we are unable to conclusively show that the DMN involvement in GSW is an epiphenomenon related to the baseline brain state used in previous studies. However, there was not a strong spatial correspondence between the GSW-related responses in the two states suggesting that the relationship between brain networks, GSW and brain state baseline requires further investigation.

Chapter 7 : Arterial Spin Labelling – differences in blood perfusion due to drug intake.

7.1 Background

Arterial spin labelling is a quantitative MRI technique that is able to measure differences in regional and global cerebral blood flow (CBF) (Williams et al., 1992). It has been used extensively in many areas of clinical research (Petersen et al., 2006) including pharmacological imaging (Wang et al., 2011; Zelaya, 2016). Cerebral blood flow is measured by magnetically labelled arterial blood water and via the pair-wise subtraction between sequentially acquired tag and control images. ASL provides whole brain maps of CBF measured in units of ml of blood/100 g tissue/min and provides cerebral blood flow estimates comparable with those obtained by other methods (Buxton et al., 1998a; Hoge et al., 1999). ASL has been particularly useful in pharmacological-MRI (phMRI) (Tracey, 2001; Detre et al., 2009). In fact, it is possible to detect drug effects on CBF during rest and during the execution of a cognitive or sensory paradigm (Wang et al., 2011).

Unlike ASL, the amplitude of conventional BOLD fMRI reflects a complex interplay between cerebral blood flow, cerebral blood volume and the change in cerebral metabolic rate of oxygen consumption (Hoge et al., 1999). Hence, an observed drug effect on the BOLD fMRI signal may in fact be the result of changes in one of the above parameters at baseline. Indeed, there have been several studies demonstrating an interaction between basal physiological and metabolic states and task-induced BOLD activation (Cohen et al., 2002; Hyder et al., 2002). Specifically, the basal CBF has been

found to affect the magnitude and the dynamics of the BOLD response induced by neural activity (Cohen et al., 2002) resulting in different BOLD activation.

In addition, studies interested in antiepileptic medication effects identified that epilepsy treatment can lead to an alteration in cerebral blood flow after drug intake (Bartenstein et al., 1991; Gaillard et al., 1996; Spanaki et al., 1999; Joo et al., 2006) suggesting an alteration of neuronal functioning related to the drug that might alter BOLD maps.

Therefore, if fMRI BOLD maps are to be compared between two conditions that consist of two different pharmacologic states, it is important to account for possible alterations in CBF, in order to distinguish between effects resulting from altered neuronal activity and those that may be caused by global haemodynamic influences (Tracey, 2001). Given that our simultaneous EEG-fMRI uses BOLD responses and these are potentially alterated by CBF changes induced by AED, we measured CBF longitudinally in patients diagnosed with GGE. CBF measures were taken using ASL before, and approximately six months after the first anti-epileptic drug treatment.

7.2 Methods

7.2.1 Subjects

Although all the patients were encouraged to complete the full MRI protocol, ASL was acquired in those patients who were able to tolerate the additional scanning time. Amongst the entire group of patients (0, Paragraph 3.3), we acquired ASL in 22 drug naïve patients (mean age=17.05, SD=7.7) and in 11 post-treatment patients (mean age=18.1, SD=8.2) (Table 7.1).

Table 7.1: Patients' demographics

CODE	AGE		GENDER	SCANNER TYPE	SCANNING TIME	
	DN	PT			DRUG NAÏVE	POST-TREATMENT
#1	6.03		M		Y	/
#2	14.00		M		Y	/
#6, #6b	13.65	14.21	F		Y	Y
#7, #7b	8.03	8.54	M		Y	Y
#9, #9b	10.28	10.77	M	1.5 T	Y	Y
#10	9.72		F		Y	/
#11, #11b	16.18	16.78	F		Y	Y
#12	7.15		M		Y	/
#13, #13b	9.26	9.78	M		Y	Y
#47, #47b	21.71	22.95	M		Y	Y
#49	16.58		F		Y	/
#50, #50b	13.64	14.14	F		Y	Y
#51, #51b	20.11	20.78	F		Y	Y
#52, #52b	35.98	36.44	M	3.0 T	Y	Y
#53	15.38		F		Y	/
#54, #54b	17.69	18.26	F		Y	Y
#55	26.04		F		Y	/
#57, #57b	25.94	26.48	F		Y	Y
#58	31.23		F		Y	/

#59	16.46	F		Y	/
#60	20.86	M		Y	/
#61	19.18	F		Y	/

Patients' demographics. DN= drug naïve, PT= post-treatment.

7.2.2 ASL acquisition

Pulse sequence parameters for the ASL sequences can be found in Chapter 3, Table 3.4.

7.2.3 ASL pre-processing

For 1.5T data, post-processing of the ASL was performed using a custom built script running in Matlab R2013b. Signal intensity values from the multi-TI non-background suppressed ASL acquisition were used to fit a TI inversion recovery curve in each voxel, to obtain maps of T1 and the reference image (M0). CBF maps were calculated offline for each patient using custom-written Matlab code using recently published guidelines (Alsop et al., 2015).

For 3T data, four control-label pairs were acquired plus a proton density (PD) image. The mean difference image was used to compute the CBF maps by dividing it by the PD image and scaling the ratio using recently published guidelines (Alsop et al., 2015). These maps were automatically computed by the scanner and written to the DICOM data-base.

For 1.5T and 3T datasets, CBF maps were visually inspected and overlaid on the M0 map to verify quality of the brain extraction. Manual segmentation was applied using FSL view where required.

7.2.4 ASL analysis

Patients from different scanners were separated in two groups. For each scanner type, we calculated the mean global CBF values using FSL for each patient (http://fsl.fmrib.ox.ac.uk/fsl/). Mean values of CBF pre-treatment versus CBF post-treatment scans were compared using a Mann-Whitney *U* test as implemented in SPSS 23 (IBM Inc). Due to the small number of participants, we did not have sufficient statistical power to carry out a whole brain, voxel-wise statistical comparison. However, we did run an exploratory Wilcoxon Signed Ranks test for those patients who performed ASL pre and post-treatment.

7.3 Results

Nine patients pre-treatment and 5 patients post-treatment (diagnosed with AE) were scanned at the 1.5T scanner and included in the first group of patients. Thirteen patients pre-treatment and 6 patients post-treatment (diagnosed with JME) were scanned at 3T and included in the second group of patients.

We found no statistically significant differences between global CBF pre-treatment compared to post-treatment in patients diagnosed with AE (U=19; p=0.69); and between CBF pre-treatment compared to CBF post-treatment in patients with JME (U=22; p=0.15) (Figure 7.1). Paired Wilcoxon Signed Ranks test was performed for those patients who had mean global CBF perfusion pre and post-treatment in the 1.5T and 3T groups. We found no differences between pre-treatment and post-treatment mean global CBF perfusion in patients diagnosed with AE (Z=-1.75; p=0.08). We did not find

significant differences between pre-treatment and post-treatment mean global CBF perfusion in patients diagnosed with JME (Z=-0.31; p=0.753).

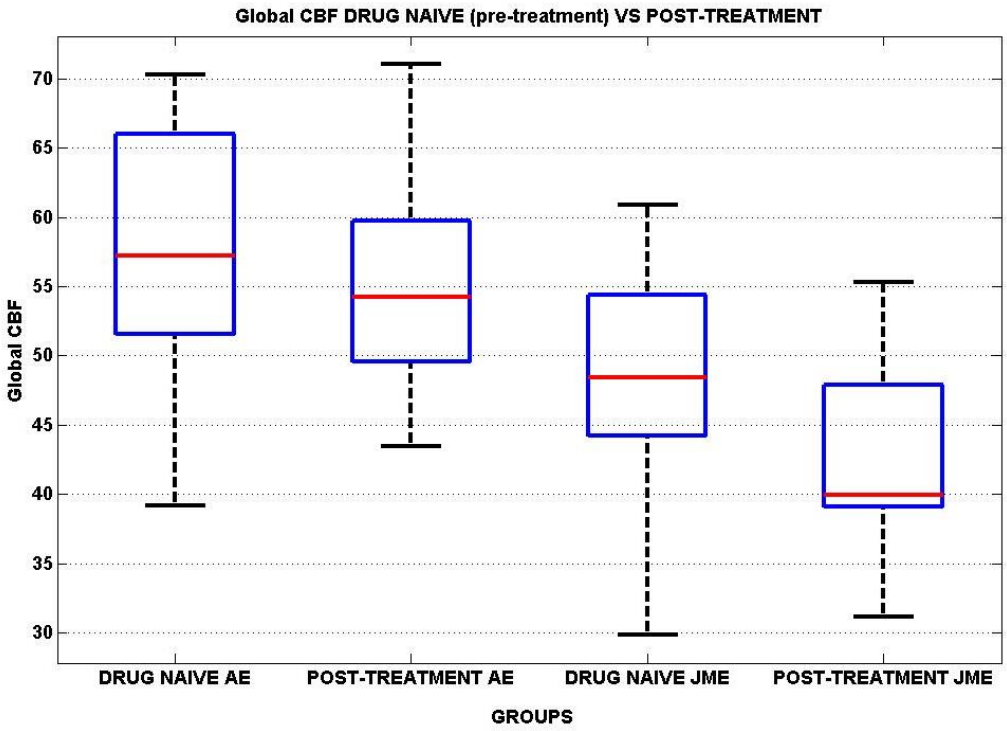

Figure 7.1: Boxplot of mean global CBF calculated mL blood per minute per 100g of tissue. Differences were calculated between i) AE drug naïve patients and AE post-treatment patients, ii) JME drug naïve patients and JME post-treatment patients. Upper limit of the box represents the upper quartile, lower limit represents the lower quartile, red line in the box is the median, error bars represent minimum and maximum values. No statistical significant differences were found longitudinally within groups.

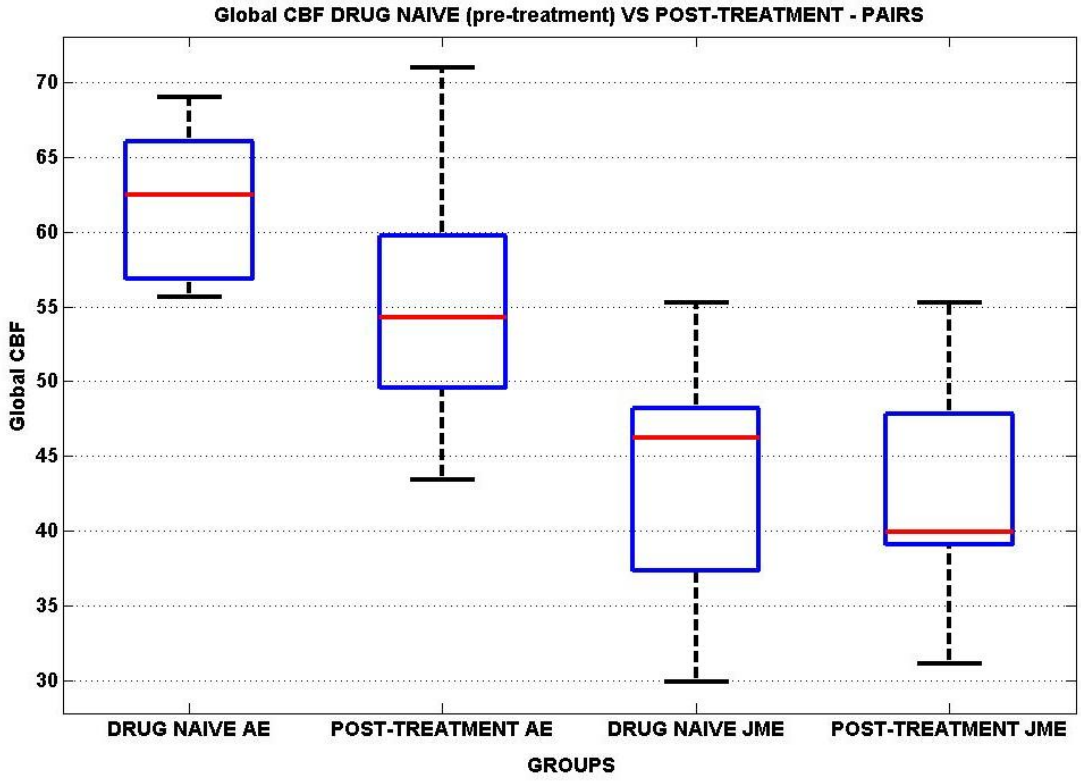

Figure 7.2: Boxplot of mean global CBF calculated mL blood per minute per 100g of tissue. Differences were calculated between pairs of patients who have drug naïve and follow-up CBF measures. Comparisons were made between i) AE drug naïve patients and AE post-treatment patients, ii) JME drug naïve patients and JME post-treatment patients. Upper limit of the box represents the upper quartile, lower limit represents the lower quartile, red line in the box is the median, error bars represent minimum and maximum values. No statistical significant differences were found longitudinally within groups.

7.4 Discussion

We did not observe statistically significant differences between global CBF pre and post treatment in drug naïve patients diagnosed with GGE. The mean global CBF in patients diagnosed with AE who came back for pre and post-treatment showed a trend towards differences in lower CBF after treatment. Interestingly, although not surviving statistical threshold, all the post-treatment mean CFB values were smaller than pre-treatment. This

is when comparing the whole group of AE and JME and those patients with longitudinally repeated measures.

Although our results suggest that there is no significant difference in CBF pre and post-treatment, previous studies have attempted to measure antiepileptic medication effects on CBF using SPECT, PET or/and SPET and they all showed significant changes due to medication (Bartenstein et al., 1991; Spanaki et al., 1999; Joo et al., 2006). Although the manner in which quantitative estimation of CBF is made in individual laboratories when using radio-tracer techniques may lead to potential differences in the results, it is important to note that they all showed decreased CBF as a consequence of medications. In addition, most studies have tested patients with focal epilepsy (Bartenstein et al., 1991; Spanaki et al., 1999). Given evidence pointing towards differences in blood perfusion depending on seizure type (Theodore et al., 1996; Nersesyan et al., 2004), and considering that we only included GGE patients, our results are difficult to compare to previous studies. In addition to this, these studies looked at AED effect on CBF using chronic patients who were taking at least one AED prior to the measurements. This may create additional differences between the effects of AED on drug naïve brain compared to already-treated brains giving reasons for the clear differences they found between CBF measures that were missing in our results.

Only one study showed differences in CBF maps as an effect of lamotrigine in drug naïve patients diagnosed with JME. Similar to our experimental paradigm, the post-treatment scans were performed 4 to 5 months after the first AED intake (Joo et al., 2006). They focused their analysis solely on lamotrigine, while we did not select based on the medication, and they found decreased CBF post-treatment. It is possible to

speculate that the different AEDs which our patients were on and different dosages might mask significant differences in CBF longitudinally (details of AEDs are listed in Table 3.1). However, given the limited number of patients available, we could not control for different AED type. Also, we had to limit our analysis to global CBF measures as we did not have sufficient statistical power to make a proper voxel-wise comparison. Therefore, regional differences as reported by Joo et al. (2006) would have been not identified.

Moreover, considering the fact that we found a trend of reduced CBF in AE and the mean global CBF values were found to be lower in the post-treatment scan compared to pre-treatment in all patients, it is possible that our non-significant results are a reflection of a lack of statistical power. We do recognize this as a limitation to our study. Therefore, given the low sample size, the trend found in the AE group and the consistency of previous results, we are unable to conclude that there is no drug effect in the post-treatment global CBF. As this analysis was performed as a prelude to future work in which pre and post-treatment maps will be compared, these preliminary results will inform future analysis in which the impact of baseline perfusion changes need to be considered in any analysis of treatment effects using BOLD fMRI.

7.5 Conclusion

We found that global CBF was not significantly different before and after treatment suggesting no influence of the drugs used in this study on global cerebral blood flow. However, given the limited number of patients and a trend found in AE patients towards decreased CBF, and that CBF values decreased in all patients post-treatment, we will

explore further potential AED effects on CBF. Therefore, any future BOLD based results we will perform, will consider the value of these preliminary results to prevent any biases by any global physiological effects related to drug intake. Differences in BOLD response pre and post-treatment will be treated as purely disease related under the insurance that AED have not affected CBF.

SECTION 4: DISCUSSION AND CONCLUSION

Chapter 8 : Discussion

In Chapters 4 to 7, I described the application of multimodal neuroimaging in a group of drug naïve patients diagnosed with GGE and related age matched groups of healthy controls and refractory patients.

The main findings of the studies in this thesis are:

- Grey matter volume reductions and shape deflection in subcortical areas were found at the very beginning of the disease.
- Simultaneous video EEG-fMRI showed that activation of the thalamic-cortical network and deactivation of the DMN are present at the drug naïve stage in presence of GSW during rest.
- Simultaneous video EEG-fMRI showed that there are BOLD changes 6s before the onset of GSW, particularly in the frontal cortex, supporting a cortical onset. Thalamus and bilateral caudate were found switching BOLD response from positive to negative 2s before GSW onsets, in concomitant with GSW generation, suggesting a later reaction subcortically that plays a role in seizures initiation and sustain.
- GSW BOLD maps during rest showed DMN areas; GSW BOLD maps during cartoon showed areas of the cartoon network. No clusters were overlapping between GSW during rest and GSW during cartoon and a trend of higher deactivation of DMN was found during rest than during cartoon. Brain state

baseline may alter GSW related BOLD changes but further investigations are needed.

- A trend for reduced CBF post-treatment was found compared to drug naïve pre-treatment CBF in GGE.

How do these findings provide further understanding of GGE? Here, I am presenting my perspective particularly focussing on treatment effect, longitudinal approach and brain state differences. I will also include what I plan to do in the near future as further analysis.

8.1 Treatment Effect

This study was conceived with the intention to fill the gap in the literature regarding the understanding of mechanisms behind GGE at the early stage of onset and when the effect of AED has not interfered with the diseases processes. The present collection of studies is the first one that presents such a big number of newly diagnosed and drug naïve patients (31 patients), possibly due to the difficulties of the recruitment of this patient population which makes this sample very rare. The possibility of excluding one confound such as AED has allowed us to disentangle its unknown effects from current knowledge of mechanisms of GGE. Below, I present the knowledge we were able to reach via the analysis of this drug naïve population.

8.1.1 Drug naïve vs treated patients

We found commonalities between changes in the volume and in the shape of subcortical areas, particularly thalamus, in drug naïve patients (Chapter 4) and those reported by previous studies using treated patients (Kim et al., 2007; Kim et al., 2013; Kim et al.,

2014). Similarly, SPM maps of GSW calculated via regressing out the effect of cartoon (classic model presented in previous studies) showed activation of thalamic-cortical network and deactivation of the DMN (Chapter 5) in accordance with previous studies (Aghakhani et al., 2004; Gotman et al., 2005; Hamandi et al., 2006; Moeller et al., 2008a). Therefore, we concluded that features reported in GGE during treatment are present already at the very early stage of the disease also when there is no treatment effect to consider as confound.

However, we cannot exclude that measures reported by previous studies in treated patients (usually refractory to treatment) are biased by treatment outcome. In fact, we can speculate that patients who will present good or bad outcome would present with differences in their brain measures. Indeed this was found as a trend of decreased grey matter volume and differences in shape in subcortical areas in patients who presented bad outcome compared to those who presented good outcome. With the current dataset, it is possible to disentangle this effect and future analysis will look into this (using a longitudinal prospective study design).

8.1.2 Dynamic activity

Exploring the time course of the BOLD response in drug naïve GGE revealed that the response to GSW is not static but it is dynamic. Following the debate of the cortical (Luders et al., 1984; Holmes et al., 2004) versus subcortical (Jasper HH, 1947) focus of onset for GGE, and the idea that dynamic changes in the brain lead to GSW (Bai et al., 2010; Petkov et al., 2014) , we explored the BOLD activity occurring up to 12 seconds before GSW electrophysiological onset. We found an early activity in the frontal cortex

followed by thalamus and caudate (Chapter 5), suggesting a more cortical focus in GGE (Gupta et al., 2011; Miao et al., 2014) and a gateway role of the thalamus which would contribute to seizures initiation and sustain as proposed by previous studies (Meeren et al., 2005).

Our results are consistent with early cortical activity found in treated patients (Benuzzi et al., 2012; Masterton et al., 2013) suggesting that treatment effect may have not played a role in altering BOLD dynamic prior to GSW. However, one study explored pre-GSW activity in 6 drug naïve patients and did not find any prior GSW BOLD changes (Moeller et al., 2008a). Reasons for this results may be related to, firstly, the limited number of patients they presented which may have led to statistical power problem; and secondly, the use of canonical HRF solely which our evidence suggests may limit the detection of changes in regions that show very different BOLD response shapes to a canonical response shape (Bagshaw et al., 2004; Bai et al., 2010).

8.2 How does the brain state change GSW related activity?

The experimental paradigm used for simultaneous EEG-fMRI was designed to improve tolerability of scanning for children during sedation free sessions (Centeno et al., 2016). However, it has also allowed us to understand if different brain state baselines (cartoon and rest) would have changed the BOLD responses related to GSW. Following the results presented in Chapter 6, we suggested the possibility of differences between GSW BOLD related activity during rest and cartoon. In fact, GSW map during rest showed the typical spatial pattern of the DMN whilst the map of GSW during cartoon did show only

right inferior frontal gyrus and right middle occipital cortex, areas of the cartoon network (Shamshiri, 2016).

However, we could not conclude strongly due to the lack of statistical significance of the results when we compared the differences between GSW during rest and GSW during cartoon.

This was the first time that comparisons of brain states and related GSW activity was made given that other studies looked at GSW activity either during rest (Aghakhani et al., 2004; Gotman et al., 2005; Hamandi et al., 2006) or during cognitive tasks (Berman et al., 2010; Moeller et al., 2010a; Chaudhary et al., 2013) separately. Shamshiri et al. (2016) reported a well-defined cartoon network suggesting a clear change in alertness and attention by the cartoon. However, this was also the first time that "Tom & Jerry" video clip was used for this purpose, thus the amount of difference in the baseline state may be insufficient. Future studies are needed to further explore these results and clarifying the influence that baseline brain state has on GSW-related brain networks. We are planning to explore functional connectivity in the DMN and in the cartoon network to identify if connectivity perturbations in the different baseline states will reveal changes in relation to GSW more sensitively than the magnitude of GSW-related BOLD responses.

8.3 Longitudinal prospective study design

Our sample allows us to compare activity at drug naïve (pre-treatment) and post-treatment stages and exploring early predictive markers of treatment outcome. The results we have presented in this thesis are just the beginning of this group of analyses

due to the limited time available to complete all post-treatment scans prior to the deadline for thesis submission. Up to now, we measured differences in grey matter volume and shape and cerebral blood flow.

For the volume and the shape of grey matter, we measured not only the differences between pre and post-treatment but also differences at the drug naïve stage between patients who subsequently had good or bad treatment outcome at the post-treatment time point (Chapter 4). We did not see any changes between pre and post-treatment neither in the volume nor in the shape suggesting the possibility that abnormalities are present since the beginning of the disease and do not progress (at least within 6 months follow-up). These results support the finding of Pulsipher et al. (2011) who also reported early changes in grey matter volume in GGE patients. However, considerations about the 6 months follow-up we used to identify longitudinal changes are relevant given that changes in the grey matter volumes at 24 months follow-up have been reported (Pulsipher et al., 2011). Though, Pulsipher et al. (2011) recorded the first time point within 12 months from the diagnoses with mean epilepsy duration of 8.36 months; hence, our post-treatment scan corresponds to their first scan. Yet, we consider our results complementary and more detailed to theirs given that they do not report any treatment outcome but they limited the comparison to between their patient group and healthy controls. In addition, our interest was to identify the earliest point in time in which it is possible to detect a marker predicting later treatment outcome (from a drug naïve stage). We identified that patients who were refractory to treatment at 6 months presented abnormalities in the shape of the left pallidum and a trend of smaller subcortical areas at the first drug-naïve scan, compared to drug naïve patients who

subsequently had a good outcome. This suggests that grey matter structural features such as volume and shape may possibly be markers predicting treatment outcome, and we identified that within 6 months from diagnoses a clinical prediction is possible allowing us to distinguish drug naïve patients who will subsequently show different treatment outcomes.

Global cerebral blood flow was measured to inform future studies in which longitudinal measures of BOLD changes will be implemented. Our results did not indicate a significant reduction in global CBF post-treatment. However, the plot of the data suggests a direction towards decreased CBF post-treatment. Evidence from previous studies supports reduction in CBF with AED intake in generalised (Joo et al., 2006) and partial epilepsies (Bartenstein et al., 1991; Spanaki et al., 1999). Given the limited number of patients in which we measured post-treatment CBF, we are aware of our limits in statistical power. Therefore, future studies will consider potential CBF reduction as confound.

8.4 Future directions

The richness of the dataset we acquired serves numerous future analyses. However, it is in our interests to prioritise specific questions which will impact our understanding of GGE: are there any differences between patients with good and bad treatment outcome? Are these differences detectable at the drug naïve stage?

In order to answer these questions, future steps will include:

- Analysis of white matter differences. It is possible that associated with the grey matter volume reduction, there are also white matter abnormalities in drug naïve

patients (Yang et al., 2012). Is has been demonstrated that there are white matter abnormalities in patients with GGE who are on treatment (Liu et al., 2011; Vollmar et al., 2011; O'Muircheartaigh et al., 2012). Therefore, we will explore which white matter abnormalities are present at the drug naïve stage and if marker of treatment outcome based on white matter features are identifiable at disease onset. This would be complementary to the trend we found in grey matter volumes in the group of drug naïve patients presented in Chapter 4 where patients who longitudinally did not respond to treatment presented smaller grey matter volumes in subcortical areas at the drug naïve stage.

- Functional connectivity. We are aware of the power of functional connectivity and the insight it can give to underpinning mechanisms of epilepsy (Kim et al., 2014; Wei et al., 2015). We will divide these analyses in two studies. Study I: we are planning to explore differences in functional connectivity across brain states to identify if DMN plays a mechanistic role in GSW or if DMN deactivation is merely due to the brain state from which GSW happened to emerge. Once this will be clarified, we will go into Study II. Here, we will explore if there may be functional connectivity differences in the core networks of GGE (as defined from Study I – GGE related only and not brain state dependent) in patients classified as refractory or responding at the post-treatment stage. We will measure if treatment response can be predicted by baseline measures of functional connectivity.
- We are planning to use the EEG signal alone to explore dynamic functional connectivity. As we identified BOLD changes prior to the electrophysiological

onset of GSW; we want to explore if the status of EEG will change prior to the appearance of GWS. On this basis, we are planning to study the baseline of functional connectivity before electrographical GSW onset and its changes toward the manifestation of GSW. We will interrogate the data to identify differences in network dynamics that generated GSW between pre-treatment, responding and refractory patients.

8.5 Limitations

Two main limitations that require considerations for planning future studies emerged from the analysis presented in this thesis.

First of all, any analysis using the longitudinal prospective needs to account for the limited numbers of patients measured at the follow-up scan. In fact, although this is still a precious dataset, it is essential to consider that 17 patients (54.8% of the drug naïve group) may limit the statistical power essential for detecting significant differences when comparing groups. This was the case we encountered in Chapter 4 when we measured differences between drug naïve and post-treatment and/or responders and not responders and we identified trends. Similarly, this was also demonstrated in Chapter 7 where the CBF values were closed to significance due to the limited statistical power.

Second of all, it is important to consider the influence of GSW, particularly when applying functional connectivity. It has been demonstrated the importance of considering IED effects in functional connectivity studies and how baseline IED-free data would provide knowledge of pathological underlying mechanisms (Coito et al., 2016; Iannotti et al., 2016; Shamshiri, 2016). As presented in Chapter 3, not all the

patients presented GSW in their EEG, as for example, we recorded GSW in only 5 patients post-treatment. Therefore, to allow comparisons between patients presenting and not presenting GSW, it is important to account for all the variance they caused. However, as demonstrated in Chapter 5, the shape of the HRF response of GSW is not clear and mostly not canonical, therefore, to fully control for the effect of GSW, it would be important to extract the best model which represents GSW response better and use it to account for all the GSW variance first. Dr. Charmichael's group is currently developing a study of HRF which may help in providing a subject-specific HRF model.

Chapter 9 : Conclusion

In this thesis I presented results on the biggest sample of drug naïve patients diagnosed with GGE currently known to us. We applied multimodal imaging to study structural and functional aspects of GGE drug naïve to disentangle treatment effect and disease mechanisms. We demonstrated that grey matter abnormalities and BOLD pattern of GSW emerging from the resting state measured with fMRI are concordant with previous literature. This suggests that treatment effect was not biasing previous findings.

In addition to a resting state session, we acquired some of the fMRI data during the projection of cartoon video clip to provide a more child friendly environment in the scanner. The mechanism underlying the deactivation of DMN during GSW at rest is not clear. Therefore, we explored differences in the BOLD response of GSW during rest and during cartoon to detect if differences in the baseline status would alter DMN activity during GSW. We demonstrated that there are differences due to brain states in the GSW BOLD maps, signalling the need for further analysis to draw clearer conclusions.

We compared pre and post-treatment measures in grey matter and in CBF to identify not only changes due to treatment but also to explore markers of future treatment outcome. We found no differences in grey matter volume and shape pre and post-treatment but we found a trend in subcortical differences when comparing drug naïve patients who reported good outcome compared to those who reported bad outcome. CBF was found not statistically different pre and post-treatment, but due to the sample size limits we abstained to draw conclusion and, due to the distribution of the sample, we support the consideration of AED effects on CBF measures in future studies.

REFERENCES

Aghakhani Y, Bagshaw AP, Benar CG, Hawco C, Andermann F, Dubeau F, Gotman J (2004) fMRI activation during spike and wave discharges in idiopathic generalized epilepsy. Brain : a journal of neurology 127:1127-1144.

Aguirre GK, Zarahn E, D'Esposito M (1998) The variability of human, BOLD hemodynamic responses. NeuroImage 8:360-369.

Allen PJ, Josephs O, Turner R (2000) A method for removing imaging artifact from continuous EEG recorded during functional MRI. NeuroImage 12:230-239.

Allen PJ, Polizzi G, Krakow K, Fish DR, Lemieux L (1998) Identification of EEG events in the MR scanner: the problem of pulse artifact and a method for its subtraction. NeuroImage 8:229-239.

Alsop DC, Detre JA, Golay X, Gunther M, Hendrikse J, Hernandez-Garcia L, Lu H, MacIntosh BJ, Parkes LM, Smits M, van Osch MJ, Wang DJ, Wong EC, Zaharchuk G (2015) Recommended implementation of arterial spin-labeled perfusion MRI for clinical applications: A consensus of the ISMRM perfusion study group and the European consortium for ASL in dementia. Magnetic resonance in medicine 73:102-116.

Amor F, Baillet S, Navarro V, Adam C, Martinerie J, Quyen Mle V (2009) Cortical local and long-range synchronization interplay in human absence seizure initiation. NeuroImage 45:950-962.

Andermann F, Berkovic SF (2001) Idiopathic generalized.
epilepsy with generalized and other seizures in adolescence. Epilepsia 42:317-320.

Anderson DR, Fite KV, Petrovich N, Hirsch J (2006) Cortical activation while watching video montage: An fMRI study. Media Psychol 8:7-24.

Anderson J, Hamandi K (2011) Understanding juvenile myoclonic epilepsy: contributions from neuroimaging. Epilepsy research 94:127-137.

Archer JS, Abbott DF, Waites AB, Jackson GD (2003) fMRI "deactivation" of the posterior cingulate during generalized spike and wave. NeuroImage 20:1915-1922.

Ashburner J (2007) A fast diffeomorphic image registration algorithm. NeuroImage 38:95-113.

Ashburner J, Friston KJ (2000) Voxel-based morphometry-the methods. NeuroImage 11:805-821.

Ashburner J, Friston KJ (2005) Unified segmentation. NeuroImage 26:839-851.

Ashburner J, Csernansky JG, Davatzikos C, Fox NC, Frisoni GB, Thompson PM (2003) Computer-assisted imaging to assess brain structure in healthy and diseased brains. Lancet Neurol 2:79-88.

Ashburner J BG, Chen C, Daunizeau J, Flandin G, Friston K, Kiebel S, Kilner J, Litvak V, Moran R, Penny W, Rosa M, Stephan K, Gitelman D, Henson R, Hutton C, Glauche V, Mattout J, Phillips C. (2012a) SPM8 Manual. London.

Ashburner J BG, Chen C, Daunizeau J, Flandin G, Friston K, Kiebel S, Kilner J, Litvak V, Moran R, Penny W, Rosa M, Stephan K, Gitelman D, Henson R, Hutton C, Glauche V, Mattout J, Phillips C. (2012b) Face Group fMRI data. In: SPM8 Manual (Group TFM, ed), pp 261-280. London.

Attwell D, Laughlin SB (2001) An energy budget for signaling in the grey matter of the brain. Journal of cerebral blood flow and metabolism : official journal of the International Society of Cerebral Blood Flow and Metabolism 21:1133-1145.

Avoli M, Kostopoulos G (1982) Participation of corticothalamic cells in penicillin-induced generalized spike and wave discharges. Brain research 247:159-163.

Avoli M, Rogawski MA, Avanzini G (2001) Generalized epileptic disorders: an update. Epilepsia 42:445-457.

Badawy R, Macdonell R, Jackson G, Berkovic S (2009) The peri-ictal state: cortical excitability changes within 24 h of a seizure. Brain : a journal of neurology 132:1013-1021.

Badawy RA, Curatolo JM, Newton M, Berkovic SF, Macdonell RA (2007) Changes in cortical excitability differentiate generalized and focal epilepsy. Annals of neurology 61:324-331.

Badawy RA, Macdonell RA, Berkovic SF, Newton MR, Jackson GD (2010) Predicting seizure control: cortical excitability and antiepileptic medication. Annals of neurology 67:64-73.

Bagshaw AP, Aghakhani Y, Benar CG, Kobayashi E, Hawco C, Dubeau F, Pike GB, Gotman J (2004) EEG-fMRI of focal epileptic spikes: analysis with multiple haemodynamic functions and comparison with gadolinium-enhanced MR angiograms. Hum Brain Mapp 22:179-192.

Bai X, Vestal M, Berman R, Negishi M, Spann M, Vega C, Desalvo M, Novotny EJ, Constable RT, Blumenfeld H (2010) Dynamic time course of typical childhood absence seizures: EEG, behavior, and functional magnetic resonance imaging. The Journal of neuroscience : the official journal of the Society for Neuroscience 30:5884-5893.

Barnea-Goraly N, Weinzimer SA, Ruedy KJ, Mauras N, Beck RW, Marzelli MJ, Mazaika PK, Aye T, White NH, Tsalikian E, Fox L, Kollman C, Cheng PY, Reiss AL, DirecN DRCN (2014) High success rates of sedation-free brain MRI scanning in young children using simple subject preparation protocols with and without a commercial mock scanner-the Diabetes Research in Children Network (DirecNet) experience. Pediatr Radiol 44:181-186.

Bartenstein P, Ludolph A, Schober O, Lottes G, Scheidhauer K, Sciuk J, Beer HF (1991) Benzodiazepine receptors and cerebral blood flow in partial epilepsy. European journal of nuclear medicine 18:111-118.

Bartolini E, Pesaresi I, Fabbri S, Cecchi P, Giorgi FS, Sartucci F, Bonuccelli U, Cosottini M (2014) Abnormal response to photic stimulation in juvenile myoclonic epilepsy: an EEG-fMRI study. Epilepsia 55:1038-1047.

Beall EB, Lowe MJ (2014) SimPACE: generating simulated motion corrupted BOLD data with synthetic-navigated acquisition for the development and evaluation of SLOMOCO: a new, highly effective slicewise motion correction. NeuroImage 101:21-34.

Benar C, Aghakhani Y, Wang Y, Izenberg A, Al-Asmi A, Dubeau F, Gotman J (2003) Quality of EEG in simultaneous EEG-fMRI for epilepsy. Clinical neurophysiology : official journal of the International Federation of Clinical Neurophysiology 114:569-580.

Benuzzi F, Mirandola L, Pugnaghi M, Farinelli V, Tassinari CA, Capovilla G, Cantalupo G, Beccaria F, Nichelli P, Meletti S (2012) Increased cortical BOLD signal anticipates generalized spike and wave discharges in adolescents and adults with idiopathic generalized epilepsies. Epilepsia 53:622-630.

Berg AT, Berkovic SF, Brodie MJ, Buchhalter J, Cross JH, van Emde Boas W, Engel J, French J, Glauser TA, Mathern GW, Moshe SL, Nordli D, Plouin P, Scheffer IE (2010) Revised terminology and concepts for organization of seizures and epilepsies: report of the ILAE Commission on Classification and Terminology, 2005-2009. Epilepsia 51:676-685.

Berkovic SF, Andermann F, Andermann E, Gloor P (1987) Concepts of Absence Epilepsies - Discrete Syndromes or Biological Continuum. Neurology 37:993-1000.

Berman R, Negishi M, Vestal M, Spann M, Chung MH, Bai X, Purcaro M, Motelow JE, Danielson N, Dix-Cooper L, Enev M, Novotny EJ, Constable RT, Blumenfeld H (2010) Simultaneous EEG, fMRI, and behavior in typical childhood absence seizures. Epilepsia 51:2011-2022.

Bernasconi A, Bernasconi N, Natsume J, Antel SB, Andermann F, Arnold DL (2003) Magnetic resonance spectroscopy and imaging of the thalamus in idiopathic generalized epilepsy. Brain : a journal of neurology 126:2447-2454.

Bernhardt BC, Rozen DA, Worsley KJ, Evans AC, Bernasconi N, Bernasconi A (2009) Thalamo-cortical network pathology in idiopathic generalized epilepsy: insights from MRI-based morphometric correlation analysis. NeuroImage 46:373-381.

Betting LE, Mory SB, Li LM, Lopes-Cendes I, Guerreiro MM, Guerreiro CA, Cendes F (2006) Voxel-based morphometry in patients with idiopathic generalized epilepsies. NeuroImage 32:498-502.

Binnie CD (2003) Cognitive impairment during epileptiform discharges: is it ever justifiable to treat the EEG? Lancet Neurol 2:725-730.

Binnie CD, Kasteleijn-Nolst Trenite DG, Smit AM, Wilkins AJ (1987) Interactions of epileptiform EEG discharges and cognition. Epilepsy research 1:239-245.

Bird CM, Burgess N (2008) The hippocampus and memory: insights from spatial processing. Nature reviews Neuroscience 9:182-194.

Biswal B, Yetkin FZ, Haughton VM, Hyde JS (1995) Functional connectivity in the motor cortex of resting human brain using echo-planar MRI. Magnetic resonance in medicine 34:537-541.

Blumenfeld H (2005a) Cellular and network mechanisms of spike-wave seizures. Epilepsia 46:21-33.

Blumenfeld H (2005b) Consciousness and epilepsy: why are patients with absence seizures absent? Prog Brain Res 150:271-286.

Bonelli SB, Powell R, Thompson PJ, Yogarajah M, Focke NK, Stretton J, Vollmar C, Symms MR, Price CJ, Duncan JS, Koepp MJ (2011) Hippocampal activation correlates with visual confrontation naming: fMRI findings in controls and patients with temporal lobe epilepsy. Epilepsy research 95:246-254.

Bonmassar G, Purdon PL, Jaaskelainen IP, Chiappa K, Solo V, Brown EN, Belliveau JW (2002) Motion and ballistocardiogram artifact removal for interleaved recording of EEG and EPs during MRI. NeuroImage 16:1127-1141.

Braga AMDS, Fujisao EK, Betting LE (2014) Analysis of generalized interictal discharges using quantitative EEG. Epilepsy research 108:1740-1747.

Brodie MJ, Dichter MA (1996) Antiepileptic drugs. The New England journal of medicine 334:168-175.

Buckner RL (1998) Event-related fMRI and the hemodynamic response. Hum Brain Mapp 6:373-377.

Buxton RB, Wong EC, Frank LR (1998a) Dynamics of blood flow and oxygenation changes during brain activation: the balloon model. Magnetic resonance in medicine 39:855-864.

Buxton RB, Frank LR, Wong EC, Siewert B, Warach S, Edelman RR (1998b) A general kinetic model for quantitative perfusion imaging with arterial spin labeling. Magnetic resonance in medicine 40:383-396.

Buzsaki G (1991) The thalamic clock: emergent network properties. Neuroscience 41:351-364.

Buzsaki G (2004) Large-scale recording of neuronal ensembles. Nat Neurosci 7:446-451.

Cabeza R, Nyberg L (2000) Imaging cognition II: An empirical review of 275 PET and fMRI studies. Journal of cognitive neuroscience 12:1-47.

Cantello R, Civardi C, Varrasi C, Vicentini R, Cecchin M, Boccagni C, Monaco F (2006) Excitability of the human epileptic cortex after chronic valproate: a reappraisal. Brain research 1099:160-166.

Caraballo RH, Dalla Bernardina B (2013) Idiopathic generalized epilepsies. Handbook of clinical neurology 111:579-589.

Carmichael DW, Hamandi K, Laufs H, Duncan JS, Thomas DL, Lemieux L (2008) An investigation of the relationship between BOLD and perfusion signal changes during epileptic generalised spike wave activity. Magn Reson Imaging 26:870-873.

Carney PR, Myers S, Geyer JD (2011) Seizure prediction: methods. Epilepsy & behavior : E&B 22 Suppl 1:S94-101.

Carney PW, Masterton RA, Harvey AS, Scheffer IE, Berkovic SF, Jackson GD (2010) The core network in absence epilepsy. Differences in cortical and thalamic BOLD response. Neurology 75:904-911.

Catani M, Jones DK, Donato R, Ffytche DH (2003) Occipito-temporal connections in the human brain. Brain : a journal of neurology 126:2093-2107.

Cauda F, D'Agata F, Sacco K, Duca S, Geminiani G, Vercelli A (2011) Functional connectivity of the insula in the resting brain. NeuroImage 55:8-23.

Cavanna AE, Trimble MR (2006) The precuneus: a review of its functional anatomy and behavioural correlates. Brain : a journal of neurology 129:564-583.

Centeno M, Carmichael DW (2014) Network Connectivity in Epilepsy: Resting State fMRI and EEG-fMRI Contributions. Front Neurol 5:1-93.

Centeno M, Tierney TM, Perani S, Shamshiri EA, StPier K, Wilkinson C, Konn D, Banks T, Vulliemoz S, Lemieux L, Pressler RM, Clark CA, Cross JH, Carmichael DW (2016) Optimising EEG-fMRI for Localisation of Focal Epilepsy in Children. PloS one 11:e0149048.

Chan CH, Briellmann RS, Pell GS, Scheffer IE, Abbott DF, Jackson GD (2006) Thalamic atrophy in childhood absence epilepsy. Epilepsia 47:399-405.

Chaudhary UJ, Duncan JS, Lemieux L (2011) A dialogue with historical concepts of epilepsy from the Babylonians to Hughlings Jackson: Persistent beliefs. Epilepsy & Behavior 21:109-114.

Chaudhary UJ, Rodionov R, Carmichael DW, Thornton RC, Duncan JS, Lemieux L (2012a) Improving the sensitivity of EEG-fMRI studies of epileptic activity by modelling eye blinks, swallowing and other video-EEG detected physiological confounds. NeuroImage 61:1383-1393.

Chaudhary UJ, Carmichael DW, Rodionov R, Thornton RC, Bartlett P, Vulliemoz S, Micallef C, McEvoy AW, Diehl B, Walker MC, Duncan JS, Lemieux L (2012b) Mapping preictal and ictal haemodynamic networks using video-electroencephalography and functional imaging. Brain : a journal of neurology 135:3645-3663.

Chaudhary UJ, Centeno M, Carmichael DW, Vollmar C, Rodionov R, Bonelli S, Stretton J, Pressler R, Eriksson SH, Sisodiya S, Friston K, Duncan JS, Lemieux L, Koepp M (2013) Imaging the interaction: epileptic discharges, working memory, and behavior. Hum Brain Mapp 34:2910-2917.

Childhood CSGf (1998) Clobazam has equivalent efficacy to carbamazepine and phenytoin as monotherapy for childhood epilepsy. Epilepsia 39:952-959.

Cho YT, Fromm S, Guyer AE, Detloff A, Pine DS, Fudge JL, Ernst M (2013) Nucleus accumbens, thalamus and insula connectivity during incentive anticipation in typical adults and adolescents. NeuroImage 66:508-521.

Chowdhury FA, Elwes RDC, Koutroumanidis M, Morris RG, Nashef L, Richardson MP (2014a) Impaired cognitive function in idiopathic generalized epilepsy and unaffected family members: An epilepsy endophenotype. Epilepsia 55:835-840.

Chowdhury FA, Pawley AD, Ceronie B, Nashef L, Elwes RDC, Richardson MP (2015) Motor evoked potential polyphasia A novel endophenotype of idiopathic generalized epilepsy. Neurology 84:1301-1307.

Chowdhury FA, Woldman W, FitzGerald THB, Elwes RDC, Nashef L, Terry JR, Richardson MP (2014b) Revealing a Brain Network Endophenotype in Families with Idiopathic Generalised Epilepsy. PloS one 9:e110136.

Ciumas C, Savic I (2006) Structural changes in patients with primary generalized tonic and clonic seizures. Neurology 67:683-686.

Coenen AM, Drinkenburg WH, Inoue M, van Luijtelaar EL (1992) Genetic models of absence epilepsy, with emphasis on the WAG/Rij strain of rats. Epilepsy research 12:75-86.

Cohen ER, Ugurbil K, Kim SG (2002) Effect of basal conditions on the magnitude and dynamics of the blood oxygenation level-dependent fMRI response. J Cerebr Blood F Met 22:1042-1053.

Coito A, Genetti M, Pittau F, Iannotti GR, Thomschewski A, Holler Y, Trinka E, Wiest R, Seeck M, Michel CM, Plomp G, Vulliemoz S (2016) Altered directed functional connectivity in temporal lobe epilepsy in the absence of interictal spikes: A high density EEG study. Epilepsia 57:402-411.

Collette F, Van der Linden M (2002) Brain imaging of the central executive component of working memory. Neuroscience and biobehavioral reviews 26:105-125.

Crunelli V, Leresche N (2002) Childhood absence epilepsy: genes, channels, neurons and networks. Nature reviews Neuroscience 3:371-382.

Dale AM, Buckner RL (1997) Selective averaging of rapidly presented individual trials using fMRI. Hum Brain Mapp 5:329-340.

Danober L, Deransart C, Depaulis A, Vergnes M, Marescaux C (1998) Pathophysiological mechanisms of genetic absence epilepsy in the rat. Progress in neurobiology 55:27-57.

David O, Guillemain I, Saillet S, Reyt S, Deransart C, Segebarth C, Depaulis A (2008) Identifying Neural Drivers with Functional MRI: An Electrophysiological Validation. Plos Biol 6:2683-2697.

Davids M, Zollner FG, Ruttorf M, Nees F, Flor H, Schumann G, Schad LR, Consortium I (2014) Fully-automated quality assurance in multi-center studies using MRI phantom measurements. Magn Reson Imaging 32:771-780.

de Kovel CGF et al. (2010) Recurrent microdeletions at 15q11.2 and 16p13.11 predispose to idiopathic generalized epilepsies. Brain : a journal of neurology 133:23-32.

Debener S, Herrmann CS (2008) Integration of EEG and fMRI. Editorial. Int J Psychophysiol 67:159-160.

Debener S, Mullinger KJ, Mazy RK, Bowtell RW (2008) Properties of the ballistocardiogram artefact as revealed by EEG recordings at 1.5, 3 and 7 T static magnetic field strength. Int J Psychophysiol 67:189-199.

Debener S, Strobel A, Sorger B, Peters J, Kranczioch C, Engel AK, Goebel R (2007) Improved quality of auditory event-related potentials recorded simultaneously with 3-T fMRI: removal of the ballistocardiogram artefact. NeuroImage 34:587-597.

Derrfuss J, Brass M, von Cramon DY (2004) Cognitive control in the posterior frontolateral cortex: evidence from common activations in task coordination, interference control, and working memory. NeuroImage 23:604-612.

Detre JA, Wang J, Wang Z, Rao H (2009) Arterial spin-labeled perfusion MRI in basic and clinical neuroscience. Current opinion in neurology 22:348-355.

Devor A, Tian PF, Nishimura N, Teng IC, Hillman EMC, Narayanan SN, Ulbert I, Boas DA, Kleinfeld D, Dale AM (2007) Suppressed neuronal activity and concurrent arteriolar vasoconstriction may explain negative blood oxygenation level-dependent signal. Journal of Neuroscience 27:4452-4459.

Di Bonaventura C, Fattouch J, Mari F, Egeo G, Vaudano AE, Prencipe M, Manfredi M, Giallonardo AT (2005) Clinical experience with levetiracetam in idiopathic generalized epilepsy according to different syndrome subtypes. Epileptic disorders : international epilepsy journal with videotape 7:231-235.

Dibbens LM, Mullen S, Helbig I, Mefford HC, Bayly MA, Bellows S, Leu C, Trucks H, Obermeier T, Wittig M, Franke A, Caglayan H, Yapici Z, Sander T, Eichler EE, Scheffer IE, Mulley JC, Berkovic SF, Consortium E (2009) Familial and sporadic 15q13.3 microdeletions in idiopathic generalized epilepsy: precedent for disorders with complex inheritance. Human molecular genetics 18:3626-3631.

Diehl B, Knecht S, Deppe M, Young C, Stodieck SR (1998) Cerebral hemodynamic response to generalized spike-wave discharges. Epilepsia 39:1284-1289.

Du H, Zhang Y, Xie B, Wu N, Wu G, Wang J, Jiang T, Feng H (2011) Regional atrophy of the basal ganglia and thalamus in idiopathic generalized epilepsy. Journal of magnetic resonance imaging : JMRI 33:817-821.

Duncan JS (2005) Brain imaging in idiopathic generalized epilepsies. Epilepsia 46 Suppl 9:108-111.

Duncan JS, Ali, R., Barkovich, J., Berkivuc, S., Chiron, C., Henry, T., Kuzniecky, R., Palmini, A., Savic, I., Theodore, W. (2000) Commission on Diagnostic Strategies: recommendations for functional neuroimaging of persons with epilepsy. Neuroimaging Subcommision of the International League Against, Epilepsy. Epilepsia 41:1350-1356.

Ellingson ML, Liebenthal E, Spanaki MV, Prieto TE, Binder JR, Ropella KM (2004) Ballistocardiogram artifact reduction in the simultaneous acquisition of auditory ERPS and fMRI. NeuroImage 22:1534-1542.

Engel J, Jr., International League Against E (2001) A proposed diagnostic scheme for people with epileptic seizures and with epilepsy: report of the ILAE Task Force on Classification and Terminology. Epilepsia 42:796-803.

Fein G, Di Sclafani V, Taylor C, Moon K, Barakos J, Tran H, Landman B, Shumway R (2004) Controlling for premorbid brain size in imaging studies: T1-derived cranium scaling factor vs. T2-derived intracranial vault volume. Psychiatry research 131:169-176.

Fischl B (2012) FreeSurfer. NeuroImage 62:774-781.

Fischl B, Dale AM (2000) Measuring the thickness of the human cerebral cortex from magnetic resonance images. Proc Natl Acad Sci U S A 97:11050-11055.

Fisher RS, Acevedo C, Arzimanoglou A, Bogacz A, Cross JH, Elger CE, Engel J, Jr., Forsgren L, French JA, Glynn M, Hesdorffer DC, Lee BI, Mathern GW, Moshe SL, Perucca E, Scheffer IE, Tomson T, Watanabe M, Wiebe S (2014) ILAE official report: a practical clinical definition of epilepsy. Epilepsia 55:475-482.

Fox MD, Raichle ME (2007) Spontaneous fluctuations in brain activity observed with functional magnetic resonance imaging. Nature reviews Neuroscience 8:700-711.

French JA et al. (2004) Efficacy and tolerability of the new antiepileptic drugs I: treatment of new onset epilepsy: report of the Therapeutics and Technology Assessment Subcommittee and Quality Standards Subcommittee of the American Academy of Neurology and the American Epilepsy Society. Neurology 62:1252-1260.

Friston K.J. H, A.P., Worsley, K.J. (1999) How Many Subjects Constitute a Study? NeuroImage 10:1-5.

Friston KJ, Penny WD, Glaser DE (2005) Conjunction revisited. NeuroImage 25:661-667.

Friston KJ, Williams S, Howard R, Frackowiak RS, Turner R (1996) Movement-related effects in fMRI time-series. Magnetic resonance in medicine 35:346-355.

Friston KJ, Zarahn E, Josephs O, Henson RN, Dale AM (1999) Stochastic designs in event-related fMRI. NeuroImage 10:607-619.

Friston KJ, Ashburner J, Frith CD, Poline JB, Heather JD, Frackowiak RSJ (1995) Spatial registration and normalization of images. Hum Brain Mapp 3:165-189.

Friston KJ, Fletcher P, Josephs O, Holmes A, Rugg MD, Turner R (1998) Event-related fMRI: characterizing differential responses. NeuroImage 7:30-40.

Gaillard WD, Zeffiro T, Fazilat S, DeCarli C, Theodore WH (1996) Effect of valproate on cerebral metabolism and blood flow: an 18F-2-deoxyglucose and 15O water positron emission tomography study. Epilepsia 37:515-521.

Gayatri NA, Livingston JH (2006) Aggravation of epilepsy by anti-epileptic drugs. Developmental medicine and child neurology 48:394-398.

Gibbs FA, Davis H, Lennox WG (1935) The electro-encephalogram in epilepsy and in conditions of impaired consciousness. Arch Neuro Psychiatr 34:1133-1148.

Gloor P (1968) Generalized Cortico-Reticular Epilepsies - Some Considerations on Pathophysiology of Generalized Bilaterally Synchronous Spike and Wave Discharge. Epilepsia 9:249-263.

Glover GH (1999) Deconvolution of impulse response in event-related BOLD fMRI. NeuroImage 9:416-429.

Goense JB, Logothetis NK (2008) Neurophysiology of the BOLD fMRI signal in awake monkeys. Current biology : CB 18:631-640.

Goldman RI, Stern JM, Engel J, Jr., Cohen MS (2000) Acquiring simultaneous EEG and functional MRI. Clinical neurophysiology : official journal of the International Federation of Clinical Neurophysiology 111:1974-1980.

Goode DJ, Penry JK, Dreifuss FE (1970) Effects of paroxysmal spike-wave on continuous visual-motor performance. Epilepsia 11:241-254.

Goodro M, Sameti M, Patenaude B, Fein G (2012) Age effect on subcortical structures in healthy adults. Psychiatry research 203:38-45.

Gotman J, Pittau F (2011) Combining EEG and fMRI in the study of epileptic discharges. Epilepsia 52 Suppl 4:38-42.

Gotman J, Grova C, Bagshaw A, Kobayashi E, Aghakhani Y, Dubeau F (2005) Generalized epileptic discharges show thalamocortical activation and suspension of the default state of the brain. P Natl Acad Sci USA 102:15236-15240.

Groppa S, Moeller F, Siebner H, Wolff S, Riedel C, Deuschl G, Stephani U, Siniatchkin M (2012) White matter microstructural changes of thalamocortical networks in photosensitivity and idiopathic generalized epilepsy. Epilepsia 53:668-676.

Grouiller F, Vercueil L, Krainik A, Segebarth C, Kahane P, David O (2010) Characterization of the Hemodynamic Modes Associated With Interictal Epileptic Activity Using a Deformable Model-Based Analysis of Combined EEG and Functional MRI Recordings. Hum Brain Mapp 31:1157-1173.

Guerrini R, Belmonte A, Parmeggiani L, Perucca E (1999) Myoclonic status epilepticus following high-dosage lamotrigine therapy. Brain & development 21:420-424.

Guerrini R, Belmonte A, Canapicchi R, Casalini C, Perucca E (1998a) Reversible pseudoatrophy of the brain and mental deterioration associated with valproate treatment. Epilepsia 39:27-32.

Guerrini R, Dravet C, Genton P, Belmonte A, Kaminska A, Dulac O (1998b) Lamotrigine and seizure aggravation in severe myoclonic epilepsy. Epilepsia 39:508-512.

Gupta D, Ossenblok P, van Luijtelaar G (2011) Space-time network connectivity and cortical activations preceding spike wave discharges in human absence epilepsy: a MEG study. Medical & biological engineering & computing 49:555-565.

Haber SN, Calzavara R (2009) The cortico-basal ganglia integrative network: the role of the thalamus. Brain research bulletin 78:69-74.

Hall EH (1879) On a new action of the magnetic on electric currents. Am J Math 2:287-292.

Hamalainen M, Hari R, Ilmoniemi RJ, Knuutila J, Lounasmaa OV (1993) Magnetoencephalography - Theory, Instrumentation, and Applications to Noninvasive Studies of the Working Human Brain. Rev Mod Phys 65:413-497.

Hamandi K, Laufs H, Noth U, Carmichael DW, Duncan JS, Lemieux L (2008) BOLD and perfusion changes during epileptic generalised spike wave activity. NeuroImage 39:608-618.

Hamandi K, Salek-Haddadi A, Laufs H, Liston A, Friston K, Fish DR, Duncan JS, Lemieux L (2006) EEG-fMRI of idiopathic and secondarily generalized epilepsies. NeuroImage 31:1700-1710.

Hampshire A, Chamberlain SR, Monti MM, Duncan J, Owen AM (2010) The role of the right inferior frontal gyrus: inhibition and attentional control. NeuroImage 50:1313-1319.

Hao Y, Creson T, Zhang L, Li P, Du F, Yuan P, Gould TD, Manji HK, Chen G (2004) Mood stabilizer valproate promotes ERK pathway-dependent cortical neuronal growth and neurogenesis. The Journal of neuroscience : the official journal of the Society for Neuroscience 24:6590-6599.

Harden CL et al. (2009) Practice parameter update: management issues for women with epilepsy--focus on pregnancy (an evidence-based review): teratogenesis and perinatal outcomes: report of the Quality Standards Subcommittee and Therapeutics and Technology Assessment Subcommittee of the American Academy of Neurology and American Epilepsy Society. Neurology 73:133-141.

Hawco CS, Bagshaw AP, Lu YL, Dubeau F, Gotman J (2007) BOLD changes occur prior to epileptic spikes seen on scalp EEG. NeuroImage 35:1450-1458.

Hedden T, Gabrieli JD (2006) The ebb and flow of attention in the human brain. Nat Neurosci 9:863-865.

Helbig I et al. (2009) 15q13.3 microdeletions increase risk of idiopathic generalized epilepsy. Nature genetics 41:160-162.

Henson RNA, Rugg, M.D., Fristson, K.J. (2001) The choise of basis functions in event-related fMRI. In: HBM01: Neuroimage.

Hoffmann A, Jager L, Werhahn KJ, Jaschke M, Noachtar S, Reiser M (2000) Electroencephalography during functional echo-planar imaging: Detection of epileptic spikes using post-processing methods. Magnetic resonance in medicine 44:791-798.

Hoge RD, Atkinson J, Gill B, Crelier GR, Marrett S, Pike GB (1999) Investigation of BOLD signal dependence on cerebral blood flow and oxygen consumption: the deoxyhemoglobin dilution model. Magnetic resonance in medicine 42:849-863.

Holmes MD, Brown M, Tucker DM (2004) Are "generalized" seizures truly generalized? Evidence of localized mesial frontal and frontopolar discharges in absence. Epilepsia 45:1568-1579.

Holmes MD, Quiring J, Tucker DM (2010) Evidence that juvenile myoclonic epilepsy is a disorder of frontotemporal corticothalamic networks. NeuroImage 49:80-93.

Hu X, Yacoub E (2012) The story of the initial dip in fMRI. NeuroImage 62:1103-1108.

Huang W, Lu G, Zhang Z, Zhong Y, Wang Z, Yuan C, Jiao Q, Qian Z, Tan Q, Chen G, Zhang Z, Liu Y (2011) Gray-matter volume reduction in the thalamus and frontal lobe in epileptic patients with generalized tonic-clonic seizures. Journal of neuroradiology Journal de neuroradiologie 38:298-303.

Hughes EJ, Bond J, Svrckova P, Makropoulos A, Ball G, Sharp DJ, Edwards AD, Hajnal JV, Counsell SJ (2012) Regional changes in thalamic shape and volume with increasing age. NeuroImage 63:1134-1142.

Hutton C, De Vita E, Ashburner J, Deichmann R, Turner R (2008) Voxel-based cortical thickness measurements in MRI. NeuroImage 40:1701-1710.

Hyder F, Rothman DL, Shulman RG (2002) Total neuroenergetics support localized brain activity: Implications for the interpretation of fMRI. P Natl Acad Sci USA 99:10771-10776.

Iannotti GR, Grouiller F, Centeno M, Carmichael DW, Abela E, Wiest R, Korff C, Seeck M, Michel C, Pittau F, Vulliemoz S (2016) Epileptic networks are strongly connected with and without the effects of interictal discharges. Epilepsia 57:1086-1096.

Irle E, Markowitsch HJ (1982) Connections of the hippocampal formation, mamillary bodies, anterior thalamus and cingulate cortex. A retrograde study using horseradish peroxidase in the cat. Exp Brain Res 47:79-94.

Isnard J, Guenot M, Sindou M, Mauguiere F (2004) Clinical manifestations of insular lobe seizures: a stereo-electroencephalographic study. Epilepsia 45:1079-1090.

Ives JR, Warach S, Schmitt F, Edelman RR, Schomer DL (1993) Monitoring the patient's EEG during echo planar MRI. Electroencephalography and clinical neurophysiology 87:417-420.

Jacobs J, Hawco C, Kobayashi E, Boor R, Levan P, Stephani U, Siniatchkin M, Gotman J (2008) Variability of the hemodynamic response as a function of age and frequency of epileptic discharge in children with epilepsy. NeuroImage 40:601-614.

Janz D, Christian, W. (1957) Impulsiv-Petit mal. Ditsch Z Nervenheilk 176:346-386.

Jasper HH DFJ (1947) Experimental studies on the functional anatomy of petit mal epilepsy. Res Publ Assoc Res Nerv Ment Dis 26:272-298.

Joo EY, Tae WS, Hong SB (2008a) Cerebral blood flow abnormality in patients with idiopathic generalized epilepsy. Journal of neurology 255:520-525.

Joo EY, Kim SH, Seo DW, Hong SB (2008b) Zonisamide decreases cortical excitability in patients with idiopathic generalized epilepsy. Clinical neurophysiology : official journal of the International Federation of Clinical Neurophysiology 119:1385-1392.

Joo EY, Hong SB, Tae WS, Han SJ, Seo DW, Lee KH, Lee MH (2006) Effect of lamotrigine on cerebral blood flow in patients with idiopathic generalised epilepsy. Eur J Nucl Med Mol Imaging 33:724-729.

Josephs O, Turner R, Friston K (1997) Event-related fMRI. Hum Brain Mapp 5:243-248.

Jueptner M, Weiller C (1995) Review: does measurement of regional cerebral blood flow reflect synaptic activity? Implications for PET and fMRI. NeuroImage 2:148-156.

Kay B, Szaflarski JP (2014) EEG/fMRI contributions to our understanding of genetic generalized epilepsies. Epilepsy & Behavior 34:129-135.

Keller SS, Ahrens T, Mohammadi S, Moddel G, Kugel H, Ringelstein EB, Deppe M (2011) Microstructural and volumetric abnormalities of the putamen in juvenile myoclonic epilepsy. Epilepsia 52:1715-1724.

Kim JB, Suh SI, Seo WK, Oh K, Koh SB, Kim JH (2014) Altered thalamocortical functional connectivity in idiopathic generalized epilepsy. Epilepsia 55:592-600.

Kim JH, Kim JB, Seo WK, Suh SI, Koh SB (2013) Volumetric and shape analysis of thalamus in idiopathic generalized epilepsy. Journal of neurology 260:1846-1854.

Kim JH, Lee JK, Koh SB, Lee SA, Lee JM, Kim SI, Kang JK (2007) Regional grey matter abnormalities in juvenile myoclonic epilepsy: a voxel-based morphometry study. NeuroImage 37:1132-1137.

Kjeldsen MJ, Corey LA, Christensen K, Friis ML (2003) Epileptic seizures and syndromes in twins: the importance of genetic factors. Epilepsy research 55:137-146.

Koepp MJ (2005) Juvenile myoclonic epilepsy-a generalized epilepsy syndrome? Acta neurologica Scandinavica Supplementum 181:57-62.

Koepp MJ, Thomas RH, Wandschneider B, Berkovic SF, Schmidt D (2014) Concepts and controversies of juvenile myoclonic epilepsy: still an enigmatic epilepsy. Expert review of neurotherapeutics 14:819-831.

Konings MK, Bartels LW, Smits HF, Bakker CJ (2000) Heating around intravascular guidewires by resonating RF waves. Journal of magnetic resonance imaging : JMRI 12:79-85.

Krakow K, Allen PJ, Lemieux L, Symms MR, Fish DR (2000a) Methodology: EEG-correlated fMRI. Advances in neurology 83:187-201.

Krakow K, Allen PJ, Symms MR, Lemieux L, Josephs O, Fish DR (2000b) EEG recording during fMRI experiments: image quality. Hum Brain Mapp 10:10-15.

Kwan P, Brodie MJ (2000) Early identification of refractory epilepsy. The New England journal of medicine 342:314-319.

Kwan P, Brodie MJ (2001) Effectiveness of first antiepileptic drug. Epilepsia 42:1255-1260.

Kwong KK (2012) Record of a single fMRI experiment in May of 1991. NeuroImage 62:610-612.

Laufs H (2012) A personalized history of EEG-fMRI integration. NeuroImage 62:1056-1067.

Laufs H, Daunizeau J, Carmichael DW, Kleinschmidt A (2008) Recent advances in recording electrophysiological data simultaneously with magnetic resonance imaging. NeuroImage 40:515-528.

Laufs H, Lengler U, Hamandi K, Kleinschmidt A, Krakow K (2006) Linking generalized spike-and-wave discharges and resting state brain activity by using EEG/fMRI in a patient with absence seizures. Epilepsia 47:444-448.

Lauritzen M (2005) Reading vascular changes in brain imaging: is dendritic calcium the key? Nature Reviews Neuroscience 6:77-85.

Lee C, Kim SM, Jung YJ, Im CH, Kim DW, Jung KY (2014) Causal influence of epileptic network during spike-and-wave discharge in juvenile myoclonic epilepsy. Epilepsy research 108:257-266.

Legatt AD, Arezzo J, Vaughan HG (1980) Averaged Multiple Unit-Activity as an Estimate of Phasic Changes in Local Neuronal-Activity - Effects of Volume-Conducted Potentials. Journal of neuroscience methods 2:203-217.

Lemieux L, Allen PJ, Franconi F, Symms MR, Fish DR (1997) Recording of EEG during fMRI experiments: patient safety. Magnetic resonance in medicine 38:943-952.

Lemieux L, Salek-Haddadi A, Lund TE, Laufs H, Carmichael D (2007) Modelling large motion events in fMRI studies of patients with epilepsy. Magn Reson Imaging 25:894-901.

Lemieux L, Salek-Haddadi A, Josephs O, Allen P, Toms N, Scott C, Krakow K, Turner R, Fish DR (2001) Event-related fMRI with simultaneous and continuous EEG: description of the method and initial case report. NeuroImage 14:780-787.

Lennie P (2003) The cost of cortical computation. Current biology : CB 13:493-497.

LeVan P, Maclaren J, Herbst M, Sostheim R, Zaitsev M, Hennig J (2013) Ballistocardiographic artifact removal from simultaneous EEG-fMRI using an optical motion-tracking system. NeuroImage 75:1-11.

Li Q, Luo C, Yang T, Yao Z, He L, Liu L, Xu H, Gong Q, Yao D, Zhou D (2009) EEG-fMRI study on the interictal and ictal generalized spike-wave discharges in patients with childhood absence epilepsy. Epilepsy research 87:160-168.

Lim YM, Cho YW, Shamim S, Solomon J, Birn R, Luh WM, Gaillard WD, Ritzl EK, Theodore WH (2008) Usefulness of pulsed arterial spin labeling MR imaging in mesial temporal lobe epilepsy. Epilepsy research 82:183-189.

Lin K, de Araujo Filho GM, Pascalicchio TF, Silva I, Tudesco IS, Guaranha MS, Carrete Junior H, Jackowski AP, Yacubian EM (2013) Hippocampal atrophy and memory dysfunction in patients with juvenile myoclonic epilepsy. Epilepsy & behavior : E&B 29:247-251.

Liu M, Concha L, Beaulieu C, Gross DW (2011) Distinct white matter abnormalities in different idiopathic generalized epilepsy syndromes. Epilepsia 52:2267-2275.

Logothetis NK (2008) What we can do and what we cannot do with fMRI. Nature 453:869-878.

Logothetis NK, Wandell BA (2004) Interpreting the BOLD signal. Annual review of physiology 66:735-769.

Logothetis NK, Pfeuffer J (2004) On the nature of the BOLD fMRI contrast mechanism. Magn Reson Imaging 22:1517-1531.

Logothetis NK, Guggenberger H, Peled S, Pauls J (1999) Functional imaging of the monkey brain. Nat Neurosci 2:555-562.

Logothetis NK, Pauls J, Augath M, Trinath T, Oeltermann A (2001) Neurophysiological investigation of the basis of the fMRI signal. Nature 412:150-157.

Lopes da Silva F (2010) EEG: Origin and Measurement. In: EEG-fMRI: Physiological Basis, Technique and Application (Mulert CL, Louis, ed), pp 19-38. London: Springer.

Lopes da Silva F, van Rotterdam, A. (2005) Biophysical Aspects of EEG and Magnetoencephalogram Generation. In: Electroencephalography Basic

Principles, Clinical Applications, and Related Fields, 5th Edition (Niedermeyer EdS, Fernando Lopes, ed), pp 108-125. Philadelphia: Lippincott Williams & Wilkins.

Lorio S, Fresard S, Adaszewski S, Kherif F, Chowdhury R, Frackowiak RS, Ashburner J, Helms G, Weiskopf N, Lutti A, Draganski B (2016) New tissue priors for improved automated classification of subcortical brain structures on MRI. NeuroImage 130:157-166.

Luders H, Lesser RP, Dinner DS, Morris HH, 3rd (1984) Generalized epilepsies: a review. Cleveland Clinic quarterly 51:205-226.

Luttjohann A, Schoffelen JM, van Luijtelaar G (2013) Peri-ictal network dynamics of spike-wave discharges: phase and spectral characteristics. Experimental neurology 239:235-247.

MacDonald D, Kabani N, Avis D, Evans AC (2000) Automated 3-D extraction of inner and outer surfaces of cerebral cortex from MRI. NeuroImage 12:340-356.

Magiorkinis E, Diamantis A, Sidiropoulou K, Panteliadis C (2014) Highights in the history of epilepsy: the last 200 years. Epilepsy research and treatment 2014:1-13.

Malonek D, Grinvald A (1996) Interactions between electrical activity and cortical microcirculation revealed by imaging spectroscopy: Implications for functional brain mapping. Science 272:551-554.

Mandelkow H, HaIder P, Boesiger P, Brandeis D (2006) Synchronization facilitates removal of MRI artefacts from concurrent EEG recordings and increases usable bandwidth. NeuroImage 32:1120-1126.

Maquet P (2000) Functional neuroimaging of normal human sleep by positron emission tomography. J Sleep Res 9:207-231.

Masterton RA, Carney PW, Abbott DF, Jackson GD (2013) Absence epilepsy subnetworks revealed by event-related independent components analysis of functional magnetic resonance imaging. Epilepsia 54:801-808.

Maziero D, Velasco TR, Hunt N, Payne E, Lemieux L, Salmon CE, Carmichael DW (2016) Towards motion insensitive EEG-fMRI: Correcting motion-induced voltages and gradient artefact instability in EEG using an fMRI prospective motion correction (PMC) system. NeuroImage 138:13-27.

Mazziotta J et al. (2001a) A probabilistic atlas and reference system for the human brain: International Consortium for Brain Mapping (ICBM). Philosophical transactions of the Royal Society of London Series B, Biological sciences 356:1293-1322.

Mazziotta J et al. (2001b) A four-dimensional probabilistic atlas of the human brain. Journal of the American Medical Informatics Association : JAMIA 8:401-430.

McCormick DA (2002) Cortical and subcortical generators of normal and abnormal rhythmicity. International review of neurobiology 49:99-114.

Mechelli A, Price CJ, Friston KJ, Ashburner J (2005) Voxel-based morphometry of the human brain: Methods and applications. Curr Med Imaging Rev 1:105-113.

Meencke HJ, Janz D (1984) Neuropathological findings in primary generalized epilepsy: a study of eight cases. Epilepsia 25:8-21.

Meeren H, van Luijtelaar G, da Silva FL, Coenen A (2005) Evolving concepts on the pathophysiology of absence seizures - The cortical focus theory. Archives of neurology 62:371-376.

Meeren HK, Pijn JP, Van Luijtelaar EL, Coenen AM, Lopes da Silva FH (2002) Cortical focus drives widespread corticothalamic networks during spontaneous absence seizures in rats. The Journal of neuroscience : the official journal of the Society for Neuroscience 22:1480-1495.

Miao A, Tang L, Xiang J, Guan Q, Ge H, Liu H, Wu T, Chen Q, Yang L, Lu X, Hu Z, Wang X (2014) Dynamic magnetic source imaging of absence seizure initialization and propagation: a magnetoencephalography study. Epilepsy research 108:468-480.

Mishra AM, Bai X, Motelow JE, Desalvo MN, Danielson N, Sanganahalli BG, Hyder F, Blumenfeld H (2013) Increased resting functional connectivity in spike-wave epilepsy in WAG/Rij rats. Epilepsia 54:1214-1222.

Moeller F, Muhle H, Wiegand G, Wolff S, Stephani U, Siniatchkin M (2010a) EEG-fMRI study of generalized spike and wave discharges without transitory cognitive impairment. Epilepsy & Behavior 18:313-316.

Moeller F, Muthuraman M, Stephani U, Deuschl G, Raethjen J, Siniatchkin M (2013) Representation and propagation of epileptic activity in absences and generalized photoparoxysmal responses. Hum Brain Mapp 34:1896-1909.

Moeller F, LeVan P, Muhle H, Stephani U, Dubeau F, Siniatchkin M, Gotman J (2010b) Absence seizures: individual patterns revealed by EEG-fMRI. Epilepsia 51:2000-2010.

Moeller F, Siebner HR, Wolff S, Muhle H, Granert O, Jansen O, Stephani U, Siniatchkin M (2008a) Simultaneous EEG-fMRI in drug-naive children with newly diagnosed absence epilepsy. Epilepsia 49:1510-1519.

Moeller F, Siebner HR, Wolff S, Muhle H, Boor R, Granert O, Jansen O, Stephani U, Siniatchkin M (2008b) Changes in activity of striato-thalamo-cortical network precede generalized spike wave discharges. NeuroImage 39:1839-1849.

Montenegro MA, Cendes F, Noronha AL, Mory SB, Carvalho MI, Marques LH, Guerreiro CA (2001) Efficacy of clobazam as add-on therapy in patients with refractory partial epilepsy. Epilepsia 42:539-542.

Montouris GBA-K, B. (2009) The first line of therapy in a girl with juvenile myoclonic epilepsy: Should it be valproate or a new agent? . Epilepsia 50:16-20.

Mufson EJ, Mesulam MM (1984) Thalamic connections of the insula in the rhesus monkey and comments on the paralimbic connectivity of the medial pulvinar nucleus. The Journal of comparative neurology 227:109-120.

Mulert C, Lemieux, L., (2010) EEG-fMRI: physiological basis, technique, and applications, 1st Edition. London: Springer.

Negishi M, Abildgaard M, Nixon T, Constable RT (2004) Removal of time-varying gradient artifacts from EEG data acquired during continuous fMRI. Clinical Neurophysiology 115:2181-2192.

Nersesyan H, Herman P, Erdogan E, Hyder F, Blumenfeld H (2004) Relative changes in cerebral blood flow and neuronal activity in local microdomains during generalized seizures. Journal of cerebral blood flow and metabolism : official

journal of the International Society of Cerebral Blood Flow and Metabolism 24:1057-1068.

Niazy RK, Beckmann CF, Iannetti GD, Brady JM, Smith SM (2005) Removal of FMRI environment artifacts from EEG data using optimal basis sets. NeuroImage 28:720-737.

Niedermeyer E (1972) The Generalized Epilepsies: A Clinical Electroencephalographical Study: Springfield, Ill: Charles C Thomas.

Niedermeyer E, Lopes da Silva, F.H. (2005) Electroencephalography: basic principles, clinical applications, and related fields, 5th Edition. Philadelphia: Lippincott Williams & Wilkins.

O'Muircheartaigh J, Vollmar C, Barker GJ, Kumari V, Symms MR, Thompson P, Duncan JS, Koepp MJ, Richardson MP (2011a) Focal structural changes and cognitive dysfunction in juvenile myoclonic epilepsy. Neurology 76:34-40.

O'Muircheartaigh J, Vollmar C, Barker GJ, Kumari V, Symms MR, Thompson P, Duncan JS, Koepp MJ, Richardson MP (2012) Abnormal thalamocortical structural and functional connectivity in juvenile myoclonic epilepsy. Brain : a journal of neurology 135:3635-3644.

O'Muircheartaigh J, Vollmar C, Traynor C, Barker GJ, Kumari V, Symms MR, Thompson P, Duncan JS, Koepp MJ, Richardson MP (2011b) Clustering probabilistic tractograms using independent component analysis applied to the thalamus. NeuroImage 54:2020-2032.

Obeid T, Panayiotopoulos CP (1989) Clonazepam in juvenile myoclonic epilepsy. Epilepsia 30:603-606.

Ogawa S, Lee TM (1990) Magnetic resonance imaging of blood vessels at high fields: in vivo and in vitro measurements and image simulation. Magnetic resonance in medicine 16:9-18.

Ogawa S, Lee TM, Nayak AS, Glynn P (1990a) Oxygenation-sensitive contrast in magnetic resonance image of rodent brain at high magnetic fields. Magnetic resonance in medicine 14:68-78.

Ogawa S, Lee TM, Kay AR, Tank DW (1990b) Brain magnetic resonance imaging with contrast dependent on blood oxygenation. Proc Natl Acad Sci U S A 87:9868-9872.

Oguni H, Uehara T, Tanaka T, Sunahara M, Hara M, Osawa M (1998) Dramatic effect of ethosuximide on epileptic negative myoclonus: implications for the neurophysiological mechanism. Neuropediatrics 29:29-34.

Olejniczak P (2006) Neurophysiologic basis of EEG. Journal of clinical neurophysiology : official publication of the American Electroencephalographic Society 23:186-189.

Panayiotopoulos CP (2005) Idiopathic geernalised epilepsies. In: The epilepsies: seizures, syndromes and management: Oxford, UK: Blandon Medical Publishing.

Panayiotopoulos CP (2010a) Principles of Therapy in the Epilepsies. In: A clinical guide to Epileptic Syndromes and their Treatment. , 2nd Edition, pp 173-236. London: Springer.

Panayiotopoulos CP (2010b) A clinical guide to epileptic syndromes and their treatment, 2nd Edition. London: Springer.

Panayiotopoulos CP (2010c) EEG and brain imaging. In: A clinical guide to Epileptic Syndromes and their Treatment, 2nd Edition, pp 147-172. London: Springer.

Papazian O, Canizales E, Alfonso I, Archila R, Duchowny M, Aicardi J (1995) Reversible dementia and apparent brain atrophy during valproate therapy. Annals of neurology 38:687-691.

Pardoe H, Pell GS, Abbott DF, Berg AT, Jackson GD (2008) Multi-site voxel-based morphometry: methods and a feasibility demonstration with childhood absence epilepsy. NeuroImage 42:611-616.

Pasley BN, Inglis BA, Freeman RD (2007) Analysis of oxygen metabolism implies a neural origin for the negative BOLD response in human visual cortex. NeuroImage 36:269-276.

Patenaude B, Smith SM, Kennedy DN, Jenkinson M (2011) A Bayesian model of shape and appearance for subcortical brain segmentation. NeuroImage 56:907-922.

Perucca E (1997) Evaluation of drug treatment outcome in epilepsy: a clinical perspective. Pharmacy world & science : PWS 19:217-222.

Petersen ET, Zimine I, Ho YC, Golay X (2006) Non-invasive measurement of perfusion: a critical review of arterial spin labelling techniques. The British journal of radiology 79:688-701.

Petkov G, Goodfellow M, Richardson MP, Terry JR (2014) A critical role for network structure in seizure onset: a computational modeling approach. Front Neurol 5:1-7.

Pillay N, Archer JS, Badawy RA, Flanagan DF, Berkovic SF, Jackson G (2013) Networks underlying paroxysmal fast activity and slow spike and wave in Lennox-Gastaut syndrome. Neurology 81:665-673.

Pizzini F, Farace P, Zanoni T, Magon S, Beltramello A, Sbarbati A, Fabene PF (2008) Pulsed-arterial-spin-labeling perfusion 3T MRI following single seizure: A first case report study. Epilepsy research 81:225-227.

Pizzini FB, Farace P, Manganotti P, Zoccatelli G, Bongiovanni LG, Golay X, Beltramello A, Osculati A, Bertini G, Fabene PF (2013) Cerebral perfusion alterations in epileptic patients during peri-ictal and post-ictal phase: PASL vs DSC-MRI. Magn Reson Imaging 31:1001-1005.

Power JD, Barnes KA, Snyder AZ, Schlaggar BL, Petersen SE (2012) Spurious but systematic correlations in functional connectivity MRI networks arise from subject motion (vol 59, pg 2142, 2012). NeuroImage 63:999-999.

Prevett MC, Duncan JS, Jones T, Fish DR, Brooks DJ (1995) Demonstration of thalamic activation during typical absence seizures using H2(15)O and PET. Neurology 45:1396-1402.

Price CJ (2010) The anatomy of language: a review of 100 fMRI studies published in 2009. Annals of the New York Academy of Sciences 1191:62-88.

Pugnaghi M, Carmichael DW, Vaudano AE, Chaudhary UJ, Benuzzi F, Di Bonaventura C, Giallonardo AT, Rodionov R, Walker MC, Duncan JS, Meletti S, Lemieux L (2014) Generalized Spike and Waves: Effect of Discharge Duration on Brain Networks as Revealed by BOLD fMRI. Brain Topogr 27:123-137.

Pulsipher DT, Dabbs K, Tuchsherer V, Sheth RD, Koehn MA, Hermann BP, Seidenberg M (2011) Thalamofrontal neurodevelopment in new-onset pediatric idiopathic generalized epilepsy. Neurology 76:28-33.

Quirk JA, Fish DR, Smith SJ, Sander JW, Shorvon SD, Allen PJ (1995) First seizures associated with playing electronic screen games: a community-based study in Great Britain. Annals of neurology 37:733-737.

Raichle ME, MacLeod AM, Snyder AZ, Powers WJ, Gusnard DA, Shulman GL (2001) A default mode of brain function. Proc Natl Acad Sci U S A 98:676-682.

Ramgopal S, Thome-Souza S, Jackson M, Kadish NE, Sanchez Fernandez I, Klehm J, Bosl W, Reinsberger C, Schachter S, Loddenkemper T (2014) Seizure detection, seizure prediction, and closed-loop warning systems in epilepsy. Epilepsy & behavior : E&B 37:291-307.

Ray A, Tao JX, Hawes-Ebersole SM, Ebersole JS (2007) Localizing value of scalp EEG spikes: a simultaneous scalp and intracranial study. Clinical neurophysiology : official journal of the International Federation of Clinical Neurophysiology 118:69-79.

Raz N, Lindenberger U, Rodrigue KM, Kennedy KM, Head D, Williamson A, Dahle C, Gerstorf D, Acker JD (2005) Regional brain changes in aging healthy adults: general trends, individual differences and modifiers. Cerebral cortex 15:1676-1689.

Reutens DC, Berkovic SF, Macdonell RA, Bladin PF (1993) Magnetic stimulation of the brain in generalized epilepsy: reversal of cortical hyperexcitability by anticonvulsants. Annals of neurology 34:351-355.

Reuter M, Tisdall MD, Qureshi A, Buckner RL, van der Kouwe AJW, Fischl B (2015) Head motion during MRI acquisition reduces gray matter volume and thickness estimates. NeuroImage 107:107-115.

Richardson MP (2012) Large scale brain models of epilepsy: dynamics meets connectomics. J Neurol Neurosur Ps 83:1238-1248.

Richardson MP, Strange BA, Duncan JS, Dolan RJ (2006) Memory fMRI in left hippocampal sclerosis: optimizing the approach to predicting postsurgical memory. Neurology 66:699-705.

Roche-Labarbe N, Zaaimi B, Mahmoudzadeh M, Osharina V, Wallois A, Nehlig A, Grebe R, Wallois F (2010) NIRS-measured oxy- and deoxyhemoglobin changes associated with EEG spike-and-wave discharges in a genetic model of absence epilepsy: the GAERS. Epilepsia 51:1374-1384.

Roger J, Bureau, M., Oller Ferrer-Vidal, L., Oller Daurella, T., Saltarelli, A., Genton, P. (1994) Clinical and electroencephalographic characteristics of idiopathic generalised epilepsies. In: Idiopathic generalised epilepsies (Malafosse A GP, Hirsch E, Marescaux C, Broglin D, Bernasconi R., ed), pp 7-18. London: John Libbey & Co. Ltd.

Rosenkranz K, Lemieux L (2010) Present and future of simultaneous EEG-fMRI. Magma 23:309-316.

Rossion B, Caldara R, Seghier M, Schuller AM, Lazeyras F, Mayer E (2003) A network of occipito-temporal face-sensitive areas besides the right middle fusiform gyrus is necessary for normal face processing. Brain : a journal of neurology 126:2381-2395.

Saini J, Sinha S, Bagepally BS, Ramchandraiah CT, Thennarasu K, Prasad C, Taly AB, Satishchandra P (2013) Subcortical structural abnormalities in juvenile

myoclonic epilepsy (JME): MR volumetry and vertex based analysis. Seizure 22:230-235.

Sakurai K, Takeda Y, Tanaka N, Kurita T, Shiraishi H, Takeuchi F, Nakane S, Sueda K, Koyama T (2010) Generalized spike-wave discharges involve a default mode network in patients with juvenile absence epilepsy: a MEG study. Epilepsy research 89:176-184.

Salek-Haddadi A, Lemieux L, Merschhemke M, Friston KJ, Duncan JS, Fish DR (2003) Functional magnetic resonance imaging of human absence seizures. Annals of neurology 53:663-667.

Salek-Haddadi A, Diehl B, Hamandi K, Merschhemke M, Liston A, Friston K, Duncan JS, Fish DR, Lemieux L (2006) Hemodynamic correlates of epileptiform discharges: an EEG-fMRI study of 63 patients with focal epilepsy. Brain research 1088:148-166.

Savic I, Osterman Y, Helms G (2004) MRS shows syndrome differentiated metabolite changes in human-generalized epilepsies. NeuroImage 21:163-172.

Schiller Y, Najjar Y (2008) Quantifying the response to antiepileptic drugs: effect of past treatment history. Neurology 70:54-65.

Schmidt H, Petkov G, Richardson MP, Terry JR (2014) Dynamics on networks: the role of local dynamics and global networks on the emergence of hypersynchronous neural activity. PLoS computational biology 10:e1003947.

Schnack HG, van Haren NE, Hulshoff Pol HE, Picchioni M, Weisbrod M, Sauer H, Cannon T, Huttunen M, Murray R, Kahn RS (2004) Reliability of brain volumes from multicenter MRI acquisition: a calibration study. Hum Brain Mapp 22:312-320.

Seeck M, Dreifuss S, Lantz G, Jallon P, Foletti G, Despland PA, Delavelle J, Lazeyras F (2005) Subcortical nuclei volumetry in idiopathic generalized epilepsy. Epilepsia 46:1642-1645.

Seneviratne U, Cook M, D'Souza W (2014) Focal abnormalities in idiopathic generalized epilepsy: a critical review of the literature. Epilepsia 55:1157-1169.

Shamshiri EA, Centeno, M., Tierney, T.M., St Pier, K., Pressler, R., Perani, S., Cross, J.H., Carmichael, D.W. (2016) Interictal activity is important for abnormal intrinsic network connectivity in paediatric focal epilepsy. Hum Brain Mapp:Under review.

Shmuel A, Augath M, Oeltermann A, Logothetis NK (2006) Negative functional MRI response correlates with decreases in neuronal activity in monkey visual area V1. Nat Neurosci 9:569-577.

Shmuel A, Yacoub E, Pfeuffer J, Van de Moortele PF, Adriany G, Hu X, Ugurbil K (2002) Sustained negative BOLD, blood flow and oxygen consumption response and its coupling to the positive response in the human brain. Neuron 36:1195-1210.

Sisodiya SM, Free SL, Stevens JM, Fish DR, Shorvon SD (1995) Widespread cerebral structural changes in patients with cortical dysgenesis and epilepsy. Brain : a journal of neurology 118:1039-1050.

Smith SJ (2005) EEG in the diagnosis, classification, and management of patients with epilepsy. Journal of neurology, neurosurgery, and psychiatry 76 Suppl 2:2-7.

Smith SM (2002) Fast robust automated brain extraction. Hum Brain Mapp 17:143-155.

Smith SM, Zhang Y, Jenkinson M, Chen J, Matthews PM, Federico A, De Stefano N (2002) Accurate, robust, and automated longitudinal and cross-sectional brain change analysis. NeuroImage 17:479-489.

Smith SM, Rao A, De Stefano N, Jenkinson M, Schott JM, Matthews PM, Fox NC (2007) Longitudinal and cross-sectional analysis of atrophy in Alzheimer's disease: cross-validation of BSI, SIENA and SIENAX. NeuroImage 36:1200-1206.

Sowell RE, Trauner, A.D., Gamst, A., Jernigan, L.T. (2002) Development of cortical and subortical brain structures in childhood and adolescence: a structural MRI study. Developmental Medicine & Child Neurology 44:4-16.

Spanaki MV, Siegel H, Kopylev L, Fazilat S, Dean A, Liow K, Ben-Menachem E, Gaillard WD, Theodore WH (1999) The effect of vigabatrin (gamma-vinyl GABA) on cerebral blood flow and metabolism. Neurology 53:1518-1522.

Speckmann EJ, Elger, C.E. (2005) Introduction to the Neurophysiological Basis of the EEG and DC Potentials. In: Electroencephalography: basic principles, clinical applications, and related fields, 5th Edition (Niedermeyer EdS, Fernando Lopes, ed), pp 18-29. Philadelphia: Lippincott Williams E Wilkins.

Srivastava G, Crottaz-Herbette S, Lau KM, Glover GH, Menon V (2005) ICA-based procedures for removing ballistocardiogram artifacts from EEG data acquired in the MRI scanner. NeuroImage 24:50-60.

Stefanovic B, Warnking JM, Pike GB (2004) Hemodynamic and metabolic responses to neuronal inhibition. NeuroImage 22:771-778.

Stefanovic B, Warnking JM, Kobayashi E, Bagshaw AP, Hawco C, Dubeau F, Gotman J, Pike GB (2005) Hemodynamic and metabolic responses to activation, deactivation and epileptic discharges. NeuroImage 28:205-215.

Storti SF, Formaggio E, Bertoldo A, Manganotti P, Fiaschi A, Toffolo GM (2013) Modelling hemodynamic response function in epilepsy. Clinical neurophysiology : official journal of the International Federation of Clinical Neurophysiology 124:2108-2118.

Storti SF, Boscolo Galazzo I, Del Felice A, Pizzini FB, Arcaro C, Formaggio E, Mai R, Manganotti P (2014) Combining ESI, ASL and PET for quantitative assessment of drug-resistant focal epilepsy. NeuroImage 102:49-59.

Szaflarski JP, Kay B, Gotman J, Privitera MD, Holland SK (2013) The relationship between the localization of the generalized spike and wave discharge generators and the response to valproate. Epilepsia 54:471-480.

Szaflarski JP, DiFrancesco M, Hirschauer T, Banks C, Privitera MD, Gotman J, Holland SK (2010) Cortical and subcortical contributions to absence seizure onset examined with EEG/fMRI. Epilepsy & behavior : E&B 18:404-413.

Tae WS, Kim SH, Joo EY, Han SJ, Kim IY, Kim SI, Lee JM, Hong SB (2008) Cortical thickness abnormality in juvenile myoclonic epilepsy. Journal of neurology 255:561-566.

Tae WS, Hong SB, Joo EY, Han SJ, Cho JW, Seo DW, Lee JM, Kim IY, Byun HS, Kim SI (2006) Structural brain abnormalities in juvenile myoclonic epilepsy patients: Volumetry and voxel-based morphometry. Korean J Radiol 7:162-172.

Tagliazucchi E, Laufs H (2014) Decoding Wakefulness Levels from Typical fMRI Resting-State Data Reveals Reliable Drifts between Wakefulness and Sleep. Neuron 82:695-708.

Tao JX, Ray A, Hawes-Ebersole S, Ebersole JS (2005) Intracranial EEG substrates of scalp EEG interictal spikes. Epilepsia 46:669-676.

Tenney JR, Fujiwara H, Horn PS, Jacobson SE, Glauser TA, Rose DF (2013) Focal corticothalamic sources during generalized absence seizures: a MEG study. Epilepsy research 106:113-122.

Theodore WH, Balish M, Leiderman D, Bromfield E, Sato S, Herscovitch P (1996) Effect of seizures on cerebral blood flow measured with 15O-H2O and positron emission tomography. Epilepsia 37:796-802.

Tierney TM, Weiss-Croft LJ, Centeno M, Shamshiri EA, Perani S, Baldeweg T, Clark CA, Carmichael DW (2016) FIACH: A biophysical model for automatic retrospective noise control in fMRI. NeuroImage 124:1009-1020.

Tracey I (2001) Prospects for human pharmacological functional magnetic resonance imaging (phMRI). Journal of clinical pharmacology Suppl:21S-28S.

Urbach H (2012) High-field magnetic resonance imaging for epilepsy. Neuroimaging clinics of North America 22:173-189.

van Houdt PJ, de Munck JC, Leijten FS, Huiskamp GJ, Colon AJ, Boon PA, Ossenblok PP (2013) EEG-fMRI correlation patterns in the presurgical evaluation of focal epilepsy: a comparison with electrocorticographic data and surgical outcome measures. NeuroImage 75:238-248.

van Luijtelaar G, Behr C, Avoli M (2014) Is there such a thing as "generalized" epilepsy? Advances in experimental medicine and biology 813:81-91.

van Luijtelaar G, Luttjohann A, Makarov VV, Maksimenko VA, Koronovskii AA, Hramov AE (2016) Methods of automated absence seizure detection, interference by stimulation, and possibilities for prediction in genetic absence models. Journal of neuroscience methods 260:144-158.

Vaudano AE, Laufs H, Kiebel SJ, Carmichael DW, Hamandi K, Guye M, Thornton R, Rodionov R, Friston KJ, Duncan JS, Lemieux L (2009) Causal Hierarchy within the Thalamo-Cortical Network in Spike and Wave Discharges. PloS one 4:e6475.

Vaudano AE, Ruggieri A, Tondelli M, Avanzini P, Benuzzi F, Gessaroli G, Cantalupo G, Mastrangelo M, Vignoli A, Bonaventura CD, Canevini MP, Bernardina BD, Nichelli PF, Meletti S (2014) The visual system in eyelid myoclonia with absences. Annals of neurology 76:412-427.

Verrotti A, Cerminara C, Domizio S, Mohn A, Franzoni E, Coppola G, Zamponi N, Parisi P, Iannetti P, Curatolo P (2008) Levetiracetam in absence epilepsy. Developmental medicine and child neurology 50:850-853.

Vollmar C, O'Muircheartaigh J, Barker GJ, Symms MR, Thompson P, Kumari V, Duncan JS, Janz D, Richardson MP, Koepp MJ (2011) Motor system hyperconnectivity in juvenile myoclonic epilepsy: a cognitive functional magnetic resonance imaging study. Brain : a journal of neurology 134:1710-1719.

Wang DJJ, Chen YF, Fernandez-Seara MA, Detre JA (2011) Potentials and Challenges for Arterial Spin Labeling in Pharmacological Magnetic Resonance Imaging. J Pharmacol Exp Ther 337:359-366.

Wang G, Dai ZY, Song W, Wang S, Shi H, Pan P, Chen F, Xu Y, Zhong J (2016) Grey matter anomalies in drug-naive childhood absence epilepsy: A voxel-based morphometry study with MRI at 3.0T. Epilepsy research 124:63-66.

Wei HL, An J, Zeng LL, Shen H, Qiu SJ, Hu DW (2015) Altered functional connectivity among default, attention, and control networks in idiopathic generalized epilepsy. Epilepsy & Behavior 46:118-125.

Westmijse I, Ossenblok P, Gunning B, van Luijtelaar G (2009) Onset and propagation of spike and slow wave discharges in human absence epilepsy: A MEG study. Epilepsia 50:2538-2548.

Whitwell JL (2009) Voxel-Based Morphometry: An Automated Technique for Assessing Structural Changes in the Brain. Journal of Neuroscience 29:9661-9664.

Wilke M (2012) An alternative approach towards assessing and accounting for individual motion in fMRI timeseries. NeuroImage 59:2062-2072.

Williams DS, Detre JA, Leigh JS, Koretsky AP (1992) Magnetic-Resonance-Imaging of Perfusion Using Spin Inversion of Arterial Water. P Natl Acad Sci USA 89:212-216.

Woermann FG, Sisodiya SM, Free SL, Duncan JS (1998) Quantitative MRI in patients with idiopathic generalized epilepsy. Evidence of widespread cerebral structural changes. Brain : a journal of neurology 121:1661-1667.

Woermann FG, Free SL, Koepp MJ, Sisodiya SM, Duncan JS (1999) Abnormal cerebral structure in juvenile myoclonic epilepsy demonstrated with voxel-based analysis of MRI. Brain : a journal of neurology 122:2101-2108.

Wolf RL, Alsop DC, Levy-Reis I, Meyer PT, Maldjian JA, Gonzalez-Atavales J, French JA, Alavi A, Detre JA (2001) Detection of mesial temporal lobe hypoperfusion in patients with temporal spin labeled lobe epilepsy by use of arterial perfusion MR imaging. Am J Neuroradiol 22:1334-1341.

Yan WX, Mullinger KJ, Geirsdottir GB, Bowtell R (2010) Physical modeling of pulse artefact sources in simultaneous EEG/fMRI. Hum Brain Mapp 31:604-620.

Yang T, Guo Z, Luo C, Li Q, Yan B, Liu L, Gong Q, Yao D, Zhou D (2012) White matter impairment in the basal ganglia-thalamocortical circuit of drug-naive childhood absence epilepsy. Epilepsy research 99:267-273.

Yao J, Dewald JP (2005) Evaluation of different cortical source localization methods using simulated and experimental EEG data. NeuroImage 25:369-382.

Zelaya Fo, Fernandez-Seara, M.A, Black,K.J., Williams, S.C., Mehta, M.A. (2016) Perfusion in pharmacological imaging. In: MR and CT perfusion and pharmacokinetic imaging (Bammer R, ed), pp 1083-1091. Philadelphia: Walters-Kluwer

Zheng TW, O'Brien TJ, Morris MJ, Reid CA, Jovanovska V, O'Brien P, van Raay L, Gandrathi AK, Pinault D (2012) Rhythmic neuronal activity in S2 somatosensory and insular cortices contribute to the initiation of absence-related spike-and-wave discharges. Epilepsia 53:1948-1958.

Zhong J, Kennan RP, Fulbright RK, Gore JC (1998) Quantification of intravascular and extravascular contributions to BOLD effects induced by alteration in oxygenation or intravascular contrast agents. Magnetic resonance in medicine 40:526-536.